

Winter 2010

Synthesis of 1,4,7-triazacyclononane pendant-armed chelators and their metal complexes

Elizabeth Garcia Cardona
University of New Hampshire, Durham

Follow this and additional works at: <https://scholars.unh.edu/thesis>

Recommended Citation

Cardona, Elizabeth Garcia, "Synthesis of 1,4,7-triazacyclononane pendant-armed chelators and their metal complexes" (2010).
Master's Theses and Capstones. 620.
<https://scholars.unh.edu/thesis/620>

This Thesis is brought to you for free and open access by the Student Scholarship at University of New Hampshire Scholars' Repository. It has been accepted for inclusion in Master's Theses and Capstones by an authorized administrator of University of New Hampshire Scholars' Repository. For more information, please contact nicole.hentz@unh.edu.

**SYNTHESIS OF 1,4,7-TRIAZACYCLONONANE PENDANT-ARMED
CHELATORS AND THEIR METAL COMPLEXES**

BY

ELIZABETH GARCIA CARDONA

B.S. Florida Southern College, 2006

THESIS

**Submitted to the University of New Hampshire
in Partial Fulfillment of the Requirements for the Degree of**

Master of Science

in

Chemistry

December, 2010

UMI Number: 1489974

All rights reserved

INFORMATION TO ALL USERS

The quality of this reproduction is dependent upon the quality of the copy submitted.

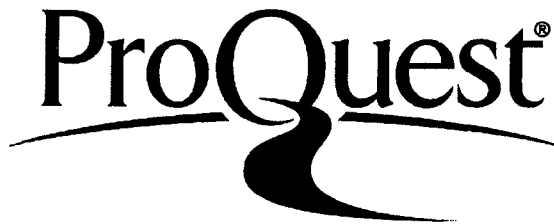
In the unlikely event that the author did not send a complete manuscript and there are missing pages, these will be noted. Also, if material had to be removed, a note will indicate the deletion.



UMI 1489974

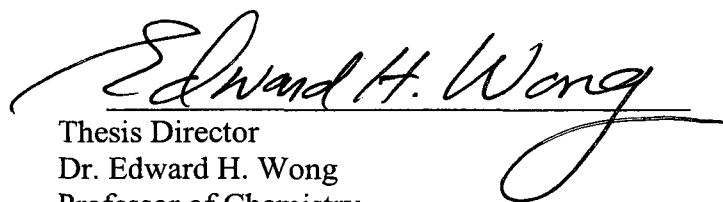
Copyright 2011 by ProQuest LLC.

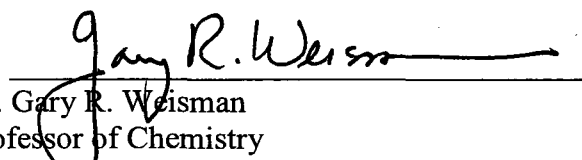
All rights reserved. This edition of the work is protected against unauthorized copying under Title 17, United States Code.




ProQuest LLC
789 East Eisenhower Parkway
P.O. Box 1346
Ann Arbor, MI 48106-1346

This thesis has been examined and approved.


Thesis Director
Dr. Edward H. Wong
Professor of Chemistry


Dr. Gary R. Weisman
Professor of Chemistry


Dr. Roy P. Panalp
Associate Professor of Chemistry

Oct 11, 2010
Date

DEDICATION

To my family for their endless love and support.

“Hay días en que somos tan móviles, tan móviles,
como las leves briznas al viento y al azar...
Tal vez bajo otro cielo la Gloria nos sonría...
La vida es clara, undívaga, y abierta como un mar...

Y hay días en que somos tan fértiles, tan fértiles,
como en Abril el campo, que tiembla de pasión;
bajo el influjo pródigo de espirituales lluvias,
el alma está brotando florestas de ilusión.

Y hay días en que somos tan sórdidos, tan sórdidos,
como la entraña oscura de obscuro pedernal;
la noche nos sorprende, con sus profusas lámparas,
en rútilas monedas tasando el Bien y el Mal.

Y hay días en que somos tan plácidos, tan plácidos...
-¡niñez en el crepúsculo! ¡lagunas de zafir!-
que un verso, un trino, un monte, un pájaro que cruza,
¡y hasta las propias penas! nos hacen sonreír...

Y hay días en que somos tan lúbricos, tan lúbricos,
que nos depara en vano su carne la mujer;
tras de ceñir un talle y acariciar un seno,
la redondez de un fruto nos vuelve a estremecer.

Y hay días en que somos tan lúgubres, tan lúgubres,
como en las noches lúgubres el llanto del pinar:
el alma gime entonces bajo el dolor del mundo,
y acaso ni Dios mismo nos pueda consolar.

Mas hay también ¡oh Tierra! un día... un día... un día
en que levamos anclas para jamás volver;
un día en que discurren vientos ineluctables...
¡Un día en que ya nadie nos puede retener!”

(Porfirio Barba Jacob)

ACKNOWLEDGEMENTS

I would like to present my sincerest gratitude to the following people: both of my research advisors and mentors, Dr. Edward Wong and Dr. Gary Weisman, for their advice, guidance, support, and patience as well as for their insightful contribution to both my research and my academic career. It has been a pleasure and an honor to be part of their research group. I would also like to recognize and thank Dr. Roy Planalp, for his lessons in inorganic chemistry and for being part of my academic committee.

To all the professors at the chemistry department, for their time and their dedication to teach. To Dr. Gonghu Li, for his financial support during the spring and the summer of 2010 as this gave me a great opportunity to explore a new area of research and allowed me to stay and finish my thesis.

To all the former members of the Weisman-Wong group, Han Wang, Orjana Terova, Matt Young, Dave Martin, Antoinette Odendaal, and Dan Stigers for their advice as senior graduate students. Special thanks to Eman Akam and Gayathri Sridhar for their moral support in life as well as in research. To the rest of the graduate students in the chemistry department for helping out every time I had questions. To these people I extend my deepest gratitude.

Additionally, I am very grateful for the help I received from Cindi Rohwer, Peggy Torch, Bob Constantine, John Wilderman, Pat Wilkinson, Amy Lindsay, and Kathy Gallagher. Their support is greatly appreciated. I also appreciate the collaboration of Dr. Arnold L. Rheingold and his group for their efforts in solving the X-ray structures, as this was an integral part in the success of my research project.

I must to say thanks to my friends and family for always being supportive. I want to give special thanks to Oszkar and Danijela. They have become a second family, offering friendship and love that will last a lifetime.

Lastly, but definitely not least, my husband, Peter Christy, as his encouragement and support was limitless.

TABLE OF CONTENTS

DEDICATION.....	iii
ACKNOWLEDGEMENTS.....	iv
TABLE OF CONTENTS.....	vi
LIST OF FIGURES.....	ix
LIST OF SCHEMES.....	xii
LIST OF TABLES.....	xiii
ABSTRACT.....	xiv
CHAPTER I: INTRODUCTION.....	1
1.1 Triazacyclononane and Related Triazamacrocyclic Compounds.....	1
1.1.1 <i>N</i> -Functionalized Triazacyclononane Derivatives.....	4
1.2 Radiopharmaceutical Applications.....	9
1.3 Coordination Chemistry of Copper (II) with NOTA.....	14
1.4 Research Goal.....	16
CHAPTER II: SYNTHESIS OF <i>N</i> -FUNCTIONALIZED 1,4,7-TRIAZACYCLONONANES.....	18
2.1 Introduction.....	18
2.2 Ligand Synthesis and Characterization.....	19
2.2.1 The Synthesis of 1-formyl-1,4,7-triazacyclononane-4,7-diacetate diethyl ester (5).....	19
2.2.2 Synthesis of 1,4,7-triazacyclonane-4,7-diacetate diethyl ester • 2HCl (6).....	22
2.2.3 Syntheses of 1,4,7-triazacyclononane-1-acetamide-4,7-diacetate diethyl	

ester (7).....	25
2.2.4 Synthesis of disodium 1,4,7-triazacyclononane-1-acetamide-4,7-diacetate (8).....	29
2.2.5 Synthesis of NOTA (2).....	34
2.3 Summary and Discussion.....	35
2.4 Future Work.....	38
CHAPTER III: COPPER(II) COORDINATION OF <i>N</i> -FUNCTIONALIZED 1, 4, 7-TRIAZACYCLONONANES.....	40
3.1 Introduction.....	40
3.2 Synthesis and Characterization of Copper (II) Complexes.....	41
3.2.1 Copper and Zinc Complexes of 1-formyl-1, 4, 7-triazacyclononane (4).....	43
3.2.2 Copper Complex of Ligand 9.....	50
3.2.3 Copper Complex of Ligand 6.....	53
3.2.4 Copper Complex of Ligand 7.....	55
3.2.5 Copper Complex of Ligand 8.....	58
3.3 Electrochemistry and Acid Inertness of Cu(II) Complexes.....	63
3.3.1 Cyclic Voltammetry.....	63
3.3.2 Acid-Assisted Decomplexation Studies.....	65
3.4 Summary and Conclusions.....	67
3.5 Future Work.....	68
CHAPTER IV: EXPERIMENTAL SECTION.....	69
4.1 General Methods and Materials.....	69
4.2 Syntheses.....	70

APPENDIX.....	80
LIST OF REFERENCES.....	104

LIST OF FIGURES

<u>Figure</u>	<u>Page</u>
Figure 1.01 1,4,7-triazacyclononane.....	1
Figure 1.02 Facial coordination mode of TACN.....	3
Figure 1.03 Facial and meridional coordination fashion in an octahedral complex of an acyclic triamine.....	4
Figure 1.04 An <i>N</i> -functionalized triazacyclononane derivative, NOTA (2).....	5
Figure 1.05 Twist angle.....	7
Figure 1.06 Five-membered chelate ring conformations.....	8
Figure 1.07 Examples of type I and type II NOTA complexes.....	8
Figure 1.08 <i>N</i> -functionalized polyazamacrocycle carboxylate-based bioconjugates.....	11
Figure 1.09 <i>N</i> -functionalized tetraazamacrocycles DOTA, TETA and CB-TE2A...11	11
Figure 1.10 Chemical structure of DOTA- 8-AOC-BBN(7-14)NH ₂ , CB-TE2A-8-AOC-BBN(7-14)NH ₂ , and NOTA -8-AOC-BBN(7-14)NH ₂	13
Figure 1.11 Two different structures for Cu-NOTA.....	15
Figure 2.01 The NOTA BFC and its simplest model, NOAM2A (8).....	18
Figure 2.02 ATR-IR spectrum of compound 5	21
Figure 2.03 ESI-TOF mass spectrum of compound 5	22
Figure 2.04 ¹ H NMR spectrum (D ₂ O, 400 MHz) of 6 •2HCl, residual EtOH set to 1.17.....	24
Figure 2.05 ¹³ C{ ¹ H} NMR spectrum (D ₂ O, 100.51 MHz) of 6 •2HCl.....	25
Figure 2.06 ATR-IR spectrum of compound 6 •2HCl.....	25

Figure 2.07	^1H NMR spectrum (CDCl_3 , 400 MHz) of compound 7	27
Figure 2.08	$^{13}\text{C}\{^1\text{H}\}$ NMR spectrum (CDCl_3 , 100.51 MHz) of Compound 7	27
Figure 2.09	ATR-IR spectrum of 7	28
Figure 2.10	ESI-TOF spectrum of 7	29
Figure 2.11	^1H NMR spectrum (D_2O , 400 MHz) of 7 after two hours in D_2O at room temperature, CH_3CN set to 2.06.....	30
Figure 2.12	^1H NMR spectrum (D_2O , 400 MHz) of 8 , EtOH set to 1.17 ppm.....	31
Figure 2.13	$^{13}\text{C}\{^1\text{H}\}$ NMR Spectrum (D_2O , 100.51 MHz) of 8 , EtOH set to 17.47 ppm.....	32
Figure 2.14	^1H NMR spectrum (D_2O , 400 MHz) of 8 after EtOH evaporation, residual solvent peak set to 4.79 ppm.....	32
Figure 2.15	$^{13}\text{C}\{^1\text{H}\}$ NMR Spectrum (D_2O , 100 MHz) of 8 after EtOH evaporation.....	33
Figure 2.16	ATR-IR spectrum of 8	34
Figure 3.01	Comparison IR spectra for copper nitrate, ligand 4 , and complex 13 ...45	
Figure 3.02	Changes in the IR (KBr) spectrum of complex 13	46
Figure 3.03	Comparison IR spectra for zinc nitrate, ligand 4 , and complex 14 ...47	
Figure 3.04	^1H NMR spectrum (D_2O , 500 MHz) of 4 and 14 , CH_3CN set to 2.06.....	48
Figure 3.05	X-ray structure of complex 14	49
Figure 3.06	ATR-IR spectrum of 15	51
Figure 3.07	X-ray structure of complex 15	52
Figure 3.08	View of the X-ray structure of complex 16	54

Figure 3.09	X-ray structure of complex 17	56
Figure 3.10	X-ray structure for complex 18	59
Figure 4.01	General design for bubbling dry HCl (g) into absolute EtOH.....	70

LIST OF SCHEMES

<u>Scheme</u>		<u>Page</u>
Scheme 1.1	Protocol for the synthesis of N,N',N''-tritosyl-1,4,7-triazacyclononane...	2
Scheme 1.2	Synthesis of NOTA.....	7
Scheme 1.3	Synthetic plan for 4, 5, 6, 7 and 8.....	17
Scheme 2.1	Synthesis of 1-formyl-1,4,7-triazacyclononane (4).....	19
Scheme 2.2	Reaction scheme used by Spiccia et al. for the synthesis of 5.....	20
Scheme 2.3	Dialkylation of 4 and formyl bond cleavage of 5.....	21
Scheme 2.4	Reported synthesis of free amine 6.....	23
Scheme 2.5	Synthesis of the monoamide diacetate analogue of NOTA, NOAM2A (8).....	26
Scheme 2.6	Synthesis of NOTA.....	35
Scheme 2.7	Suggested protonation sequence of NOTA.....	37
Scheme 2.8	Suggested first protonation site of 11.....	37
Scheme 2.9	Suggested second, third, and fourth protonation sites of 11.....	38
Scheme 3.1	General protocol for M (II) complexation with ligands 4, 5, 6, and 7...41	
Scheme 3.2	Delocalization of nitrogen's lone Pair into a π system leading to favorable binding at the more basic carbonyl oxygen.....	43
Scheme 3.3	Synthesis of compound 7.....	56
Scheme 3.4	Cu (II) complexation with ligand 8.....	58
Scheme 3.5	Potential species formed during electrochemistry studies.....	65

LIST OF TABLES

<u>Table</u>		<u>Page</u>
Table 1.01	Examples of TACN derivatives.....	6
Table 2.01	Protonation constants of NOTA (2) and TACN-diacetate (11), values in square brackets were determined from ¹ H NMR titration.....	36
Table 3.01	List of ligands and metal complexes.....	42
Table 3.02	Selected bond length (Å) and angles (°) for complex 14.....	49
Table 3.03	Selected bond length (Å) and angles (°) for complex 15.....	52
Table 3.04	Bond length (Å) and angles (°) for complex 16.....	55
Table 3.05	Selected bond length (Å) and angles (°) for complex 17.....	57
Table 3.06	Selected bond length (Å) and angles (°) for complex 18.....	60
Table 3.07	Crystal data for compounds 14, 15, and 16.....	61
Table 3.08	Crystal data for compounds 17 and 18.....	62
Table 3.09	Electrochemical studies of copper (II) complexes.....	64
Table 3.10	Acid decomplexation studies of copper (II) complexes.....	66

ABSTRACT

SYNTHESIS OF 1,4,7-TRIAZACYCLONONANE PENDANT-ARMED CHELATORS AND THEIR METAL COMPLEXES

by

Elizabeth Garcia Cardona

University of New Hampshire, December, 2010

Pendant-armed cyclic polyamines have been demonstrated to be promising ligands for the development of new metal-based radiopharmaceuticals for positron-emission tomography (PET). Macrocyclic polyamines bearing pendant arms can effectively bind specific metals with suitable complexation kinetics and stability while attached to a tumor-targeting vector or peptide. ^{64}Cu -radiolabeled peptides containing the chelator 1,4,7-triazacyclononane 1,4,7-triacetate have been shown to possess superior properties which overcome commonly observed problems such as demetallation and accumulation of the radio-metal in non-targeted tissues. To model these radiolabeled bioconjugates and to gain insight into this observed bio-stability, the synthesis of a copper (II) complex of a new triazacyclononane derivative containing one amide and two acetate groups (NOAM2A) has been performed. Studies of its acid inertness and electrochemistry behavior have been investigated. Complementary, copper (II) complexes of other triazacyclononane intermediates have also been explored.

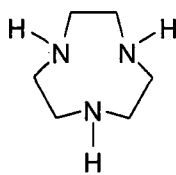
CHAPTER I

INTRODUCTION

1.1 1, 4, 7- Triazacyclononane and Related Triazamacrocyclic Compounds

The use of cyclic polyamine compounds as ligands for metal complexation has expanded over the years.¹⁻⁴ Interest in the coordination chemistry of these chelators is due in part to their relevance in bioinorganic and catalytic studies, as well as their applications in biology, medicine, and modern clinical imaging protocols.¹⁻⁵

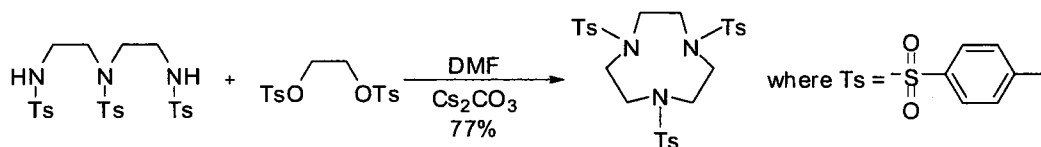
Cyclic polyamine compounds include a large group of polydentate ligands containing nitrogen donor atoms within a ring.² 1,4,7-Triazacyclononane (**1**) (TACN) contains nine atoms of which three are nitrogen and it is the parent of a family of ligands which have been used for the complexation of a myriad of metals. This tridentate ligand has three-fold symmetry (**Figure 1.01**) and usually occupies one hemisphere of the metal coordination sphere.¹



1

Figure 1.01: 1,4,7-triazacyclononane

The synthesis of TACN was reported by Koyama and Yoshino in 1972.⁶ TACN was obtained from its precursor, 1-4-di-*p*-toluenesulfonyl-1-4-7-triazacyclononane, via hydrolysis of the tosylamide groups with hydrobromic acid and glacial acetic acid.⁶ The synthesis of its precursor had been reported in 1937 in a very low yield, 18%, thus it was not ideal.⁷ Other approaches towards the synthesis of cyclic tosylamines were reported by Stetter and Roos. Condensation of terminal dihalides with bisulfonamide sodium salts under high dilution were performed to obtain moderate cyclization yields.⁸ In 1974, Richman and Atkins reported a modified and efficient method for the preparation of 9- to 21-membered saturated macrocycles containing three to seven heteroatoms. Use of preformed bisulfonamide sodium salts and sulfonate ester leaving groups in a dipolar aprotic solvent eliminated the need of high dilution techniques, allowing preparation on a large scale.⁹ The free amine TACN is efficiently obtained by the oxidative cleavage of the tosyl groups with concentrated sulfuric acid at 100 °C, followed by basification of the tris-sulfate salt.^{1,9} Modified procedures have been also reported by McAuley et al.,¹⁰ Graeme et al.,¹¹ Sherry et al.,¹² and Kellogg.¹³ In our group, the cyclization is performed using a modification of the Kellogg procedure (**Scheme 1.1**).



Scheme 1.1 : Protocol for the synthesis of N, N', N''-tritosyl-1,4,7-triazacyclononane

Following the development of a simplified synthetic approach, metal complexes of TACN have been extensively investigated. Early work, much of it by Wieghardt and coworkers, focused on the basic chemistry of TACN and were compiled in a review by

Chaudhuri and Wieghardt.¹ It was recognized that TACN is a remarkable ligand in supporting both mono- and bi-metallic complexes containing labile coordination sites. Thus, a variety of TACN complexes have been used to model both structural and functional metallo-enzymes.^{14,15} Metal complexes of the type [Metal-TACN]^{3+/2+} have been synthesized with transition and main group metals in common oxidation states. TACN metals complexes with Cr(III), V(IV), Mn(II), Mn(IV), Fe(III), Co(II), Co(III), Ni(II), Cu(II), Zn(II), Au(III), Pt(II), Pt(IV), Pd(II), Mo(II), W(II), Re(I), Ru(III), Ru(II), Rh(III), Os(II), Ga(III), In(III), Tl(III), Tc(II), Tc(III), and Tc(IV) have been reported in the literature and their coordination chemistry has been investigated by Wieghardt and others.^{1,6,14-19}

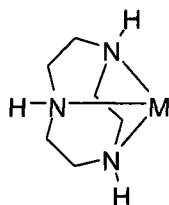


Figure 1.02: Facial coordination mode of TACN

TACN coordinates very strongly to metal ions with the metal ion above the triaza plane (**Figure 1.02**). The medium-ring size restricts its coordination to a facial manner, as opposed to its acyclic analogues, which can coordinate in either a facial or a meridional fashion (**Figure 1.03**).^{1,2} The thermodynamic stabilities for most reported TACN-metal complexes surpass those of their open-chain analogues, this trend is also observed by macrocyclic molecules and it is commonly known as the macrocyclic effect stating that complexes of macrocyclic ligands are more stable than their acyclic counterparts.^{1,2,20,21} Moreover, the medium-ring sized, TACN, has shown higher stability

constants for the formation of some 1:1 ligand-metal complexes compared to the larger 1,4,7-triazacyclododecane, 1,4,8-triazacycloundecane, and 1,5,9-triazacyclododecane macrocycles.¹

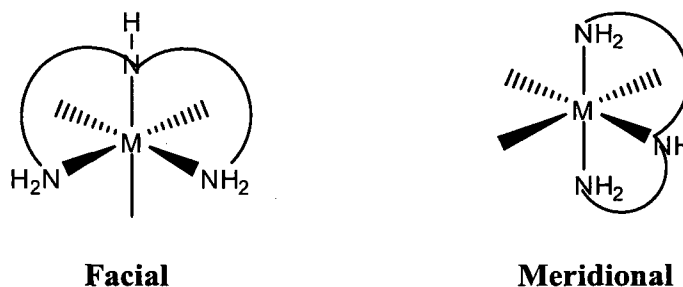


Figure 1.03: Facial and meridional coordination fashion in an octahedral complex of an acyclic triamine

The thermodynamic stability and the kinetic inertness of coordinated triazamacrocyclic complexes are two important aspects that have made these ligands very useful in fostering advances in inorganic chemistry as well as applications in other scientific fields. For example biological activity data of $[\text{Au}(\text{TACN})\text{Cl}_2]\text{Cl}$ has shown higher cytotoxicity than cisplatin against A-549 and HCT-116 tumor cell lines.¹⁹ To further optimize metal binding, this ligand system has been frequently modified by the attachment of pendant donor groups, typically onto nitrogens, in order to fill out additional metal coordination sites.

1.1.1 N-Functionalized Triazacyclononane Derivatives

Attachment of functional groups (R,R',R'') to the secondary amine positions in the medium sized ring (**Figure 1.04**) tunes ligand properties and enhances its complexation with a large variety of metal ions, providing additional control over the

ligand environment around the metals as well as overall charge. Furthermore, ligands of this class combine the attractive features of a chelating ring as well as faster binding kinetics of an open-chain.² The selection of the pendant arms and their functional groups is based on the metal of interest, its oxidation state, and its potential applications. Gasser et al. reported the synthesis of a TACN derivative with two pyridyl pendant groups to increase its stability when complexed to copper(II) ion as compared to the parent TACN copper complex.²² There are many other examples of TACN derivatives with a variety of pendant arms shown in Table 1.01 as compounds A,²³⁻²⁶ B,²⁷ C²⁸, D, E,^{29, 30} G,³¹ H,³² etc. One of the original and most useful *N*-functionalized TACN derivative is the tri-*N*-substituted *N,N',N''*-tris(carboxymethyl)-14,7-triazacyclononane, **NOTA**, **(2)** (**Figure 1.04**).²³⁻²⁶

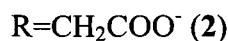
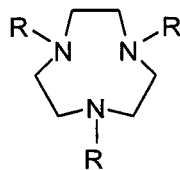
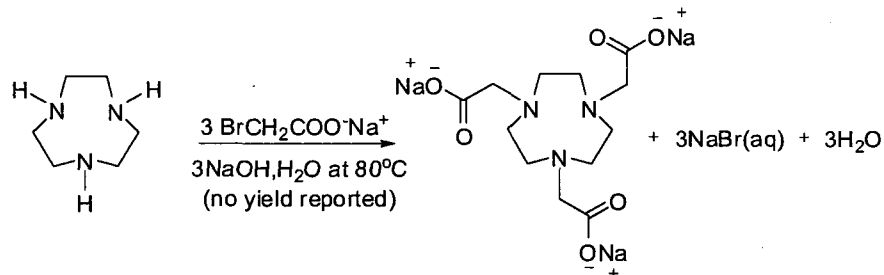


Figure 1.04: An *N*-functionalized triazacyclononane derivative, **NOTA (2)**

Compound	R
A	
B	
C	
D	
E	
F	
G	
H	

Table 1.01: Examples of TACN derivatives

NOTA has been synthesized by reacting TACN with sodium bromoacetate and sodium hydroxide in aqueous solution at 80 °C as shown in **Scheme 1.2**.²⁶ Its coordination chemistry has been studied with Ca(II), Mg(II), Al(III), Cr(III), V(IV), Mn(II), Mn(III), Fe(II), Fe(III), Co(II), Co(III), Ni(II), Ni(III), Cu(II), Cd(II), Pb(II), Ga(III), In(III), Tl(III) to form in most cases complexes of the type $[M\text{-NOTA}]^{0/-1}$, where M is one of the above metals commonly in either (II) or (III) oxidation state.¹ Formation constants show higher stabilities in comparison to the parent TACN metal complexes where formation constants range from 5.8 up to 16.2 as compared to 8.8 up to 28.3 for NOTA complexes.¹⁻³



Scheme 1.2: Synthesis of NOTA²⁶

NOTA is a potentially hexadentate ligand with a N_3O_3 -donor set that has a favorable binding geometry for many metal complexes. The nine-membered ring coordinates facially to the metal ion which is enveloped simultaneously by the *N*-acetate arms to give octahedral to trigonal prismatic geometries around the metal.^{1-3,23-26,33} These geometries are defined by the degree of distortion from the regular octahedral arrangement which is given by the twist angle, θ , illustrated in **Figure 1.05**. Here θ is 0° in a trigonal prism and 60° in a regular octahedron.

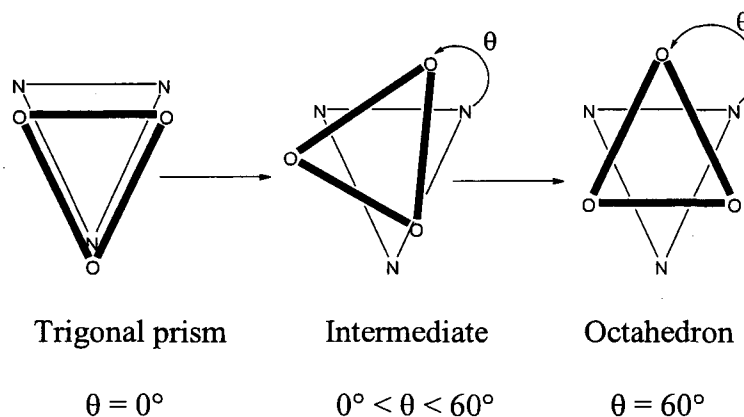


Figure 1.05: Twist angle

The compactness of the TACN ring and the low steric requirement of the acetate arms lead to the formation of unusually stable metal complexes.² The 9-membered ring, TACN, is chiral when coordinated to the metal ion, having a [3,3,3] conformation of the 9 membered ring and ($\delta\delta\delta$) or ($\lambda\lambda\lambda$) conformation of the five-membered M-N-C-C-N chelate rings (**Figure 1.06**). In addition, the acetate arms on the pseudooctahedral complexes of NOTA can exist in two possible orientations, clockwise or counterclockwise to which the literature refers as type I or type II respectively (**Figure 1.07**).¹

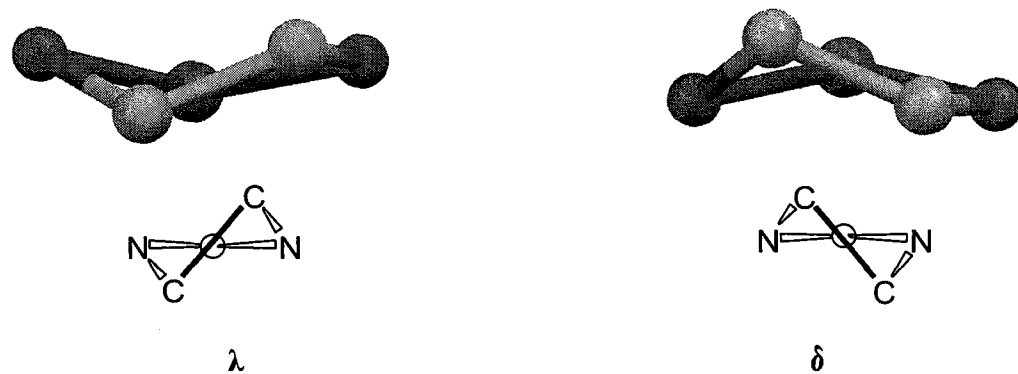


Figure 1.06: Five-membered chelate ring conformations³⁴

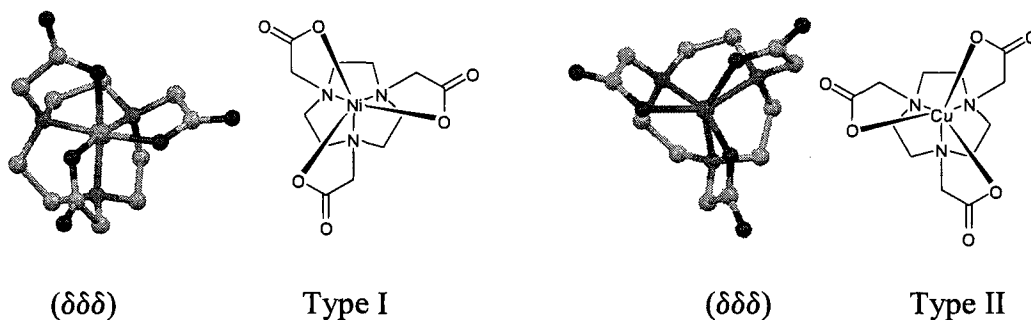


Figure 1.07: Examples of type I and type II NOTA complexes¹

NOTA has been used to make complexes with an assortment of metal ions and it is now well-established as a useful metal chelator for many tri- and divalent transition metals.^{1,3,26} Recently, radiometal complexes of this ligand have attracted attention in development of new carriers for radiopharmaceutical applications.

1.2 Radiopharmaceutical Applications

Radiopharmaceuticals utilizing radiometal-labeled complexes is a rapidly growing medicinal area.³⁵⁻³⁷ Scintigraphy, single photon emission computer tomography (SPECT), and positron emission tomography (PET) are current imaging modalities using radio-metal isotopes to image a wide range of diseases including heart disease, cancer, brain disorders, thrombosis, kidney and liver abnormalities.³⁸⁻⁴⁰

There are important factors in the selection of the proper radionuclides in designing radiopharmaceuticals, these include their mode of decay, energy emitted, half-life, production methods and cost.³⁸⁻⁴¹ The half-life of the radionuclide must be long enough for the synthesis of the radiopharmaceutical and to allow accumulation in the target tissue.³⁹⁻⁴¹ Among these modalities PET has advantages in terms of sensitivity and resolution.^{38,39} In these modalities, radiolabeled pharmaceuticals are injected in the body and imaging is obtained via detection of the decay from the targeted radioisotope inside the body. Different imaging modalities require pharmaceuticals with specific decay characteristics according to the equipment of the detection. Scintigraphy and SPECT require a radiopharmaceutical that possesses a gamma (γ) emitting radionuclide with an energy range of between 100 to 250 keV. PET requires radiopharmaceuticals with a

positron-emitting (β^+) radionuclide that would eventually result in two photon emissions $\sim 180^\circ$ apart with energy of 511 keV.³⁹⁻⁴¹

Additionally, the use of radiometals in molecular imaging applications requires metal ions that bind strongly to the ligands to form radionuclide complexes with kinetic inertness *in vivo* in order to prevent release of the radioisotope.⁴²

Copper (II) presents good characteristics as a radiometal ion for applications in diagnosis and therapy of disease in nuclear medicine since it provides an extensive selection of radioisotopes. In particular ^{60}Cu , ^{61}Cu , ^{62}Cu , ^{64}Cu , and ^{67}Cu can be used for molecular imaging and/or radiotherapy.³⁵ These copper nuclides have half-lives ranging from 10 minutes up to 62 hours, and they decay by positron (β^+), electron (β^-), or gamma (γ) emission. For instance, ^{64}Cu has a half-life of 12.7 hours and decay of $\beta^+=0.653$ MeV (19%) and $\beta^-=0.579$ MeV (39 %). The emitted positron is ideal for PET imaging and the β^- suitable for targeted radiotherapy of cancer.⁴⁰ Complementarily, copper has a well-known coordination chemistry that allows its reactions with a large number of ligands which can be linked to proteins, peptides, and other biologically-relevant molecules.⁴⁰

In order to target radiometal ions to tumors or other tissues, a bifunctional chelator (BFC) is required to conjugate to a peptide. This chelator should react rapidly enough to avoid radioactivity loss from the radiometal before injecting it to the patient. Structurally, it should contain a functional group for the covalent attachment of the targeting agent and enough donor sites remaining for complexing the radiometal ion (**Figure 1.08**).

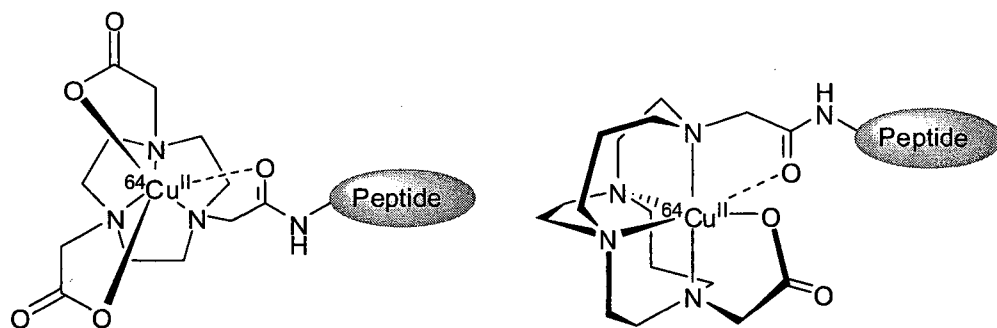


Figure 1.08: *N*-functionalized polyazamacrocyclic carboxylate-based bioconjugates

Cu(II) forms complexes with azamacrocycles that have large thermodynamic stability constants which make them attractive for the design of radiopharmaceuticals.^{2,3} These chelators provide excellent binding environments for Cu(II) ions, providing rapid metal complexation, and aqueous solubility.^{3,43} Specifically, *N*-functionalized polyazamacrocyclic carboxylate derivatives have been used in the development of ⁶⁴Cu-based imaging agents for detection and treatment of cancer. 1,4,7,10-tetraazacyclododecane-1,4,7,10-tetraacetic acid (DOTA) (Figure 1.09) and 1,4,8,11-tetraazacyclotetradecane-1,4,8,11-tetraacetic acid TETA (Figure 1.09) are two important chelators that have been used for conjugation with peptides and radiolabeling with ⁶⁴Cu as radioactive agents for PET.⁴⁴⁻⁴⁶

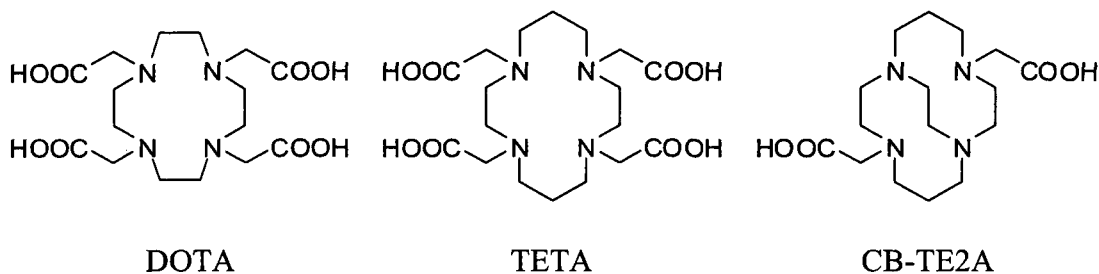


Figure 1.09: *N*-functionalized tetraazamacrocycles DOTA, TETA and CB-TE2A

The Cu(II) complexes of DOTA and TETA have the desired high thermodynamic stability constants ($\log K_{\text{Cu(II)-DOTA}}=22.7$ and $\log K_{\text{Cu(II)-TETA}}=21.9$), but unfortunately these are only moderately stable *in vivo*, resulting in significant demetallation and subsequent accumulation of the radiometal in nontarget tissues, decreasing the effectiveness of the radiopharmaceutical.^{35,47,48}

To improve the *in vivo* properties of the ^{64}Cu complexes of the BFCs, researchers have developed and investigated other chelators. A novel family of cross-bridged tetraamine chelators was developed by the Weisman-Wong group^{49,50} and used to prepare ^{64}Cu -imaging agents.^{35,47,48} Specifically, a compound of this cross bridge class, 4,11-bis(carboxymethyl)-1,4,8,11-tetraazabicyclo[6.6.2]hexadecane (CB-TE2A), is a hexadentate ligand that forms a very stable six-coordinate Cu(II) complex by complete encapsulation of the metal center.⁵⁰ In a collaborative effort between the Weisman-Wong group and the Anderson group, the efficacy of CB-TE2A in PET imaging agents was evaluated by conjugation to a somatostatin analogue peptide, radiolabeled with $^{64}\text{Cu(II)}$, and its biological activity in tumor bearing rats investigated.^{35,47,48} These studies showed reduced demetallation or accumulation of radioactivity in nontarget tissues observed in chelators, DOTA and TETA.

Hoffman et al. have also reported the synthesis and characterization of a ^{64}Cu -CB-TE2A conjugated with bombesin (BBN), ^{64}Cu -CB-TE2A-8-AOC-BBN(7-14) NH_2 (**Figure 1.10**), where BBN is a peptide able to bind to receptors that are expressed on a variety of human cancers and 8-AOC is the covalent linker.⁵¹ They have evaluated its biological activity in tumor-bearing rats and compared side by side with ^{64}Cu -DOTA-8-AOC-BBN(7-14) NH_2 confirming superior kinetic stability of the ^{64}Cu -

CB-TE2A-8-AOC-BBN(7-14)NH₂ over ⁶⁴Cu-DOTA-8-AOC-BBN(7-14)NH₂ with considerably less accumulation in non-targeted organs.⁵¹

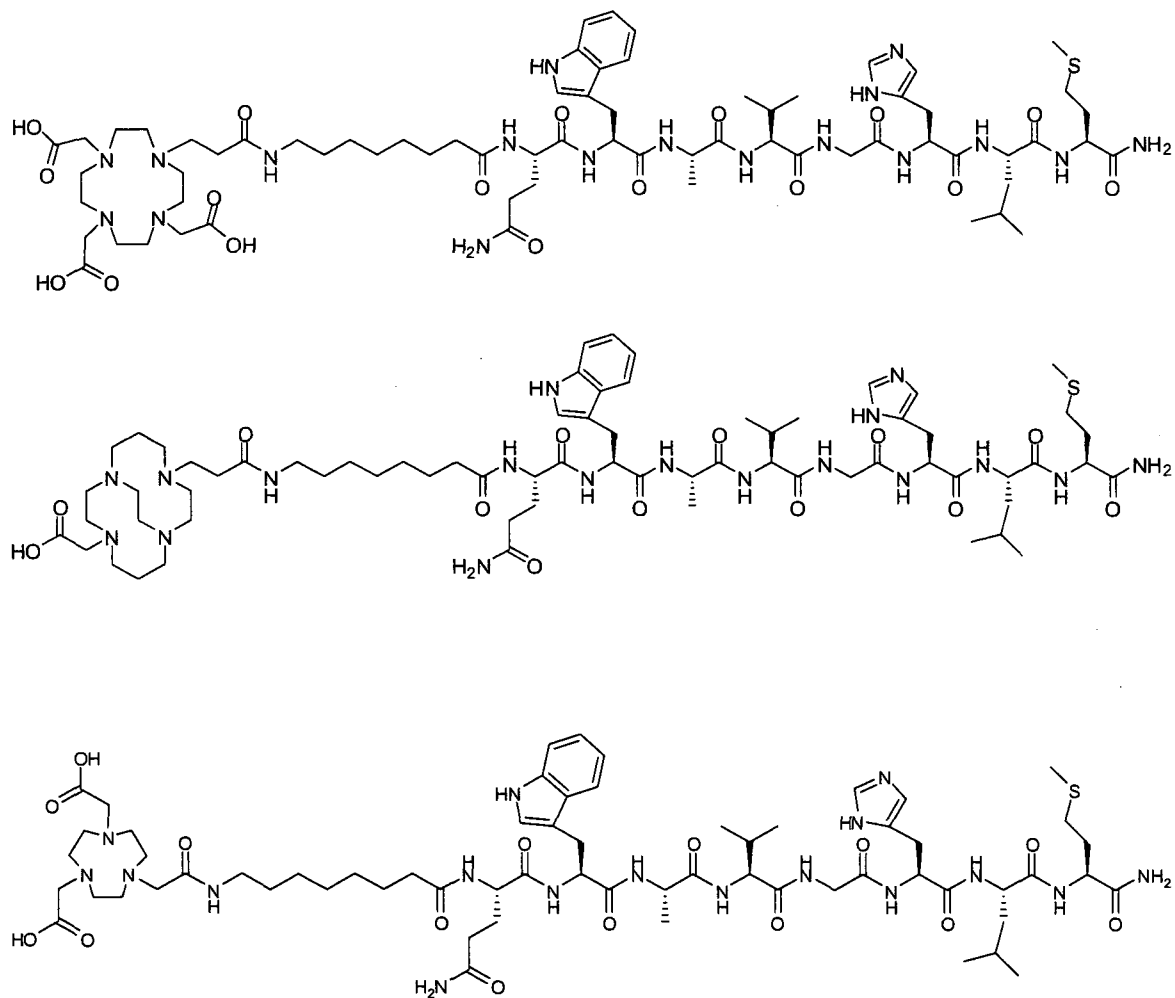


Figure 1.10: Chemical structure of DOTA- 8-AOC-BBN(7-14)NH₂, CB-TE2A-8-AOC-BBN(7-14)NH₂, and NOTA -8-AOC-BBN(7-14)NH₂^{51,52,53}

Hoffman and Smith have also explored the well known *N*-functionalized trizacyclononane system, NOTA, as the BFC bioconjugated BBN as compared to DOTA-BBN (Figure 1.10).^{52,53} Biodistribution studies of ⁶⁴Cu-NOTA-8AOC-BBN(7-14)NH₂

have shown resistance to demetallation, accumulation and retention of the conjugate in renal organs while producing microPET images that are clearly superior to the ^{64}Cu -DOTA-conjugate.^{52,53} ^{64}Cu -NO2A-8-AOC-BBN(7-14) NH_2 gave no radioactivity in collateral nontarget tissues while resulting in higher target-to-nontarget accumulation ratios. Consequently high-quality images were obtained as compared to other ^{64}Cu -BBN tracers.^{52,53}

CB-TE2A-8-AOC-BBN(7-14) NH_2 and NOTA-8-AOC-BBN(7-14) NH_2 possess improved *in vivo* properties for PET in comparison to other BFCs.⁵¹⁻⁵³ At present, it is not well understood whether the observed properties are due to the enhanced stability provided by the ligand or simply the effect of superior *in vivo* pharmacokinetics of its conjugate.

1.3 Coordination Chemistry of Copper (II) with NOTA

The coordination chemistry of the metals must be satisfied to allow for their successful incorporation into a pharmaceutical. Inorganic chemistry plays an important role in the design of target specific radiopharmaceuticals, since it is possible to correlate *in vivo* behavior of the metal complexes to their *in vitro* chemical properties such as redox stability, charge, and solubility.

Complexes of NOTA with Cu(II) were first reported by Hama and Takamoto and later structurally characterized by Wieghardt and Hancock.^{1,26,33} Two different coordination modes have been described. First, Wieghardt reported that the central copper(II) ion is six-coordinated to three nitrogens and three oxygens of the hexadentate ligand. The structure consists of the anionic unit $[\text{Cu(II)-NOTA}]^-$ with Na^+ as counter ion

(Figure 1.11), where the donor atoms are disposed in a bifacial arrangement. Three N ring atoms occupy one facial plane while three carboxylate O atoms form the other plane. A twist angle, θ , between $26-27^\circ$ indicates an intermediate geometry between an octahedral and a prismatic geometry of the $\text{Cu(II)N}_3\text{O}_3$ coordination sphere.

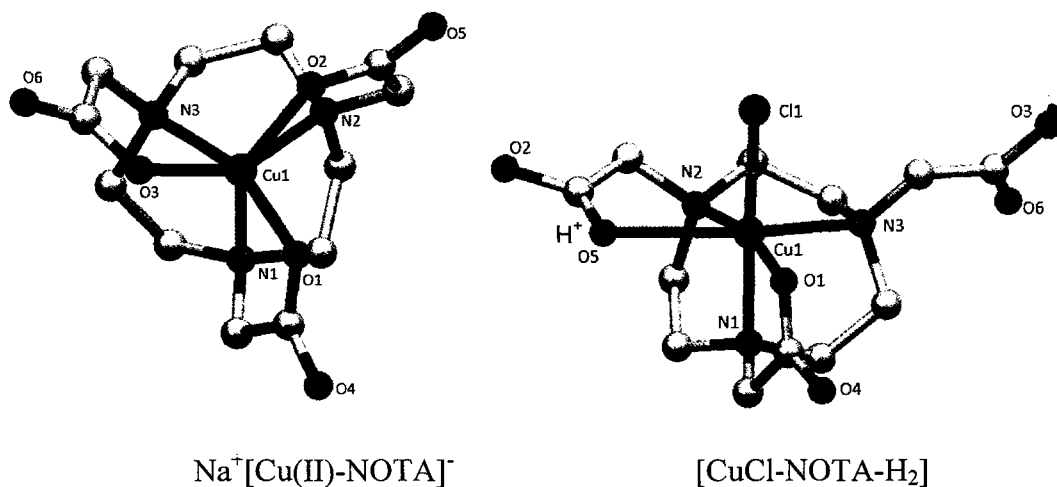


Figure 1.11: Two different structures for Cu-NOTA

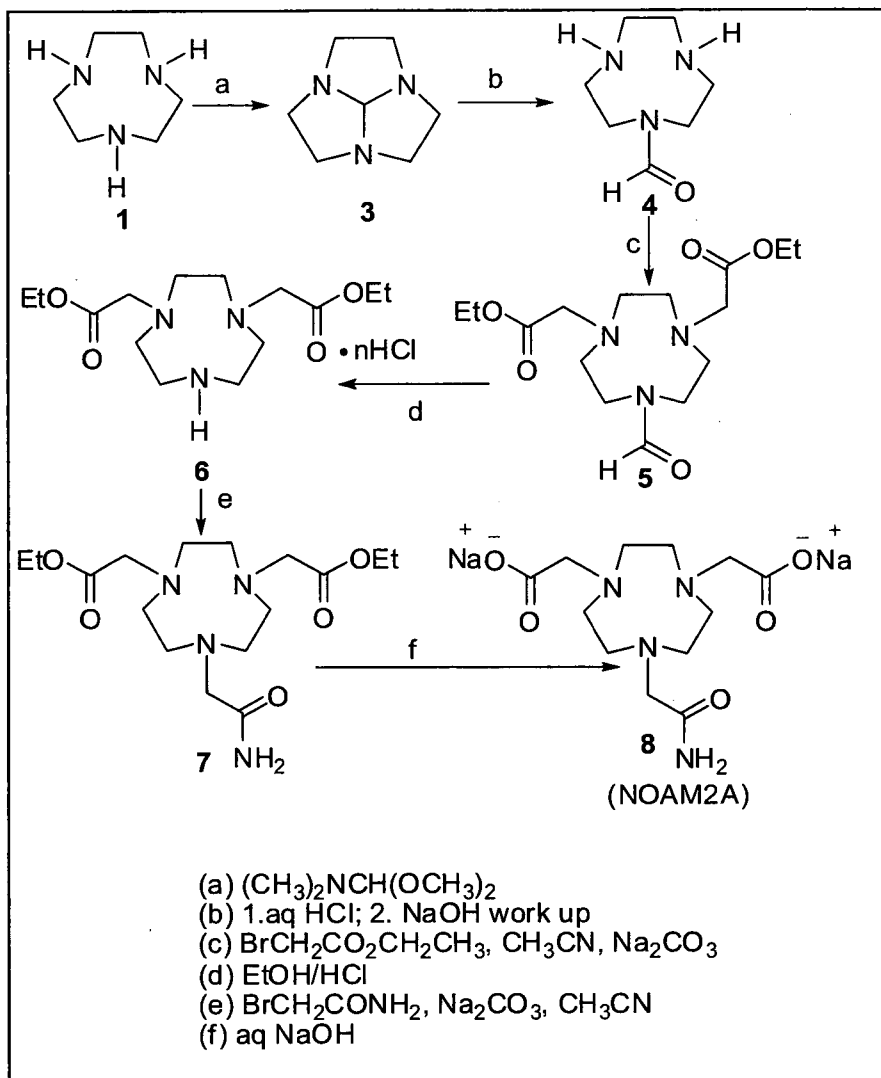
Hancock and coworkers have described the coordination of Cu(II) with protonated ligand, NOTA-H_2 .³³ In this particular case, NOTA-H_2 serves as a pentadentate ligand where three nitrogens and one acetate arm are coordinated to the metal in a similar way as described by Wieghardt. The other two pendant acetate arms are protonated in which one is weakly interacting with the metal center and the other is not coordinated at all. The coordination sphere is defined by $\text{N}_3\text{O}_2\text{Cl}$ and a twist angle of 33° , giving an intermediate geometry between octahedral and trigonal prismatic. This structure, $[\text{CuCl-NOTA-H}_2]$ (Figure 1.11), presents a higher level of distortion with respect to the bond lengths of the coordination sphere in comparison to $[\text{Cu-NOTA}]$. The reported bond lengths for $[\text{CuCl-NOTA-H}_2]$ has Cu-N bond lengths of 2.07, 2.04, and 2.38 Å; one

regular and one weak Cu-O bonds of 1.96, and 2.56 Å respectively and a Cu-Cl bond length of 2.30 Å filling the sixth coordination site. In the structure described by Wieghardt, [Cu-NOTA]⁻, the Cu-N bond lengths are 2.04, 2.12, and 2.20 Å and the Cu-O bond lengths are 1.98, 2.14, and 2.21 Å. Therefore it is noted that in [Cu-NOTA]⁻, the metal is interacting with all donor groups of the ligand, while in [Cu-NOTA-H₂], protonation of the ligand resulted in a pentadentate chelator with one weak metal-donor (O5-Cu1) interaction. For both structures a type II orientation is observed.

Peptide conjugation of NOTA converts one acetate arm to an amide by reaction with an N-terminal peptide. To gain insight into the high *in vivo* stability of the reported ⁶⁴Cu-NOTA conjugate, a monoamide dicarboxylate analogue of NOTA (NOAM2A) was proposed as a target for this research. While the synthesis and full characterization of the copper complex of the mono-amide version of Cu(II)-CB-TE2A, Cu(II)-CB-TEAMA, have been previously accomplished by the Weisman-Wong lab⁵⁴, there is no report of any NOTA derivative with one amide and two acetate arms.

1.4 Research Goal

The aim of this thesis research was the synthesis and characterization of the *N*-functionalized TACN, NOAM2A, as a model of the NOTA-peptide conjugate. Its coordination chemistry with copper(II), electrochemistry and acid inertness have been studied to gauge its resistance to demetallation. We have synthesized NOAM2A in six-steps from TACN (**Scheme 1.3**). In addition, we have attempted to prepare Cu(II) complexes of these intermediates and to characterize them as well.



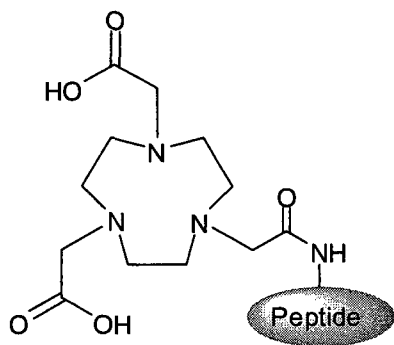
Scheme 1.3: Synthetic plan for 4, 5, 6, 7 and 8

CHAPTER II

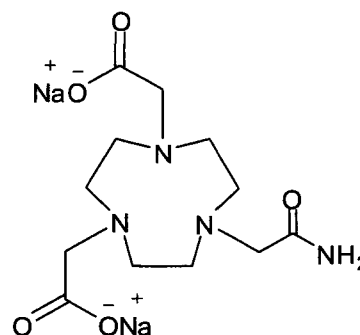
SYNTHESIS OF *N*-FUNCTIONALIZED 1, 4, 7-TRIAZACYCLONONANES

2.1 Introduction

The chelator NOTA has been shown to possess superior *in vivo* properties for PET overcoming common limitations observed with prior BFCs.⁵² To gain insight into this improved bio-stability, studies of simple models of these bioconjugates are proposed. Our interest in synthesizing an *N*-functionalized-triazacyclononane with an amide in addition to the two acetate pedant arms is to prepare such a simple model of the conjugated BFC used by Hoffman et al.^{52,53}



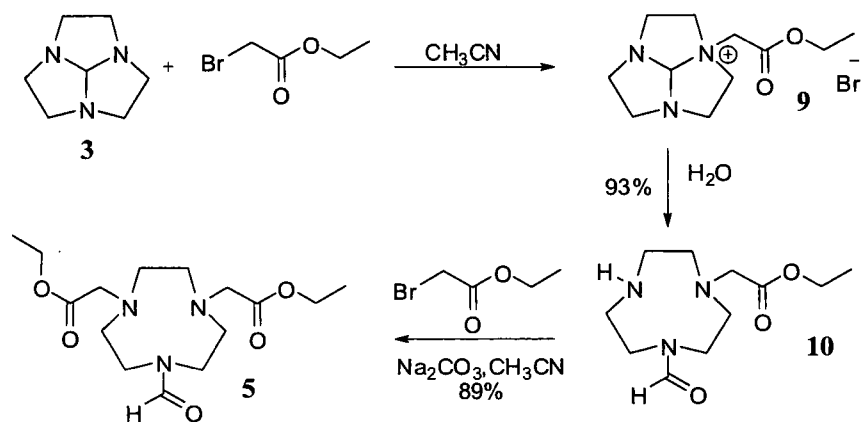
A NOTA-derived bioconjugate



Disodium salt of our bioconjugate model (8)

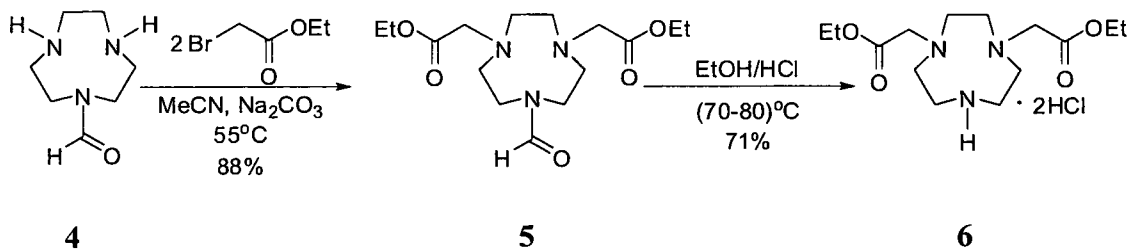
Figure 2.01: The NOTA BFC and its simplest model, NOAM2A (8)

reported. Spiccia et al. also utilized **3** as the starting material but a different approach for the introduction of the pendant arms and the formation of **5**. Their approach (**Scheme 2.2**) carried out alkylations in two separate steps. The first arm was added by the reaction of **3** with ethyl bromoacetate to form the quaternary ammonium bromide salt (**9**), which was hydrolyzed to yield the formyl-monoester derivative (**10**). The second carboxylate ester group was then attached in a similar fashion as before, but in presence of a base.⁶²



Scheme 2.2: Reaction scheme used by Spiccia et al. for the synthesis of **5**⁶²

In our approach, the two *N*-alkylations were achieved in the same step (**Scheme 2.3**), starting with the *N*-formyl monoprotected TACN **4**. The two pendant carboxylate esters were attached similar to the second alkylation by Spiccia et al. to give **5** as a clear yellowish oil in 80-90% yields. Characterization data including ^1H -NMR and $^{13}\text{C}\{^1\text{H}\}$ -NMR were obtained and corroborated with the reported data.⁶² Additional data such as mass spectrometry and IR spectroscopy were also obtained.



Scheme 2.3: Dialkylation of 4 and formyl bond cleavage of 5

The attenuated total reflectance infrared (ATR-IR) spectrum of compound **5** (**Figure 2.02**) shows typical CH₂ bands at 2979, 2909, and 2848 cm⁻¹. The carbonyl stretches are observed at 1735 and 1664 cm⁻¹, corresponding to the carboxylate ester groups and the formyl group respectively. The electrospray ionization time-of-flight (ESI-TOF) mass spectrum (**Figure 2.03**) exhibits a major peak at 352.1823 m/z which is consistent with the [5]Na⁺ cation with the formula (C₁₅H₂₇N₃NaO₅)⁺. A second peak at 330.2007 m/z is consistent with the [5]H⁺ cation and a composition of (C₁₅H₂₈N₃O₅)⁺.

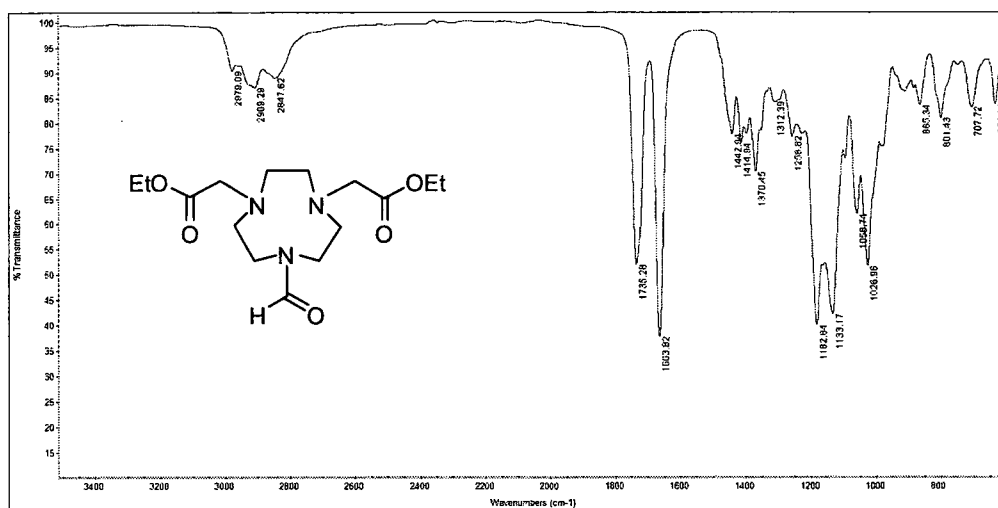


Figure 2.02: ATR-IR spectrum of compound 5

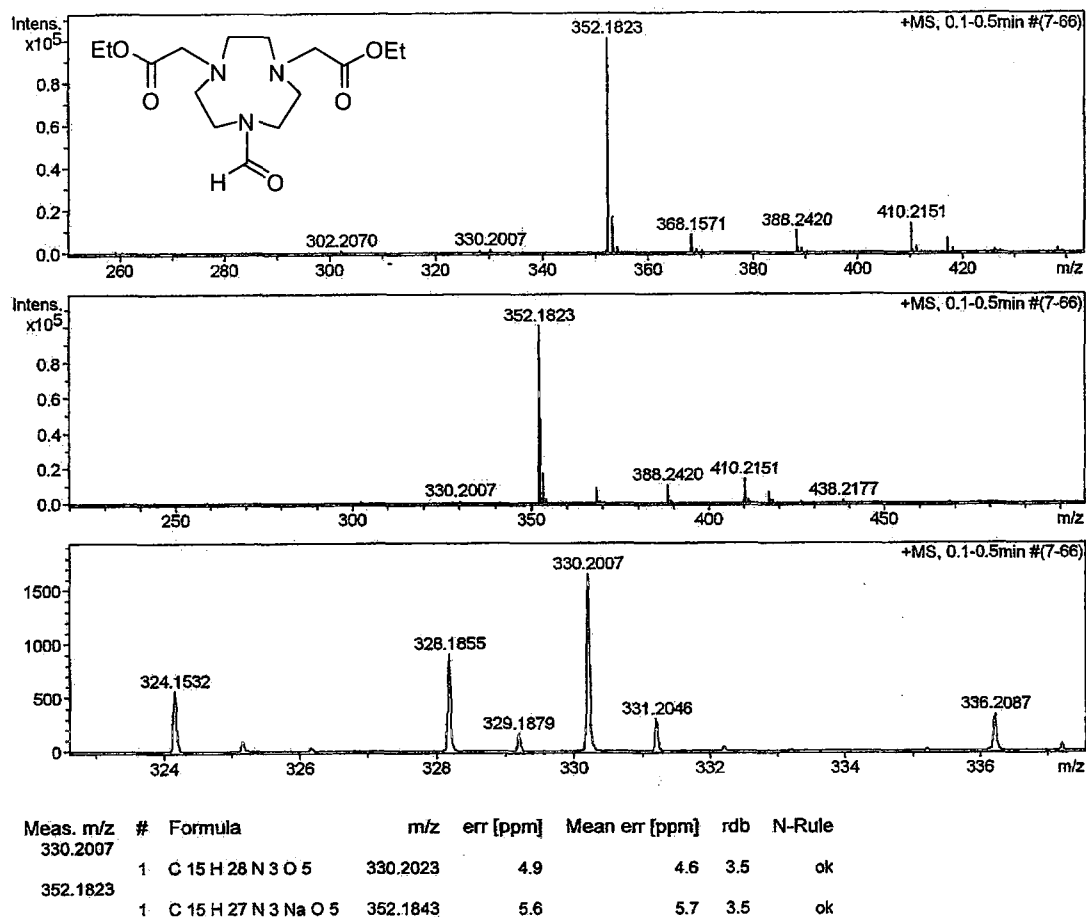
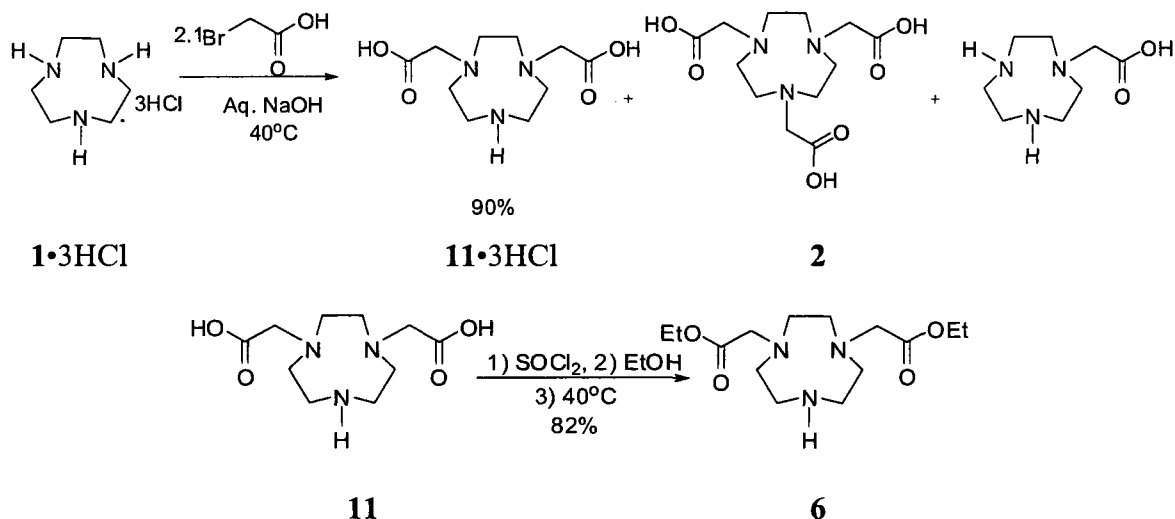


Figure: 2.03: ESI-TOF mass spectrum of compound 5

2.2.2 Synthesis of 1,4,7-triazacyclonane-4,7-diacetate diethyl ester • 2HCl (6)

Compound **6** has been previously reported by Sherry et al.⁶³ One drawback, however, is that the described synthetic pathway yielded a mixture of di- and tri-substituted intermediates that required relatively long, tedious purification techniques. Sherry et al. obtained **6** by a three-step synthesis from TACN•3HCl. In this approach, the hydrochloric salt of TACN is dissolved in water at pH 9.5 with 2.1 equivalents of bromoacetic acid (**Scheme 2.4**). It was reported that the reaction gave a mixture of products with the primary product being TACN diacetate. This mixture was then purified

by ion-exchange chromatography using aqueous hydrochloric acid as the eluent to give the pure TACN diacetate tri-hydrochloric salt. This product is then added to a premade cold solution of thionyl chloride and ethanol, stirred and warmed to 40 °C. Finally, base work up of this reaction mixture gives free amine, **6**.⁶³



Scheme 2.4: Reported synthesis of free amine 6⁶³

In our approach, the access to **6** is attained by cleavage of the formyl group in compound **5**. This was accomplished by the reaction of **5** with a dry ethanolic solution of hydrogen chloride (**Scheme 2.3**). Base work up and organic solvent extraction to obtain the free amine gave **6** as a yellow oil in very low yields. This was likely because partial hydrolysis of the ethyl ester groups had taken place in the work up and most of the product remained in the aqueous solution in the hydrolyzed form. Consequently, base work up was omitted and the hydrochloride salt of **6** (**Scheme 2.3**) was purified in a 71% yield and used for the next alkylation step. The number of HCl equivalents per molecule of **6** was determined to be two by elemental analysis. The same experimental sample was used for other characterizations, i.e. IR and NMR spectroscopy.

The structure of **6**·2HCl was confirmed by ^1H and $^{13}\text{C}\{^1\text{H}\}$ NMR spectra (**Figure 2.04**) and (**Figure 2.05**) and these agree with the assignment of time-averaged C_{2v} symmetry. The proton spectrum features a triplet at δ 1.28 and a quartet at δ 4.27 which are consistent with the ethyl ester groups, a singlet at δ 3.29, and a multiplet at δ 3.42-3.54 corresponding to the ring protons, and finally a singlet at δ 3.96 assignable to the methylene protons of the pendant arms.

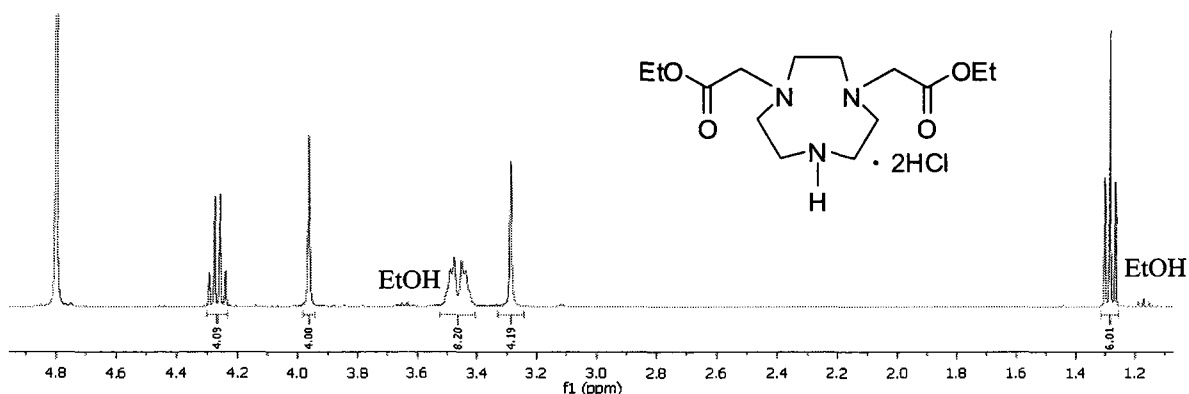


Figure 2.04: ^1H NMR spectrum (D_2O , 400 MHz) of **6**·2HCl, residual EtOH set to δ 1.17

The $^{13}\text{C}\{^1\text{H}\}$ NMR spectrum is in agreement with the reported spectrum⁶³ with seven carbon resonances in support of an averaged C_{2v} symmetry of the molecule. The IR (neat) spectrum (**Figure 2.06**) of compound **6**·2HCl contains bands in the 2800-3000 cm^{-1} region which correspond to the aliphatic C-H stretches from the ring and from the pendant arms as well. The broad N-H bands observed in the 2300 and 2600 cm^{-1} region may be attributed to H-bonding within the molecule. The C=O stretch of the carboxylic ester group is observed at 1738 cm^{-1} .

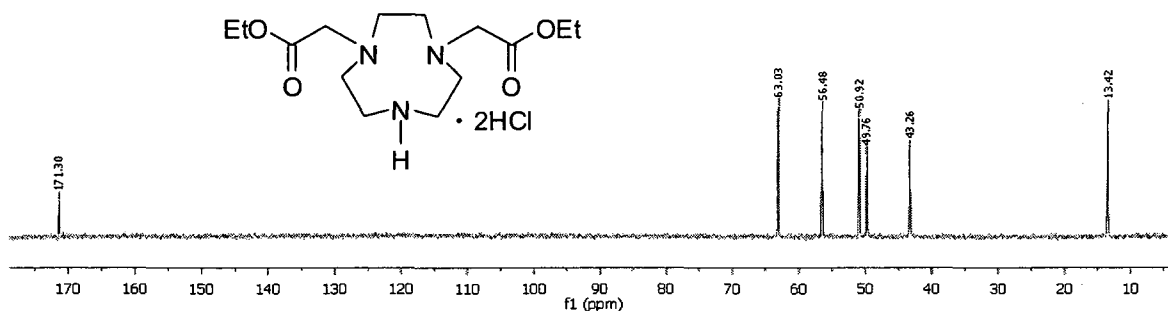


Figure 2.05: $^{13}\text{C}\{^1\text{H}\}$ NMR spectrum (D_2O , 100.51 MHz) of **6**·2HCl

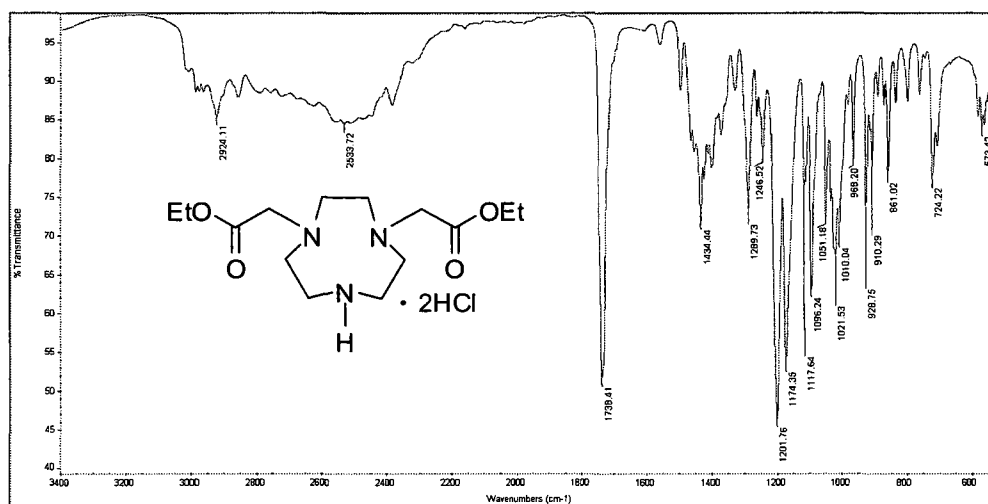
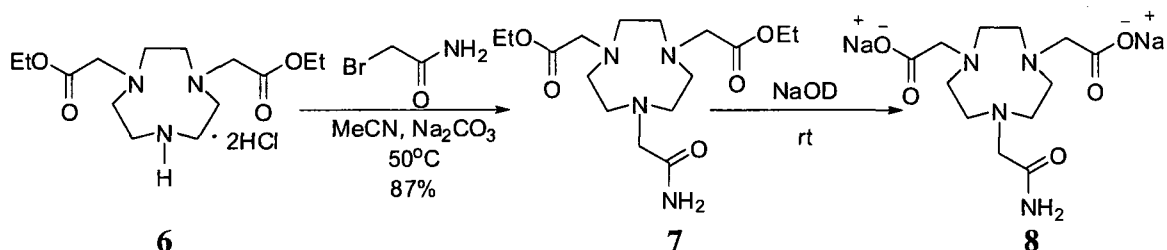


Figure 2.06: ATR-IR spectrum of compound **6**·2HCl

2.2.3 Syntheses of 1,4,7-triazacyclononane-acetamide-4,7-diacetic acid diethyl ester(7)

Using standard alkylation conditions, compound **6** was treated with one equivalent of 2-bromoacetamide and excess potassium carbonate in acetonitrile at 50°C . After a reaction time of one day, the crude material was isolated as a yellow oil (Scheme 2.5). Analysis of this crude material by ^1H -NMR spectroscopy confirmed the presence of the desired product along with impurity peaks. Base work up of this crude

material afforded compound **7** sufficiently pure to proceed to the next step. Purity assay was based on the ^1H NMR and $^{13}\text{C}\{^1\text{H}\}$ NMR spectra of the product, **Figure 2.07** and **Figure 2.08** respectively.



**Scheme 2.5: Synthesis of the monoamide diacetate derivative of NOTA,
NOAM2A (8)**

The structure of compound **7** presents an averaged C_{2v} symmetry as confirmed by ^1H and $^{13}\text{C}\{^1\text{H}\}$ NMR spectroscopy. As expected, the proton spectrum shows a splitting pattern similar to its precursor with additional singlets at 3.27, 5.43 and 9.29 ppm consistent with the new methylene and amide protons. The triplet and quartet of the methyl and methylene protons of the ethyl ester arms are displayed at 1.27 and 4.15 ppm respectively and finally, the other resonances for the ethylene protons within the ring are shown at the 2.80-2.90 ppm region. The $^{13}\text{C}\{^1\text{H}\}$ NMR spectrum reveals 9 different carbon resonances in agreement with the C_2 symmetry of compound **7**.

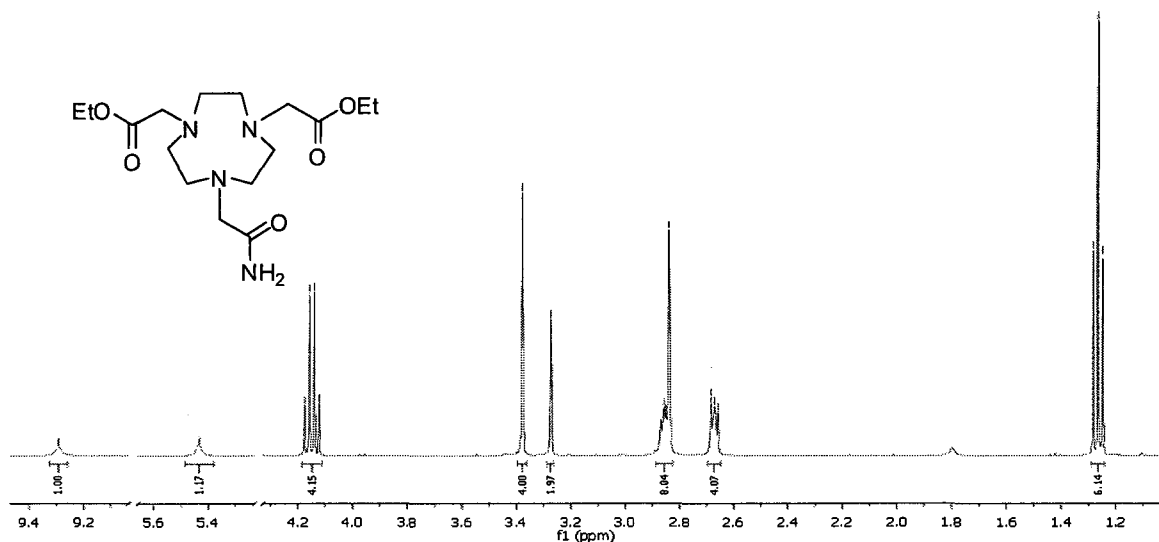


Figure 2.07: ^1H NMR spectrum (CDCl_3 , 400 MHz) of compound 7

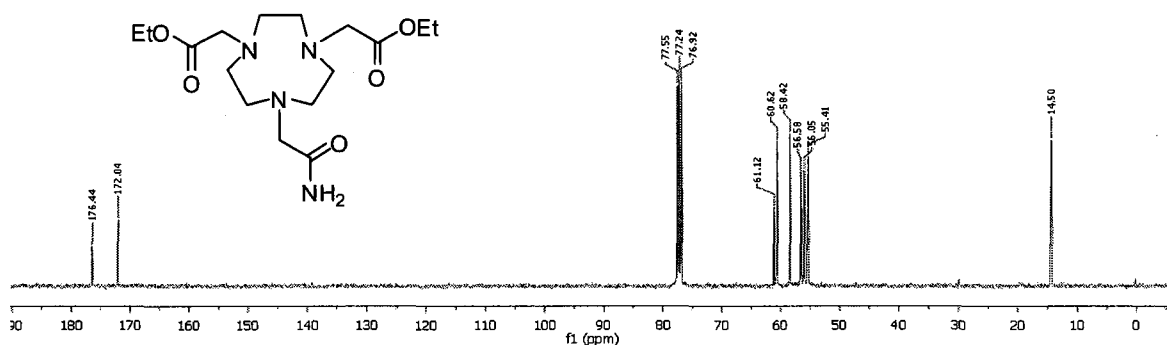


Figure 2.08: $^{13}\text{C}\{^1\text{H}\}$ NMR spectrum (CDCl_3 , 100.51 MHz) of compound 7

The IR spectrum (neat) (Figure 2.09) of compound 7 shows aliphatic CH stretches at 2841 and 2930 cm^{-1} . The strong bands at 1671 and 1734 cm^{-1} correspond to the two carbonyl stretches of the amide and ester groups respectively. There is a broad band in the 3100-3500 cm^{-1} region which is assignable to the presence of water obscuring any NH bands. Proton NMR spectrum also confirms the presence of water by a small singlet at δ 1.56.

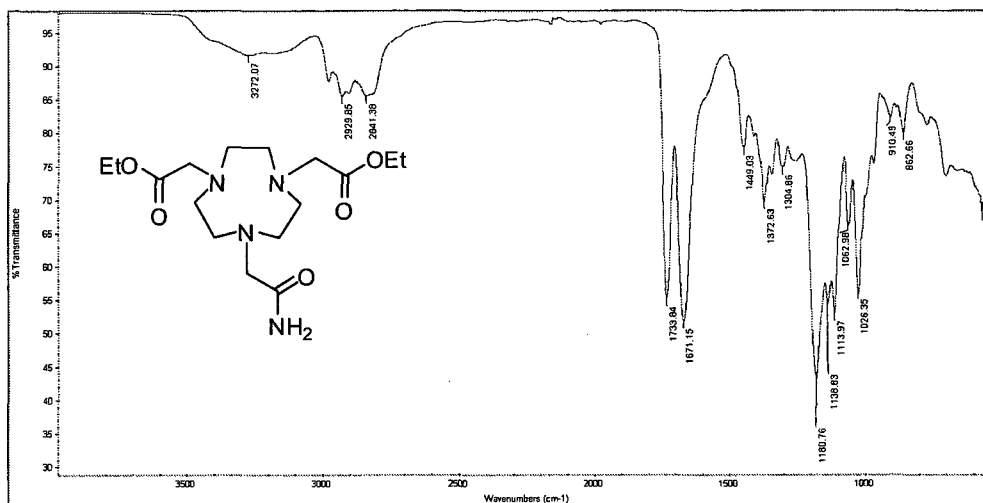


Figure 2.09: ATR-IR spectrum of 7

The ESI-TOF mass spectrum of **7** (Figure 2.10) exhibits a major peak at 359.2283 which is consistent with compound **7** agreement with the cation $[7]H^+$ with a composition of $(C_{16}H_{31}N_4O_5)^+$.

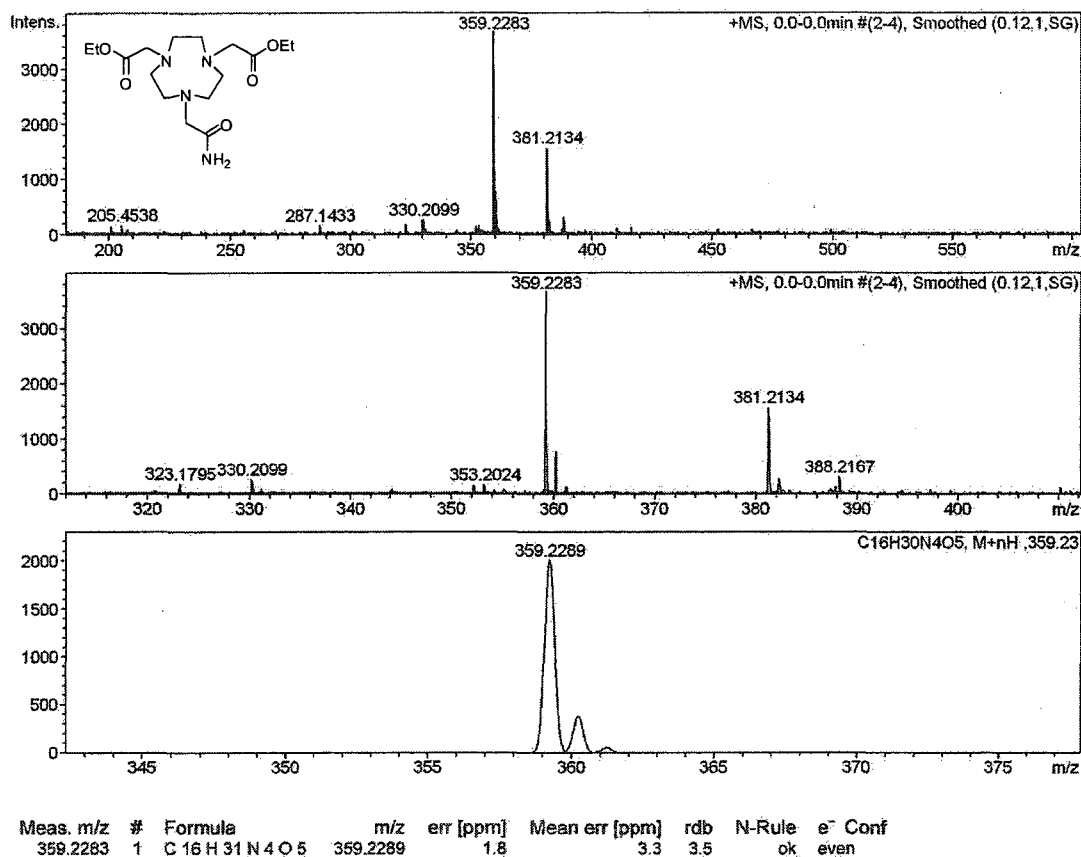


Figure 2.10: ESI-TOF spectrum of 7

2.2.4 Synthesis of disodium 1,4,7-triazacyclononane-acetamide-4,7-diacetate (8)

As previously observed in compound 6, hydrolysis of the ester groups can be carried out under mildly conditions. Initially, attempts to dissolved compound 7 in D₂O gave emulsion mixtures, which contained unhydrolyzed and hydrolyzed compound 7 as proved by proton NMR. D₂O is, in this case, just enough to partially hydrolyzed this molecule, but not strong enough to completely hydrolyze it. Figure 2.11 shows the proton NMR of 7 after two days in D₂O. It is most likely that solvent was slightly acidic, which allowed for an acid-catalysed ester hydrolysis and an acid catalysed ester formation equilibrium. Given that the hydrolysis of esters in acidic media leads to the equilibrium

between unhydrolyzed and hydrolyzed species, basic conditions were preferred for this step.

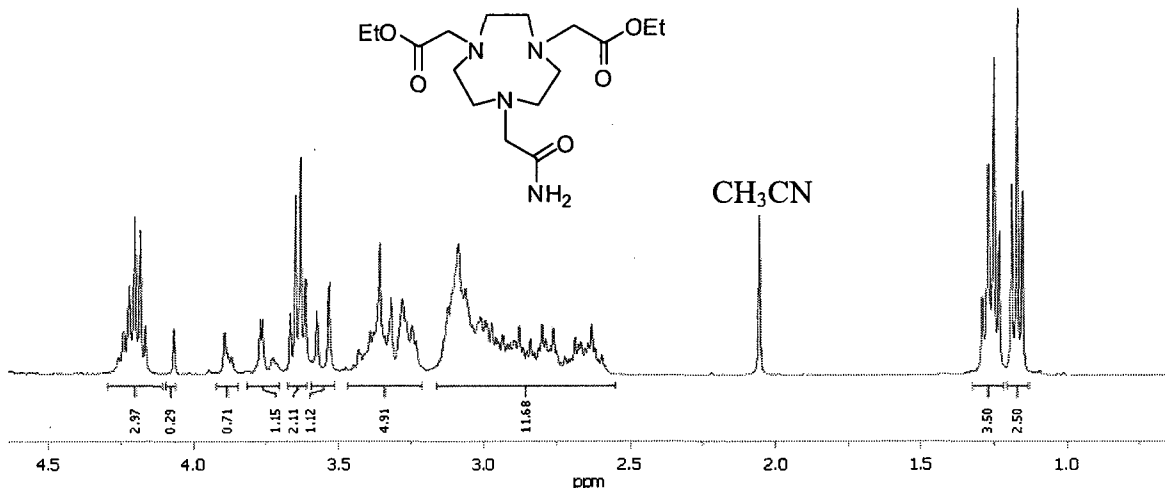


Figure 2.11: ¹H NMR (D₂O, 400 MHz) of 7 after two hours in D₂O at room temperature, CH₃CN set to 2.06 ppm

Ester groups of compound 7 were hydrolyzed using 1M NaOD at room temperature and monitored by ¹H NMR spectroscopy. Figure 2.12 shows the proton NMR spectrum after complete ester hydrolysis, which is supported by the appearance of resonances at 1.17 and 3.64 ppm corresponding to the protons of the ethanol formed. Nevertheless, this shows irreproducible NMR results and therefore, no definitive NMR spectra were obtained.

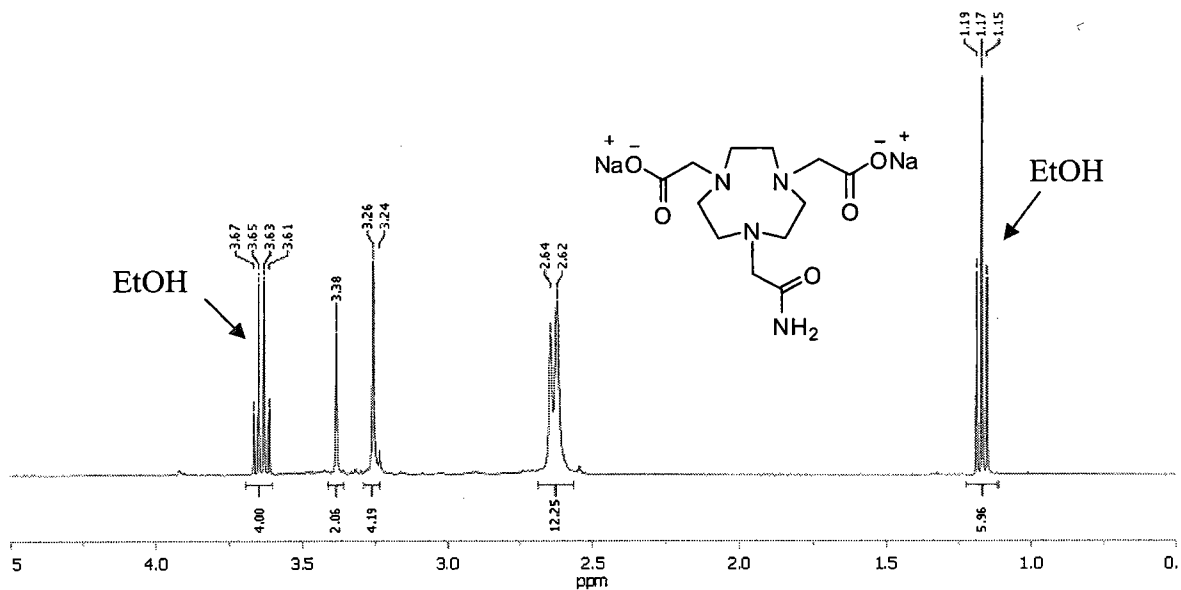


Figure 2.12: ^1H NMR spectrum (D_2O , 400 MHz) of **8**, EtOH set to 1.17 ppm

Three resonances at δ 2.62-2.65, 3.22-3.27, and 3.38 with relative integrations of twelve, four, and two respectively coincide with the expected number of protons in compound **8**. However, this is not always the case. For example, differences in the splitting pattern and their relative integrations have been observed in other samples. The $^{13}\text{C}\{^1\text{H}\}$ NMR spectrum (**Figure 2.13**) of the hydrolyzed product exhibits only seven carbon resonances; two of which are assigned to ethanol carbons from the hydrolysis and only five belong to compound **8**. For other samples, six or seven resonances assignable to the compound were observed.

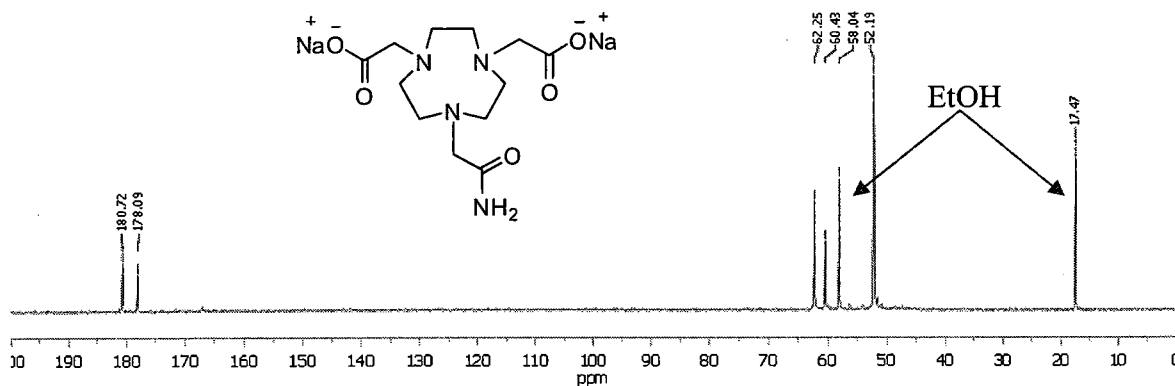


Figure 2.13: $^{13}\text{C}\{^1\text{H}\}$ NMR spectrum (D_2O , 100.51 MHz) of **8,**

EtOH set to 17.47 ppm

After complete hydrolysis of compound **7**, the solvent was evaporated and the residue was re-dissolved in D_2O , its ^1H and $^{13}\text{C}\{^1\text{H}\}$ NMR spectra confirm the expected disappearance of the ethanol and shows resonances assigned to compound **8** (Figure 2.14).

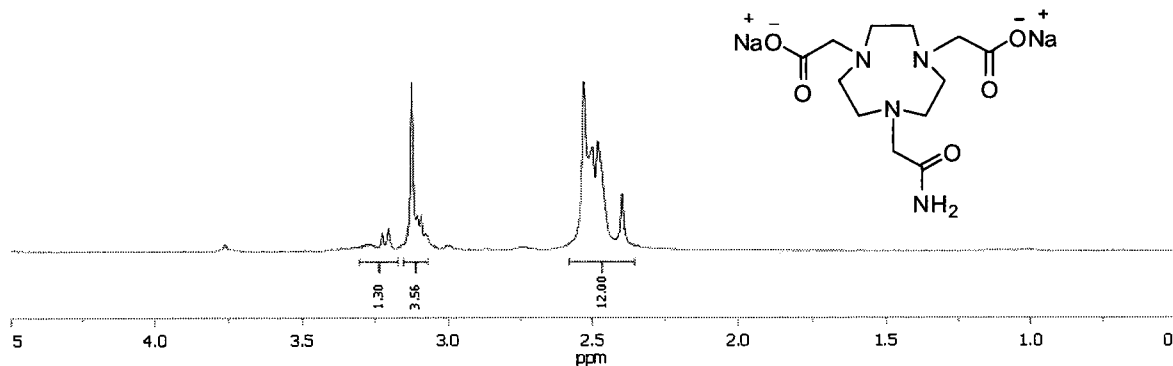


Figure 2.14: ^1H NMR spectrum (D_2O , 400 MHz) of **8 after EtOH evaporation,**

residual solvent peak set to 4.79 ppm

The displayed ^1H NMR presents three major resonances with relative integrations of 12, 3.6 and 1.3. In the $^{13}\text{C}\{^1\text{H}\}$ NMR spectrum, (Figure 2.15) nine distinct carbon

resonances are observed. Unfortunately, no internal reference for the NMR spectra was used; therefore chemical shifts are not very accurate. The obtained spectra allow for several interpretations about what is possibly happening. These include possible protonation at one or two sites of the molecule and therefore a potential hydrogen bonding with the carboxylate oxygens as previously seen in NOTA and TACN diacetate (**11**).^{1,64,65} Partial hydrolysis of the amide group to a carboxylate group can result in a mixture of **8** and NOTA trianion. Amide rotation may be slow enough on the NMR scale to differentiate both acetates. Also, a likely deuterium exchange at methylene pendant arm protons could explain the observed smaller relative integrations.

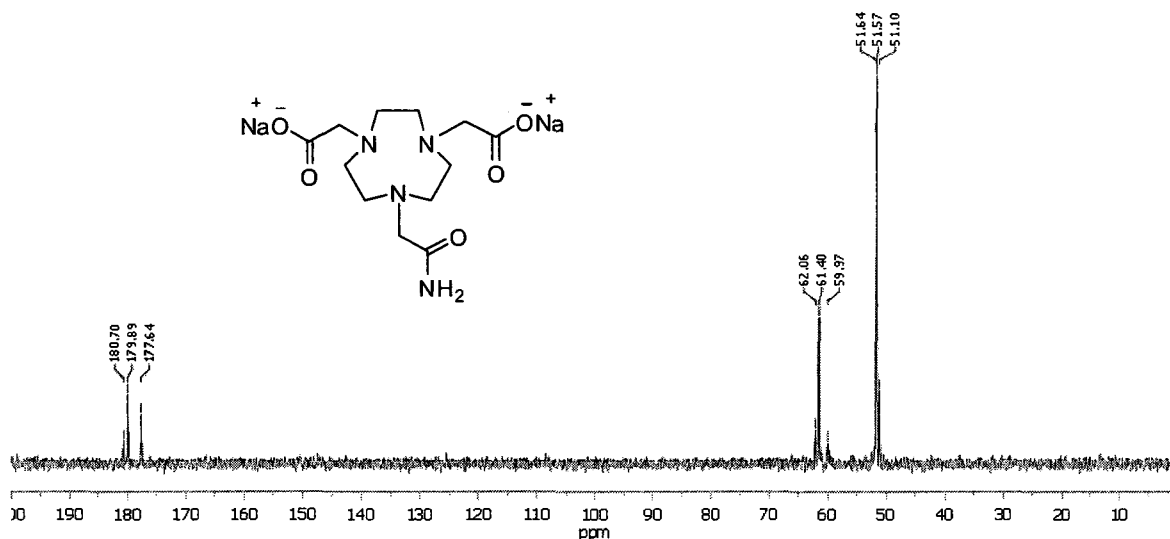


Figure 2.15: $^{13}\text{C}\{^1\text{H}\}$ NMR spectrum (D_2O , 100.51 MHz) of **8** after EtOH evaporation

In the ATR-IR spectrum (**Figure 2.16**), three assignable bands are observed at 3300, 2807, and 1583 cm^{-1} which correspond to O-H, C-H, and carboxylate stretches respectively.

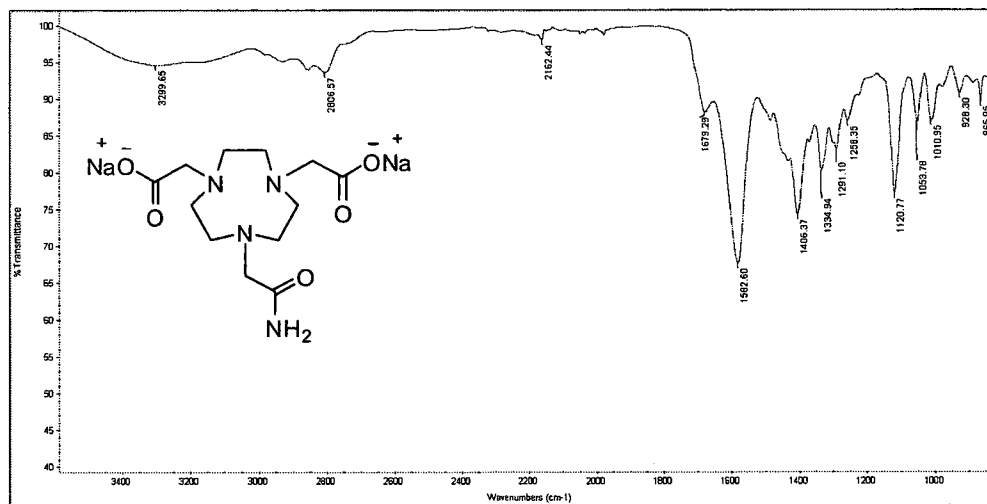
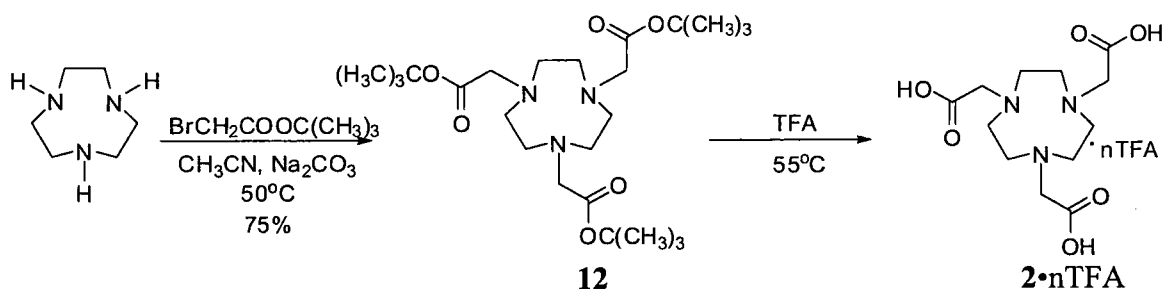


Figure 2.16: ATR-IR spectrum of 8

For additional characterization data, two samples of **8** were sent for ESI-TOF mass spectrometry analysis. However, the major species observed were not in accordance with compound **8**.

2.2.5 Synthesis of NOTA (2)

The synthesis of NOTA was performed following a modified approach by Sherry from that reported by Wiegardt described in Chapter I.^{26,66} NOTA was prepared from the tri-substituted tert-butyl acetate TACN intermediate and subsequent deprotection of the tert-butyl ester groups with trifluoroacetic acid (TFA) gave the TFA salt of NOTA. The tri-substituted intermediate is formed by reacting TACN with three equivalents of tert-butyl bromoacetate followed by regular base work up to give the tri-tert-butyl acetate TACN (**12**) as an oil.



Scheme 2.6: Synthesis of NOTA

2.3 Summary and discussion

This chapter described an efficient route to incorporate different functional groups into the macrocycle TACN. Compound **7** was selectively prepared through a five-step route from TACN. This was accomplished by the addition of a protecting group (1-formyl) onto one ring nitrogen followed by the alkylation of the other two nitrogens with two ethyl ester groups to form intermediate **5**. Hydrolysis of the 1-formyl protecting group of compound **5** led to the formation of intermediate **6**. Finally, incorporation of an acetamido group into at the available nitrogen gave **7**. This compound has been fully characterized through ^1H and $^{13}\text{C}\{\text{H}\}$ NMR, IR, and ESI MS spectroscopy. NMR spectra confirm the expected C_{2v} symmetry for the molecule. Presence of water provides a broad peak in the $3100\text{-}3400\text{ cm}^{-1}$ region of the neat IR spectrum obscuring the NH bands. Characteristic IR bands corresponding to CH_2 and carbonyl stretches contributed to the characterization of **7**.

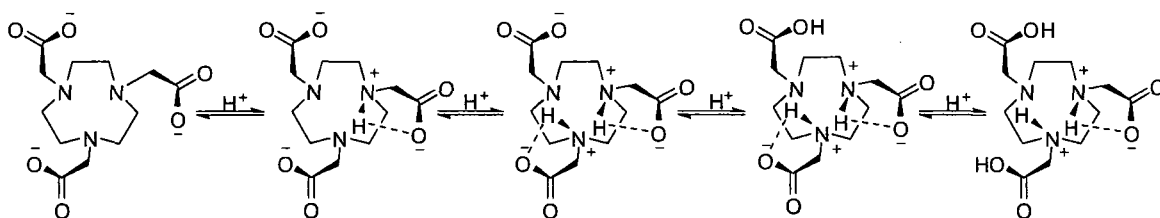
The previously-reported intermediates **5** and **6** were prepared and confirmed by ^1H and/or $^{13}\text{C}\{\text{H}\}$ NMR spectroscopy and additional characterization data including IR, ESI MS, and elemental analysis.

A sodium salt of compound **8** was prepared by combining **7** with aqueous NaOD. However, its ^1H and $^{13}\text{C}\{^1\text{H}\}$ NMR spectra were irreproducible. To account for this irreproducibility, it is proposed that additional species are due to hydrogen bonding with various protonated ring nitrogens as was observed for other TACN-acetate compounds **2** and **11**.^{64,65}

Geraldes and others demonstrated that at high pH (Table 2.01) NOTA exhibits two protonated amine groups, and as a consequence hydrogen bond formation is possible between two protonated nitrogens and the two adjacent nonprotonated carboxylates as illustrated in Scheme 2.7. The protonation sequence is followed by the protonation of the carboxylate groups, leaving the third amine nitrogen to be protonated last only at very low pH.^{1,33,64}

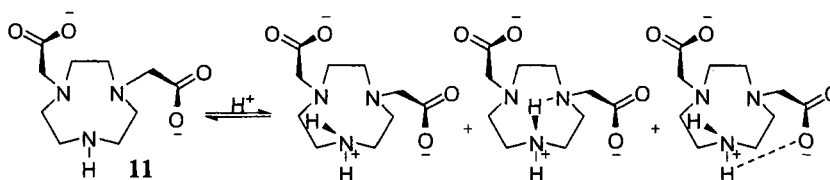
	2 ($\text{I}=1\text{M KCl}$)	11 ($\text{I}=0.1\text{M KCl}$)
$\log K_1^H$	11.96[11.3]	11.82[12.05]
$\log K_2^H$	5.66[5.59]	6.70[6.85]
$\log K_3^H$	3.37[2.88]	2.87[3.3]
$\log K_4^H$	1.71	1.02[1.6]

Table 2.01: Protonation constants of NOTA (2) and TACN-diacetate (11), values in square brackets were determined from ^1H NMR titration^{33,64,65}



Scheme 2.7: Suggested protonation sequence of NOTA

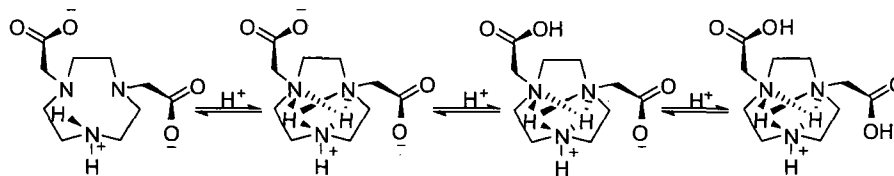
For compound **11**, Lazar et al. concluded that when compound **11** is protonated stepwise, the first proton is localized on the secondary amino group the majority of the time and this is shared with the two carboxylates and the other two nitrogens (**Scheme 2.8**). Lazar et al. also stated that the carboxylate groups have a significant contribution in the first protonation step and their relative high protonation ratio indicates hydrogen bonding between a carboxylate and the protonated nitrogen atom.⁶⁵ In **Scheme 2.8**, the illustrated hydrogen bonding is just a possibility, but it was not determined whether hydrogen bonds were of intramolecular or intermolecular nature. The protonation constants of **11** are shown in **Table 2.01**.⁶⁵



Scheme 2.8: Suggested first protonation site of 11

Introduction of the second proton changes significantly the hydrogen bonding arrangement. As a result the two protons end up evenly shared by the three ring nitrogens. This is associated with possible conformational changes that lead to the weakening of the hydrogen bonding between the carboxylates and the ring nitrogen

protons. Finally, the third and the fourth protons add to the carboxylate groups with an increase of proton density on the tertiary amino groups. (Scheme 2.9).⁶⁵



Scheme 2.9: Suggested second, third and fourth protonation sites of 11

It is likely that compound **8** can undergo similar protonation steps as the described for NOTA. Therefore even at high pH, at least one amine may be protonated leading to hydrogen bonding and conformational changes of **8**. The major difference in the structure of **8** compared to NOTA is the presence of an amide group instead of an acetate group, thus it is likely that at low pH the carbonyl oxygen of the amide group gets protonated and cause a hydrolysis. This and other hypothesis can be used to provide significant support and explanation for the observed variable spectra of the compound. However, more experiments are required in order to corroborate or disprove them.

Although, mass spectrometry did not correlate to possible species of compound **8** and no definite NMR data have been obtained to prove the formation of pure compound **8**, its copper (II) complex has been isolated and fully characterized. The coordination chemistry of **8** and its precursors will be discussed in Chapter III.

2.4 Future Work

The structural behavior of compound **8** in solution is not well understood. It is therefore necessary to further investigate this to a complete understanding and full characterization of this compound. Potentiometric and NMR studies can be use to

provide the protonation scheme of compound **8** and an explanation to the changeable NMR.

Temperature variable NMR studies may provide additional information regarding to the amide rotation, however hydrolysis of amide group would be very likely to take place at high temperature and something that it should be considered.

Further characterization for compound **8** including elemental analysis and mass spectrometry remains to be made.

CHAPTER III

COPPER (II) COORDINATION OF N-FUNCTIONALIZED 1, 4, 7- TRIAZACYCLONONANES

3.1 Introduction

As mentioned in Chapters 1 and 2, radioisotopes of copper have become increasingly important in radio-imaging techniques because copper offers a selection of several nuclides with a broad range of nuclear properties for both diagnostic and therapeutic purposes. In order to prepare radio-copper carriers, it is essential that ligands satisfy copper's coordination chemistry, forming stable complexes that will survive *in vivo* redox reactions and demetallations.

Normally, copper can exist in three different oxidation states of (3+)d⁸, (2+)d⁹, and (1+)d¹⁰. Copper in the oxidation states I and II is typically found in most biological environments. Cu(II) is a borderline acid and favors borderline bases such as nitrogen and chloride. In contrast, Cu(I) prefers softer sulfur-based ligands.⁶⁷ However, copper(II) is the oxidation state with the most common aqueous chemistry. The most observed coordination numbers for copper(II) are 4, 5, and 6 and it can adopt square planar, square pyramidal/trigonal bipyramidal, as well as tetragonal geometries. Copper(I) ion is often found in a pseudo-tetrahedral geometry, but, its coordination number varies a lot. Copper(III) is relatively uncommon and difficult to obtain. Copper complexes in this

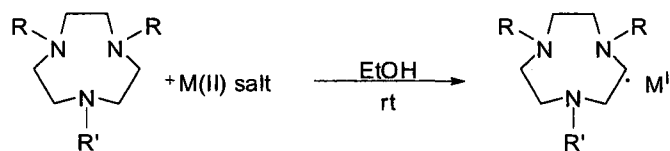
oxidation state usually adopt a square planar geometry.⁶⁸ Since copper (II) is more stable and easier to manipulate, it is therefore the oxidation state used in the design of radiopharmaceuticals.

Zinc is a constituent of many enzymes which are present in several metabolic processes and is therefore essential for life.⁶⁷ The predominant and almost invariant oxidation state of Zn is 2+ and it is the form found in all living systems. Similar to Cu(II), Zn(II) is a borderline acid which forms stable complexes with a variety of donor ligands including oxygen, nitrogen, sulfur, and halogen donors. An assortment of high and low coordination numbers and various stereochemistries are found in Zn(II) complexes, however 4-coordinate tetrahedral geometry seems to be favored biologically.⁶⁸

In this chapter the coordination chemistry of Cu(II) and Zn(II) with *N*-functionalized pendant arms TACN ligands containing *O*- and *N*-donors will be described.

3.2 Synthesis and Characterization of Copper (II) Complexes

Copper complexes of ligands 4, 5, 6, and 7 were prepared following a general procedure. This is illustrated in **Scheme 3.1**



Scheme 3.1: General protocol for M (II) complexation with ligands 4, 5, 6, and 7

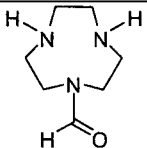
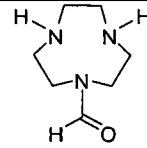
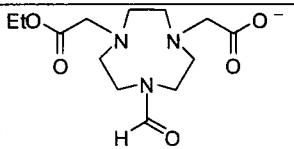
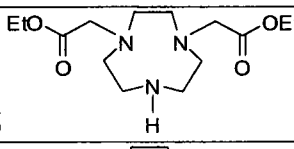
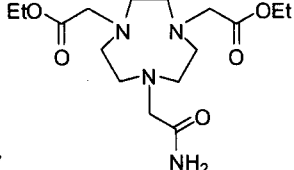
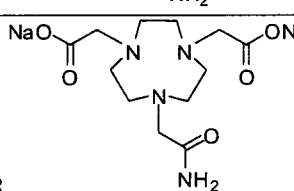
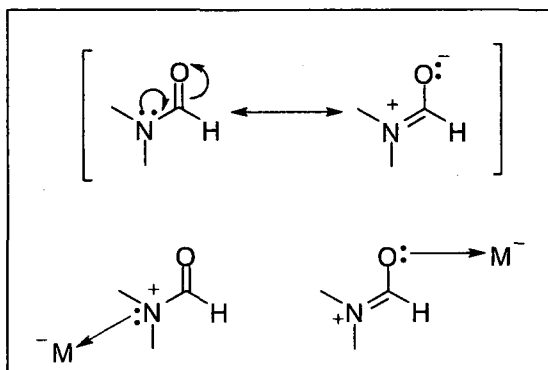
M(II) salt	Ligand	Complex
$\text{Cu}(\text{NO}_3)_2$	 4	$\text{Cu}(\text{NO}_3)_2 \cdot 4$ (13)
$\text{Zn}(\text{NO}_3)_2$	 4	$\text{Zn}(\text{NO}_3)_2 \cdot 4$ (14)
CuCl_2	 9	$\text{Cu}(\text{II})\text{Cl} \cdot 9$ (15)
CuCl_2	 6	$\text{CuCl}_2 \cdot 6$ (16)
CuCl_2	 7	$[\text{CuCl} \cdot 7]_3$ (17)
CuCl_2	 8	$\text{Cu} \cdot 8$ (18)

Table 3.01: List of ligands and metal complexes

The general complexation procedure consisted of dissolving the ligand and the metal (II) salts in absolute ethanol, followed by their combination and stirring overnight at room temperature.

3.2.1 Copper and Zinc Complexes of 1-formyl-1, 4, 7-triazacyclononane (4)

Our interest in the coordination chemistry of **4** was piqued by the presence of a tertiary amide. Metal complexes containing *N*-coordinated tertiary amides are rare and very few well-characterized examples have been reported to date.⁶⁹⁻⁷⁴ Typically, amide groups bind the metal through their carbonyl oxygen given that amides are resonance delocalized and *N*-coordination precludes such resonance (**Scheme 3.2**).^{69,75}



Scheme 3.2: Delocalization of nitrogen's lone pair into a π system leads to favorable binding at the more basic carbonyl oxygen

Copper (II) complex formation with ligand **4** was observed by the appearance of an instant precipitate when the ligand and the copper nitrate solutions were combined. This precipitate was collected and dried to give **13** as a lilac-blue solid in very good yield. Several attempts to obtain X-ray quality crystals for compound **13** were unsuccessful.

The neat infrared spectrum of **13** (**Figure 3.01**) shows the characteristic NH and C=O stretches at 3305 cm^{-1} and 1676 cm^{-1} respectively. The carbonyl peak of the complex has shifted to higher energy with respect to the free ligand value of 1641 cm^{-1} . This suggests a possible interaction of the amide nitrogen with the metal center. It is known that delocalization of the lone pair of the nitrogen of amides leads to the

resonance form illustrated in **Scheme 3.2**. Nitrogen metal coordination would decrease that delocalization, thus the double bond character between carbon oxygen should increase as a result.

Other observed bands at 1469 and 1286 cm^{-1} suggest a coordinated nitrate.⁷⁶ The UV-Vis spectrum of **13** displays an absorption maximum at 661 nm and a molar absorptivity of 46 $\text{M}^{-1}\text{cm}^{-1}$, which is similar to other copper complexes of TACN **1**.⁷⁷ The elemental analyses confirm the formula $\text{CuC}_7\text{H}_{15}\text{N}_5\text{O}_7$ which constitutes a ratio of 2:1:1 (nitrate: ligand: metal).

It was interesting to see a solid-state reaction of **13** in the KBr pellet. A color change was observed a few hours after making the pellet as the coordinated nitrate peaks disappeared from the IR spectrum. **Figure 3.02** illustrates these changes in the IR (KBr) spectrum of **13** over time. The bromide ion is likely substituting for the coordinated nitrates. This is in accord with literature reports that the nitrate ion is generally considered to be a weak ligand.⁷⁷ By contrast, attenuated total reflectance infrared (ATR-IR) spectra of **13** did not change over time.

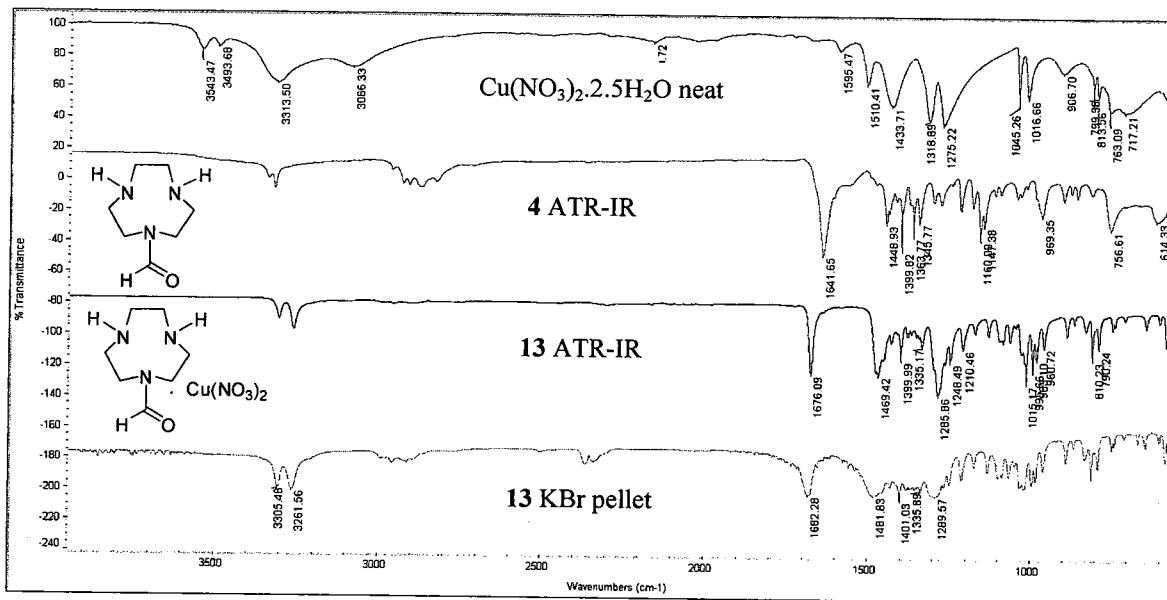
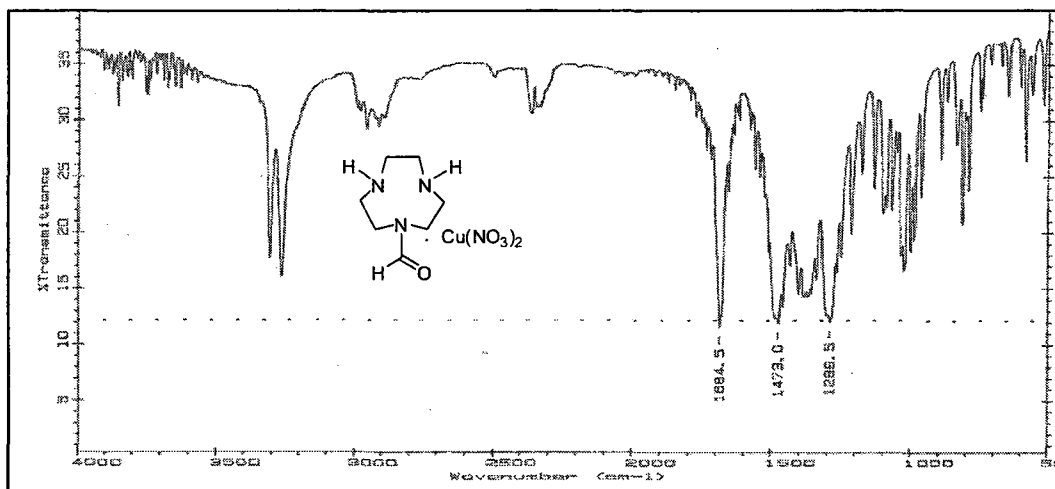
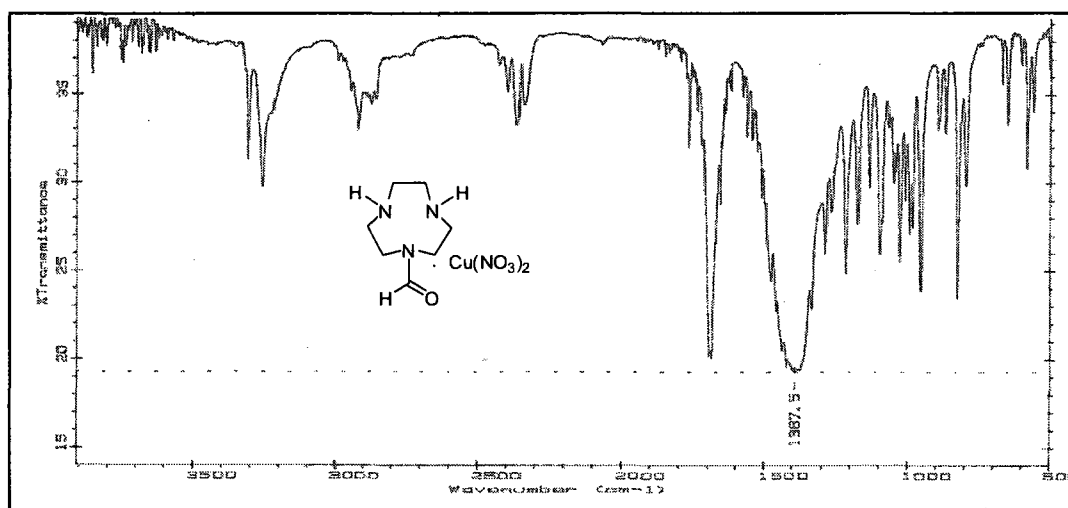


Figure 3.01: Comparison IR spectra for copper nitrate, ligand 4, and complex 13



Time: 0 hours



Time: 24 hours

Figure 3.02: Changes in the IR(KBr) spectrum of complex 13

Compound **14**, a $\text{Zn}(\text{NO}_3)_2$ complex of ligand **4**, was obtained in 27% yield. This complex is a white solid that seems to decompose readily over time, color changes of complex **14** were observed from white to yellowish. Characterization of data of **14** such as ATR-IR, ^1H NMR, and X-ray crystallography provides good evidence of amide nitrogen metal interaction. In the IR the ν_{CO} amide stretch of **14** was observed at 1656

cm^{-1} , this is shifted slightly towards higher energy from that of the free ligand value of 1641 cm^{-1} . Coordinated nitrate bands are seen at 1464 and 1290 cm^{-1} . A KBr pellet of **14** showed a different IR spectrum compared to its neat spectrum since non-coordinated nitrate peaks are seen as soon as the KBr pellet was made (**Figure 3.03**). Presumably, a solid state reaction occurred similar to that observed for complex **13**.

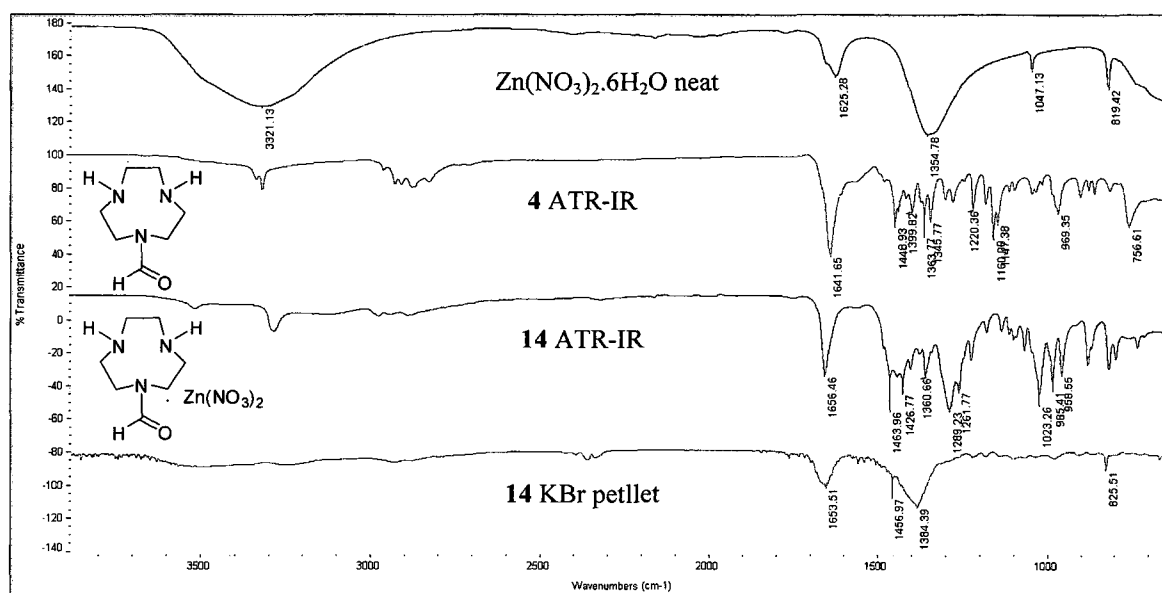


Figure 3.03: Comparison IR spectra for zinc nitrate, ligand 4, and complex 14

Since complex **14** was insoluble in all organic solvents and just slightly soluble in water $^{13}\text{C}\{^1\text{H}\}$ NMR was not well resolved and only good proton NMR data was obtained (**Figure 3.04**). This spectrum reveals six multiplets at δ 2.90-2.95, δ 3.04-3.09, δ 3.12-3.17, δ 3.24-3.29, δ 3.50-3.54, and δ 3.57-3.62 and a singlet at δ 8.14. This is important since the time-averaged C_s symmetry indicates that amide rotation is fast on the NMR time confirming an amide N-coordination. In addition, single-crystal X-ray crystallographic data of a crystalline sample corroborated the amide N-metal interaction

and the formation of compound **14** despite the fact that its elemental analysis did not provide useful characterization data.

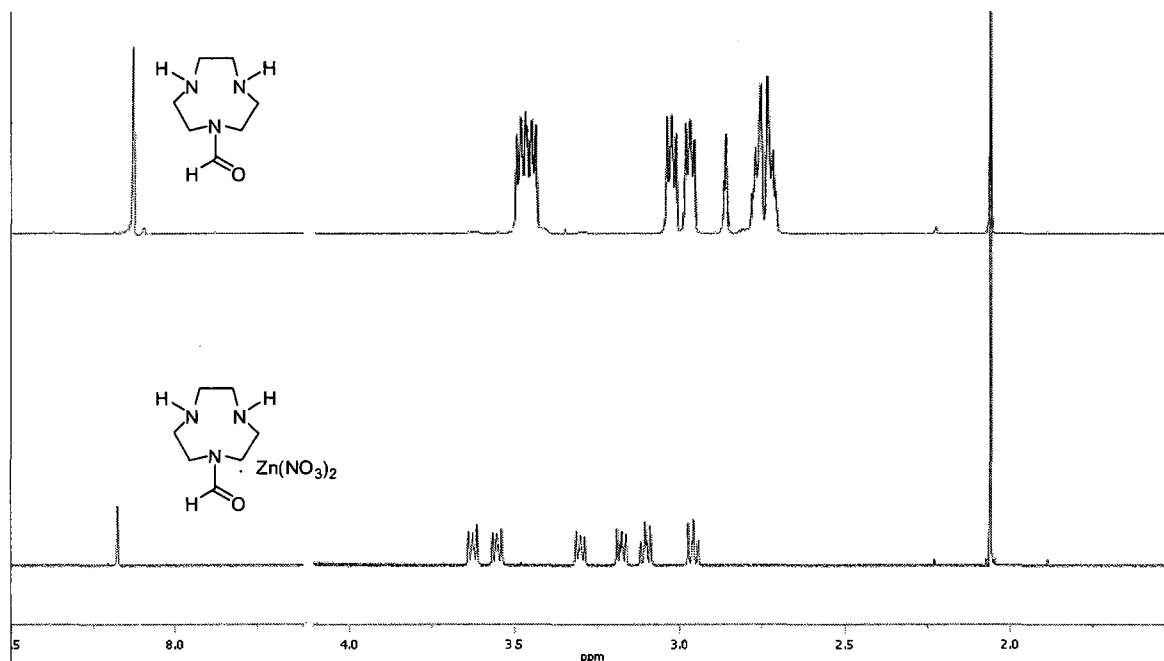


Figure 3.04: ^1H NMR spectrum (D_2O , 500 MHz) of **4** and **14**, CH_3CN set to 2.06

The coordination chemistry around the metal center of **14** can be described as a distorted octahedral geometry. Its X-ray structure (**Figure 3.05**), shows two nitrogen donors from the medium sized ring strongly coordinated to the metal; three other Zn coordination sites are occupied by two nitrate groups, and an ethanol molecule. Most interestingly, zinc cation shows an additional interaction with the nitrogen N(4) of the tertiary amide at a Zn(1)-N(4) distance of 2.795(1) Å completing the sixth coordination site. This interaction allows for deviations from planarity of the tertiary amide function, thus the nitrogen atom N(4) is no longer truly sp^2 hybridized and the sum of the C-N(4)-C angles add up to 355°. Important bond lengths and bond angles are summarized in (**Table 3.02**).

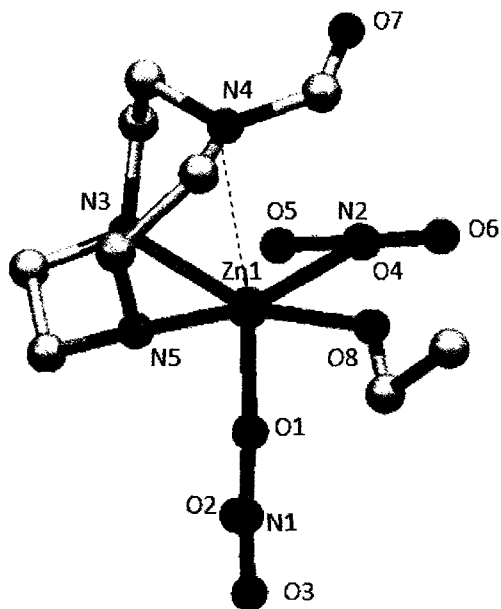


Figure 3.05: X-ray structure of complex 14

Zn(1)-O(1)	2.073(1)	Zn(1)-O(8)	2.066(2)	Zn(1)-N(5)	2.123(1)
Zn(1)-O(4)	2.093(1)	Zn(1)-N(3)	2.102(2)	Zn(1)-N(4)	2.795(1)
O(1)-Zn(1)-O(4)	90.12(5)	O(4)-Zn(1)-O(8)	79.21(5)	O(8)-Zn(1)-N(5)	96.03(5)
O(1)-Zn(1)-O(8)	104.39(5)	O(4)-Zn(1)-N(3)	96.05(5)	N(3)-Zn(1)-N(5)	81.53(5)
O(1)-Zn(1)-N(3)	97.82(5)	O(4)-Zn(1)-N(5)	161.82(5)		_____
O(1)-Zn(1)-N(5)	108.06(5)	O(8)-Zn(1)-N(3)	157.25(5)		_____

*esd in parentheses. Refer to the end of section 3.2 for additional crystallographic data.

Table 3.02: Selected bond lengths (Å) and angles (°) for complex 14

3.2.2 Copper Complex of Ligand 9



The coordination chemistry of compound **5** is also of interest due to the presence of a ring tertiary amide as well as ester pendant arms. Complex **15** was formed by the procedure described in **Scheme 3.1**, whereby ethanolic solutions of copper chloride and ligand **5** were combined forming a homogenous green solution. After the solvent was evaporated, the crude material was dissolved in methanol and precipitated with ethyl acetate. X-ray quality blue crystals were grown by layering ethyl acetate onto a MeOH solution of the complex. Ligand **5** is in this case hydrolyzed at some point during the complexation or recrystallization procedure. Characterization data, such as ATR-IR spectroscopy and X-ray crystallography, provided evidence for the formation of complex **15**. Its structure, which is displayed in **Figure 3.07**, reveals that one of the ester arms of ligand **5** has been hydrolyzed. The most likely cause of this hydrolysis is the presence of water. It is important to mention that similar ester hydrolysis has also been observed with previously described compound **6**.

The IR spectrum of this complex (**Figure 3.06**) shows four bands at 1734, 1714, 1669, and 1646 cm^{-1} characteristic of carbonyl and carboxylate stretches in accordance with the ester, acetate, and probably two amide rotamers. The elemental analyses match best the molecular formula $\text{CuC}_{13}\text{H}_{22}\text{N}_3\text{O}_5\text{Cl}$ (NaCl) ($1.3 \text{ CH}_3\text{CH}_2\text{OH}$) which correspond to compound **15**. The electronic spectrum of **15** in water shows an absorption maximum at 666 nm with a molar absorptivity of $\epsilon = 69 \text{ M}^{-1}\text{cm}^{-1}$.

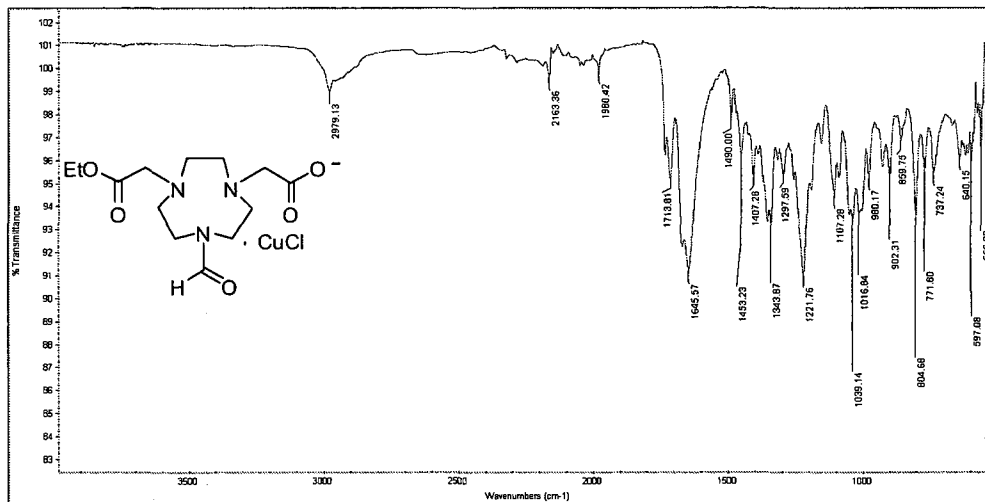


Figure 3.06: ATR-IR spectrum of 15

The X-ray structure of **15** is displayed in **Figure 3.07** and selected bond lengths and angles are listed in **Table 3.03**. The coordination mode of this complex is categorized by five different types of donor atoms illustrating a very distorted arrangement, therefore it was difficult to assign a definite geometry. The interactions with the copper center are defined by one acetate oxygen, one chloride and two nitrogen atoms from the medium sized ring with an average distance of 2.075 Å. In addition, an ester carbonyl oxygen O(2) and a tertiary amide nitrogen N(3) are weakly interacting with this metal center with distances of Cu(1)-O(2) and Cu(1)-N(3) of 2.618(4) Å and 2.609(4) Å respectively. The interaction of the amide nitrogen with the metal center affects the structure around this nitrogen causing a small pyramidalization. This distortion is similar to the described for the amide nitrogen of compound **14** with the sum of the C-N(3)-C angles also equal to 355°. Moreover, compound **15** shows a slightly longer bond length of the N(3)-C(formyl) with a distance of 1.366 Å in comparison to the N(3)-C(formyl) bond of the ligand with a

value of 1.335 Å. Orientation of pendant arms described a type II mode, forming two five-member chelate rings.

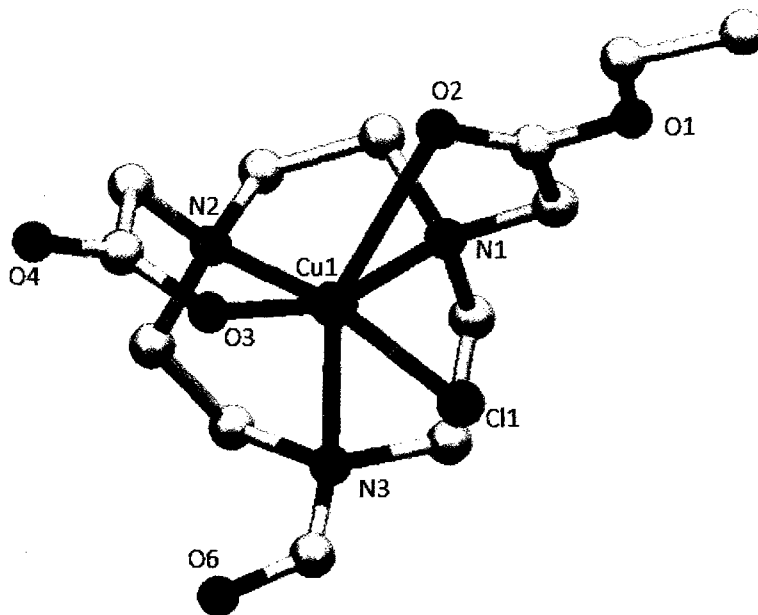


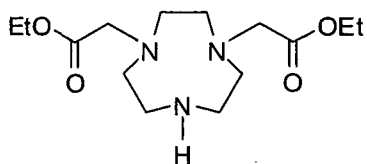
Figure 3.07: X-ray structure of complex 15

Cu(1)-Cl(1)	2.261(1)	Cu(1)-O(2)	2.618(4)	Cu(1)-O(3)	1.939(4)
Cu(1)-N(1)	2.060(4)	Cu(1)-N(2)	2.041(4)	Cu(1)-N(3)	2.609(4)
Cl(1)-Cu(1)-O(2)	83.5(1)	O(2)-Cu(1)-O(3)	96.8(1)	O(3)-Cu(1)-N(2)	84.2(2)
Cl(1)-Cu(1)-O(3)	95.5(1)	O(2)-Cu(1)-N(1)	71.8(1)	O(3)-Cu(1)-N(3)	113.9(1)
Cl(1)-Cu(1)-N(1)	99.6(1)	O(2)-Cu(1)-N(2)	107.7(2)	N(1)-Cu(1)-N(2)	83.6(2)
Cl(1)-Cu(1)-N(2)	168.8(1)	O(2)-Cu(1)-N(3)	149.3(1)	N(1)-Cu(1)-N(3)	79.5(1)
Cl(1)-Cu(1)-N(3)	91.0(1)	O(3)-Cu(1)-N(1)	159.7(2)	N(2)-Cu(1)-N(3)	79.0(2)

*esd in parentheses. Refer to the end of section 3.2 for additional crystallographic data.

Table 3.03: Selected bond lengths (Å) and angles (°) for complex 15

3.2.3 Copper Complex of Ligand 6



The coordination chemistry of ligand **6** is of interest for its five potential donor sites for coordination with metal ions. Pentadentate ligands of this class are currently of interest since they can be used to anchor mononuclear octahedral complexes that have a single open coordination site for binding and activation of small molecules.⁷⁸

The synthesis of complex **16** from **6** was carried out similarly as the complexes described above (**Scheme 3.1**). This complex was characterized by elemental analysis, IR and UV-vis spectra and X-ray crystallography. The maximum absorption in the visible region of the electronic spectrum is observed at 694 nm. Elemental analysis of this product confirmed the formula $\text{CuC}_{14}\text{H}_{27}\text{N}_3\text{O}_4\text{Cl}_2(0.5\text{H}_2\text{O})$.

In its IR spectrum, a sharp and strong band appeared at 1732 cm^{-1} , this is consistent with typical ester carbonyl stretches. Thus despite presence of both coordinated and uncoordinated esters in the X-ray structure (**Figure 3.08**), only one resolved carbonyl peak was seen. This is likely the result of a weak interaction of the O(1)-Cu(1), which has a distance of 2.743 \AA , and does not really affect the ester carbonyl stretches. The bond distances for the C=O of the uncoordinated and coordinated esters are 1.205 \AA and 1.220 \AA respectively.

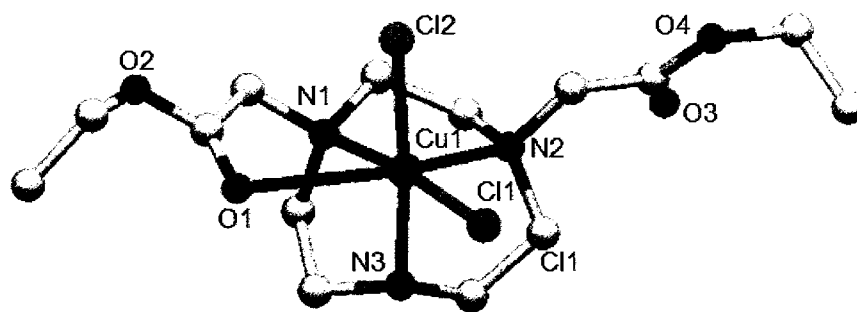


Figure 3.08: View of the X-ray structure of complex **16**

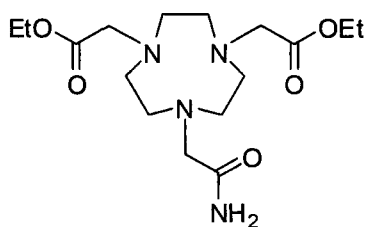
Blue rhombic plates of X-ray quality were grown by slow cooling of a hot solution of **16** in ethanol. The structure of the complex consists of monomeric, neutral molecules of Cu-6 (**Figure 3.08**). The copper ion is coordinated by just four atoms of the pentadentate ligand. Three nitrogens occupy one facial position of a distorted octahedron and the other face is occupied by an oxygen atom from one pendant arm and two chlorides. The Jahn-Teller distortion in this complex is evident by the elongation of one of the axial bonds with a very long distance Cu(1)-O(1) of 2.743(2) Å and Cu(1)-N(2) bond of 2.308(2) Å. Compression of the *trans* angles to less than the ideal angle (180)° are observed for Cl(1)-Cu(1)-N(1), Cl(2)-Cu(1)-N(3), N(2)-Cu(1)-O(1) which are 173.16(7), 174.26(7), 151.83(7) respectively. Other bond distances and bond angles are summarized in **Table 3.04**.

Cl(1)-Cu(1)	2.315(1)	Cl(2)-Cu(1)	2.300(1)	Cu(1)-N(1)	2.115(2)
Cu(1)-N(2)	2.308(2)	Cu(1)-N(3)	2.051(3)	Cu(1)-O(1)	2.743(2)
Cl(1)-Cu(1)-Cl(2)	94.07(3)	Cl(2)-Cu(1)-N(1)	91.32(7)	N(1)-Cu(1)-N(3)	83.37(9)
Cl(1)-Cu(1)-N(1)	73.16(7)	Cl(2)-Cu(1)-N(2)	99.69(6)	N(1)-Cu(1)-O(1)	69.95(8)
Cl(1)-Cu(1)-N(2)	100.86(6)	Cl(2)-Cu(1)-N(3)	174.26(7)	N(2)-Cu(1)-N(3)	81.82(9)
Cl(1)-Cu(1)-N(3)	91.07(7)	Cl(2)-Cu(1)-O(1)	86.29(5)	N(2)-Cu(1)-O(1)	151.83(7)
Cl(1)-Cu(1)-O(1)	106.18(5)	N(1)-Cu(1)-N(2)	82.34(9)	N(3)-Cu(1)-O(1)	89.82(8)

*esd in parentheses. Refer to the end of section 3.2 for additional crystallographic data.

Table 3.04: Selected bond lengths (Å) and angles (°) for complex 16

3.2.4 Copper Complex of Ligand 7



Complex **17** was obtained by the reaction of **7** with copper chloride as in **Scheme 3.1**. This complex was characterized spectroscopically and structurally. The electronic spectra of **17** in aqueous solution shows a maximum at 716 nm with a molar absorptivity $\epsilon = 57 \text{ M}^{-1} \text{ cm}^{-1}$. Its solid state IR spectrum displays three carbonyl stretches assignable to both uncoordinated and coordinated esters at 1738 and 1723 cm^{-1} respectively and one amide carbonyl at 1660 cm^{-1} . Its elemental analysis corresponds to the empirical formula $\text{CuC}_{16}\text{H}_{30}\text{N}_4\text{O}_5\text{Cl}_2 (0.3\text{NaCl})(0.7\text{H}_2\text{O})$.

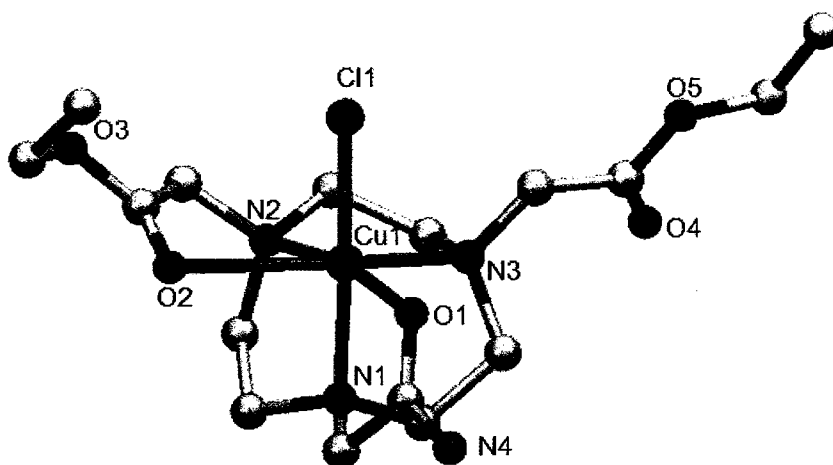
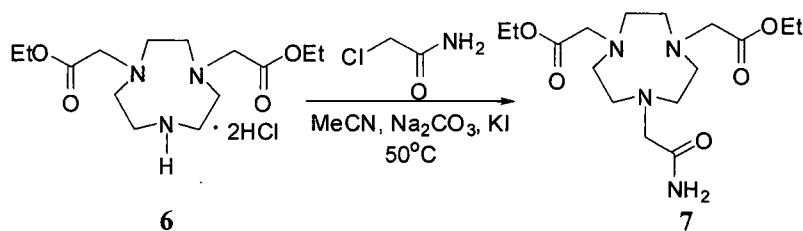


Figure 3.09: X-ray structure of complex 17

The X-ray structure of **17** consists of the complex cation $[\text{CuCl-7}]^+$ (**Figure 3.09**), an uncomplexed triiodide ion, and a molecule of ethanol. Triiodide ion is not a reagent in the complexation reaction; however potassium iodide is part of the reagents in the ligand synthesis. Therefore, the most likely reason for the presence of triiodide ion is that traces of KI were present in the ligand solution used. Iodide can be easily air oxidized to I_2 to give I_3 . Compound **17** was prepared using the crude material of the ligand synthesis shown in **Scheme 3.3**. Note that synthesis of compound **7** was reported in Chapter 2 and it is slightly different than the synthesis in **Scheme 3.3**.



Scheme 3.3: Synthesis compound 7

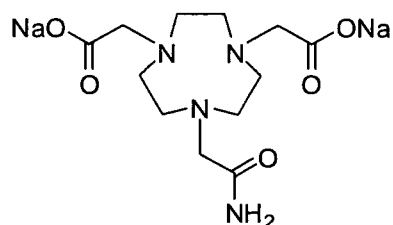
Ligand **7** contains six potential donor atoms for complexation with metals ions, however only five are coordinated to the copper center in complex **17**. Its coordination is defined by the N₃O₂Cl sphere, where three nitrogens occupy one face of a distorted octahedron while the other face is occupied by two ester carbonyl oxygens, and a chloride. The Jahn-Teller elongated Cu(1)-O(2) bond length of 2.566(6) Å and Cu(1)-N(3) distance of 2.265(7)Å as well as non-ideal Cl(1)-Cu(1)-N(1), N(3)-Cu(1)-O(2), N(2)-Cu(1)-O(1) *trans* angles of 173.8(2), 155.5(2), 166.9(2)° respectively are observed. Additional structural data for the complex are listed in **Table 3.05**.

Cl(1)-Cu(1)	2.258(1)	Cu(1)-N(1)	2.043(5)	Cu(1)-N(2)	2.072(5)
Cu(1)-N(3)	2.265(7)	Cu(1)-O(1)	2.004(4)	Cu(1)-O(2)	2.566(6)
Cl(1)-Cu(1)-N(1)	73.8(2)	N(1)-Cu(1)-N(2)	85.1(2)	N(2)-Cu(1)-O(1)	166.9(2)
Cl(1)-Cu(1)-N(2)	98.9(2)	N(1)-Cu(1)-N(3)	83.9(2)	N(2)-Cu(1)-O(2)	72.4(2)
Cl(1)-Cu(1)-N(3)	101.2(1)	N(1)-Cu(1)-O(1)	82.4(2)	N(3)-Cu(1)-O(1)	99.0(2)
Cl(1)-Cu(1)-O(1)	93.3(1)	N(1)-Cu(1)-O(2)	90.7(2)	N(3)-Cu(1)-O(2)	155.5(2)
Cl(1)-Cu(1)-O(2)	86.1(1)	N(2)-Cu(1)-N(3)	83.3(2)	O(1)-Cu(1)-O(2)	104.0(2)

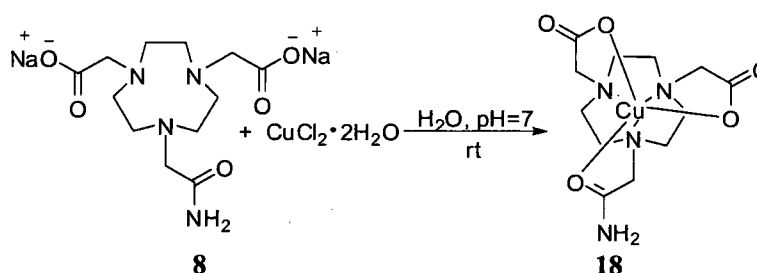
*esd in parentheses. Refer to the end of section 3.2 for additional crystallographic data.

Table 3.05: Selected bond lengths (Å) and angles (°) for complex 17

3.2.5 Copper Complex of Ligand 8



The synthesis of compound **18** is shown in **Scheme 3.4**. An aqueous solution of ligand **8** at pH 7 was combined with an aqueous solution of $\text{CuCl}_2 \cdot 2\text{H}_2\text{O}$ and the reaction mixture readjusted to pH 7. This homogeneous solution was stirred at room temperature overnight under nitrogen atmosphere. At this point, water was evaporated and the residual blue crystalline film was dissolved in absolute ethanol. An insoluble light-blue material was removed by centrifugation and the supernatant was evaporated to dryness to give blue crystals. The final product was recrystallized by slow cooling from ethanol and water to give cubic crystals suitable for X-ray analysis.



Scheme 3.4: Cu(II) complexation with ligand 8

In the IR spectrum of complex **18** the N-H and carbonyl stretches are displayed. The N-H stretches are shown at 3450 and 3305 cm^{-1} . The amide C=O stretch is observed at 1652 cm^{-1} , which is at a lower wavenumber than value observed for the free ligand, 1678 cm^{-1} , and it is consistent with carbonyl oxygen coordination. For the carboxylate carbonyl stretches the free ligand is 1583 cm^{-1} while for the complex is 1605 cm^{-1} . Its

maximum absorption in aqueous solution is observed at 719 nm with a molar absorptivity of $\epsilon = 68 \text{ M}^{-1} \text{ cm}^{-1}$.

The X-ray crystal structure of Cu-8 shows an intermediate geometry between distorted octahedral and trigonal prismatic given by a twist angle of 33° (**Figure 3.10**) as compared to 27° for Cu-NOTA. Copper (II) is enveloped by all three nitrogens and three oxygens of the ligand with the acetate groups oriented counterclockwise in a type II conformation. This coordination mode is similar to that of Cu-NOTA reported by Wieghardt.²⁶

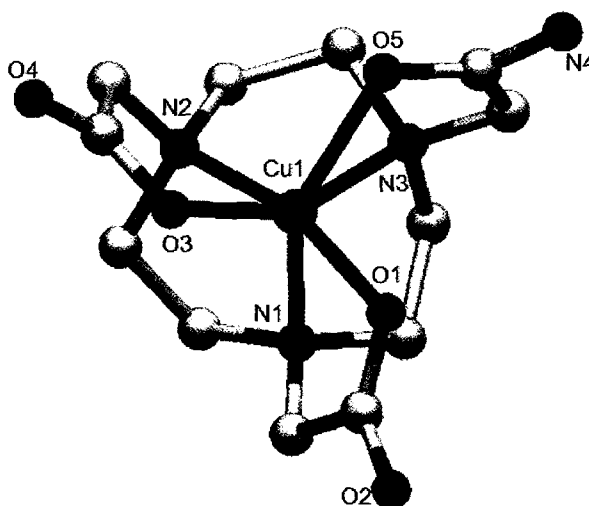


Figure 3.10: X-ray structure for complex 18

Cu-NOTA presents Cu-N bond lengths of 2.04, 2.12, and 2.20 Å as compared to 2.00, 2.12, and 2.20 Å for Cu-8. The Cu-O bond lengths are 1.98, 2.14, and 2.21 Å as compared to 1.97, 2.05, and 2.28 Å for Cu-8.

Cu(1)-O(1)	1.973(1)	Cu(1)-O(3)	2.045(1)	Cu(1)-O(5)	2.284(1)
Cu(1)-N(1)	2.122(2)	Cu(1)-N(2)	2.001(2)	Cu(1)-N(3)	2.200(2)
O(1)-Cu(1)-O(3)	93.88(6)	O(3)-Cu(1)-O(5)	91.64(5)	O(5)-Cu(1)-N(2)	107.15(6)
O(1)-Cu(1)-O(5)	88.82(5)	O(3)-Cu(1)-N(1)	117.00(6)	O(5)-Cu(1)-N(3)	73.90(6)
O(1)-Cu(1)-N(1)	81.56(6)	O(3)-Cu(1)-N(2)	82.32(6)	N(1)-Cu(1)-N(2)	85.98(7)
O(1)-Cu(1)-N(2)	163.62(6)	O(3)-Cu(1)-N(3)	155.51(6)	N(1)-Cu(1)-N(3)	81.50(6)
O(1)-Cu(1)-N(3)	105.22(6)	O(5)-Cu(1)-N(1)	150.19(6)	N(2)-Cu(1)-N(3)	83.26(6)

*esd in parentheses. Refer to the end of this section for additional crystallographic data.

Table 3.06: Selected bond lengths (Å) and angles (°) for complex 18

	Complex 14	Complex 15	Complex 16
Identification code	Complex 14	Complex 15	Complex 16
Empirical formula	C ₁₀ H ₂₅ N ₅ O _{8.50} Zn	C ₁₅ H ₂₅ Cl Cu N ₄ O ₅	C ₁₈ H ₃₄ Cl ₂ Cu N ₃ O ₄
Formula weight	416.72	440.38	490.92
Temperature	123(2) K	100(2) K	150(2) K
Wavelength	0.71073 Å	0.71073 Å	0.71073 Å
Crystal system	Triclinic	Monoclinic	Monoclinic
Space group	P-1	P2(1)/n	P2(1)/c
Unit cell dimensions			
a (Å)	7.8884(5)	7.0767(9)	12.289(7)
b (Å)	9.8961(6)	17.242(2)	14.298(8)
c (Å)	11.4324(7)	15.315(2)	12.931(7)
α (°)	68.1680(10)	90	90
β (°)	89.3730(10)	94.817(2)	102.835(7)
γ (°)	89.1390(10)	90	90
Volume (Å ³)	828.35(9)	1862.1(4)	2215(2)
Z	2	4	4
Density (calculated)	1.671 g/cm ³	1.571 Mg/m ³	1.472 Mg/m ³
Absorption coefficient	1.537 mm ⁻¹	1.350 mm ⁻¹	1.255 mm ⁻¹
F(000)	436	916	1032
Crystal size (mm ³)	0.30 x 0.27 x 0.24	0.20 x 0.15 x 0.12	0.29 x 0.16 x 0.08
Crystal color, habit		blue / block	Blue-Green Plate
Theta range for data collection	1.92 to 25.75°	1.78 to 26.53°	1.70 to 27.48°
Index ranges	-9<=h<=9, -12<=k<=12, -13<=l<=13	-8<=h<=8, 0<=k<=21, 0<=l<=19	-15<=h<=15, -17<=k<=18, -16<=l<=15
Reflections collected	9500	22,417	20498
Independent reflections	3162 [R(int) = 0.0181]	3849 [R(int) = 0.0510]	4913 [R(int) = 0.0535]
Completeness to theta = 25.00°	99.8 %	99.6 %	99.8 %
Absorption correction			
Max. and min. transmission	None	multi-scan/sadabs	Multi-scan
Refinement method	0.7093 and 0.6557	0.8547 and 0.7739	0.9030 and 0.7153
Data / restraints / parameter	Full-matrix least-squares on F ²	Full-matrix least-squares on F ²	Full-matrix least-squares on F ²
Goodness-of-fit on F ²	3162 / 0 / 235	3849 / 0 / 236	4913 / 0 / 249
Final R indices [I>2sigma(I)]	1.111	1.065	1.040
R indices (all data)	R1 = 0.0215, wR2 = 0.0564	R1 = 0.0625, wR2 = 0.1783	R1 = 0.0430, wR2 = 0.0959
Largest diff. peak and hole	R1 = 0.0224, wR2 = 0.0569	R1 = 0.0721, wR2 = 0.1842	R1 = 0.0641, wR2 = 0.1057
	0.374 and -0.588 e Å ⁻³	1.184 and -0.832 e Å ⁻³	0.630 and -0.515 e Å ⁻³

Table 3.07: Crystal data for compounds 14, 15, and 16

	Complex 17	Complex 18
Identification code	Complex 17	Complex 18
Empirical formula	C ₁₈ H ₃₆ Cl Cu I ₃ N ₄ O ₆	C ₁₂ H ₂₆ Cu N ₄ O ₈
Formula weight	884.20	417.91
Temperature	150(2) K	173(2) K
Wavelength	0.71073 Å	0.71073 Å
Crystal system	Triclinic	Monoclinic
Space group	P-1	P2(1)/n
Unit cell dimensions		
a (Å)	14.7261(10)	9.0561(7)
b (Å)	5.0430(10)	12.9139(11)
c (Å)	15.3459(11)	14.4933(11)
α (°)	77.1670(10)	90
β (°)	61.8290(10)	93.0990(10)
γ (°)	84.4100(10)	90
Volume (Å ³)	2921.8(3)	1692.5(2)
Z	4	4
Density (calculated)	2.010 Mg/m ³	1.640 g/cm ³
Absorption coefficient	4.046 mm ⁻¹	1.341 mm ⁻¹
F(000)	1700	876
Crystal size (mm ³)	0.37 x 0.35 x 0.24	0.24 x 0.22 x 0.10
Crystal color, habit	Red Block	Pale blue plate
Theta range for data collection	1.85 to 28.29°	2.11 to 25.69°
Index ranges	-19<=h<=19, -19<=k<=20, -20<=l<=19	-11<=h<=11, -15<=k<=15, -17<=l<=11
Reflections collected	33196	16761
Independent reflections	12875 [R(int) = 0.0254]	3169 [R(int) = 0.0387]
Completeness to theta = 25.00	97.9 %	98.8 %
Absorption correction	Multi-scan	Multi-scan
Max. and min. transmission	0.4435 and 0.3160	
Refinement method	Full-matrix least-squares on F ²	Full-matrix least-squares on F ²
Data / restraints / parameter	12875 / 0 / 603	3169 / 9 / 244
Goodness-of-fit on F ²	1.047	1.055
Final R indices [I>2sigma(I)]	R1 = 0.0565, wR2 = 0.1526	R1 = 0.0271, wR2 = 0.0616
R indices (all data)	R1 = 0.0633, wR2 = 0.1579	R1 = 0.0321, wR2 = 0.0650
Largest diff. peak and hole	4.669 and -4.138 e.Å ⁻³	0.391 and -0.416 e Å ⁻³

Table 3.08: Crystal data for compounds 17 and 18

3.3 Electrochemistry and Acid Inertness of Cu(II) Complexes

Dissociation of copper from bioconjugate complexes *in vivo* compromises their efficacy for PET. This has been observed with ^{64}Cu BFCs of TETA and DOTA, but higher resistance to such dissociation has been observed with the BFC of NOTA. Possible *in vivo* reduction of Cu(II) in its chelate complexes can play a detrimental role in that the less stable Cu(I) complex can dissociate and bind to a variety of biomolecules. Other feasible *in vivo* dissociations of the $^{64}\text{Cu(II)}$ from the bioconjugate can take place by reaction of the BFC with protons or biological metal ions. We have therefore examined the cyclic voltammetry as well as the acid inertness of these new model complexes. These experiments were performed by Dr. Edward Wong.

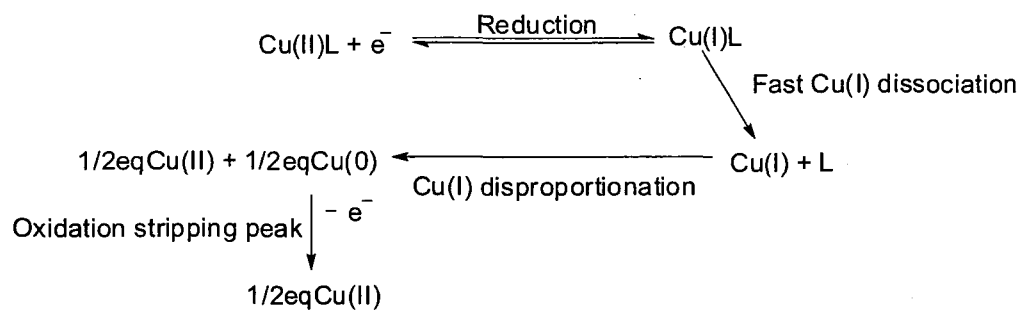
3.3.1 Cyclic voltammetry

Cyclic voltammetry experiments were carried out in 0.1 N aqueous sodium acetate solutions at room temperature. Table 3.09 shows the reduction potentials for relevant copper complexes.

Complex	Reduction Peak Potentials (0.1N NaOAc, Ag/AgCl ref.)
[Cu-(1)] ²⁺	-0.5 V, -1.3 V Irreversible
[Cu-(1) ₂] ²⁺	-0.5 V, -1.3 V Irreversible
[Cu-4] ²⁺ or (13)	-0.3V Irreversible
[Cu-5] ²⁺ or (15-15')	-0.07V Irreversible
[Cu-6] ²⁺ or (16)	-0.5V Irreversible
[Cu-7] ²⁺ or (17)	-0.7V Irreversible
[Cu-NOTA] ⁻ or [Cu-2] ⁻	-0.9 V, -1.2 V Irreversible
[Cu-NOAM2A] or (18)	-0.8V Irreversible
Cu-CB-TE2A	-1.03V Quasi-reversible ⁷⁹

Table 3.09: Electrochemical studies of copper (II) complexes

All copper complexes studied here yielded irreversible reductions. None of the ligands seem to be able to adapt to the coordination of Cu(I) and stabilize it. It is most likely that for all complexes, Cu(I) readily dissociated from the ligand after reduction and then the free Cu(I) disproportionated to yield Cu(0) and Cu(II) (Scheme 3.5). Large stripping peaks indicative of Cu(0) are present in all voltammograms upon return scanning.



Scheme 3.5: Potential species formed during electrochemistry studies

3.3.2 Acid-Assisted Decomplexation Studies

Aqueous acid dissociation studies of copper complexes can be used to predict whether or not the complexes will survive *in vivo*. Such half-lives are frequently used as first indicators of how long a compound will persist under harsh conditions. Copper complexes in 1M acid at various temperatures and their half-lives were therefore determined spectroscopically. In these studies, decomplexation was quantitatively monitored using UV-vis spectroscopy. The d-d transitions for these copper complexes occur in the range between 600 and 750nm. The slope of the $\ln(\text{absorbance})$ vs. time of the λ_{max} peak from the kinetic data gives the pseudo first order half-life of the complex. These results are summarized in **Table 3.10**.

Complex	Half life in 1M HCl 30°C	Half life in 1M HCl 90°C	Half life in 5M HCl 30°C
[Cu-(1)Cl ₂]	< 1min	—	—
[Cu-(1) ₂]Cl ₂	< 1min	—	—
[Cu-2] ⁻	Months	23(4) days	< 1min
18	Months	32(1) days	< 1min
Cu-CB-TE2A	—	—	>350 days

Table 3.10: Acid decomplexation studies of copper(II) complexes

Even though Cu-TACN, Cu-(TACN)₂ and Cu-NOTA are well-known complexes, their half-lives in acidic media have not been determined. These complexes were synthesized, and their stabilities in acidic solutions were determined.

At room temperature both Cu-TACN and Cu-(TACN) decomplexated immediately after dissolution in 1M HCl solution as opposed to Cu-NOTA which did not change over a month. Another solution of this complex was then tested at 90°C with the same acid concentration. In this case a half life of 23(4) days was determined. Lastly, Cu-NOTA was dissolved with 5M aqueous HCl yielding an instantaneous decomplexation.

The same procedure was followed to determine the half life of the model copper bioconjugate analogue, Cu-NOAM2A. Like Cu-NOTA, this complex showed no change in 1M HCl at room temperature and instant dissociation in 5M acid. Its half life was determined to be 32 days when kept in 1M aqueous HCl at 90°C.

3.4 Summary and Conclusions

Zn(II) and Cu(II) complexes of ligand **4** were obtained and fully characterized. The X-ray structure of the Zn complex verified an N-amide interaction with metal center with a distance of 2.8Å. There was not an X-ray structure for Cu-**4** to confirm such an interaction, but an IR band at 1676 cm⁻¹ for the carbonyl of Cu-**4** is higher in energy than of the ligand at 1641 cm⁻¹, supporting a similar rare amide N-Cu coordination.

Disappearance of nitrate peaks in the IR spectrum when a KBr pellet was used for analysis of both of these complexes led us to conclude that a solid state reaction occurred. Presumably, the Br⁻ ions displaced the coordinated nitrates.

Cu(II) complexes with ligands **5**, **6**, **7**, and **8** have been prepared. These complexes have been fully characterized and X-ray structures have been obtained. Typical distorted octahedral geometry is observed in all structures. These complexes presented a UV-vis λ_{max} from 600 to 750nm with molar absorptivities of less than 100 M⁻¹cm⁻¹ which are typical for d-d transitions of pseudo-octahedral Cu(II) complexes.

Even though electrochemistry studies showed irreversible reductions for all copper complexes, the reduction peak potentials of -0.9V and -0.8V for Cu-NOTA and Cu-NOAM2A are most likely negative enough to resist biological reduction.

The kinetic inertness studies confirmed that both Cu-NOTA and Cu-NOAM2A are significantly more stable kinetically than the copper complex of the unsubstituted TACN. While neither approach the extreme inertness of the Cu-CBTE2A, they appear sufficiently robust for typical *in vivo* pH's.

In conclusion, our coordination chemistry, acid inertness, and electrochemistry studies suggest that coordination of the pendant arms in the chelating ligand NOTA and

its derivatives likely to contribute significantly to the *in vivo* stability of the radio-labeled bioconjugates.

3.5 Future Work

The copper complex of compound **8** was made as a model of the ^{64}Cu -NOTA-bioconjugate, however the use of a TACN-diacetate derivative containing a secondary amide instead of a primary amide can be a better model of this bioconjugate.

Although, 2-chloro-*N*-phenylacetamide was initially used to synthesize a monoamide TACN-diacetate diethyl ester derivative, further exploration of this compound remains to be made. The hydrolysis of the ester groups can be performed in basic solution and concerns about the hydrolysis of amide group may be diminished for the presence of a secondary amide. Complexation with copper (II) can be performed similar to how compound **18** was prepared.

NMR studies of a zinc complex of compound **8** may be useful to explore the behavior of this ligand in aqueous solution when complexed to metal centers. Other metals such gallium (III) and indium (III) may be used as well.

CHAPTER IV

EXPERIMENTAL SECTION

4.1 General Methods and Materials

Elemental Analysis (CHN) was performed by Atlantic Micro-Labs Inc., Atlanta Georgia, USA. High Resolution Mass Spectra Electrospray Ionization Time-of-Flight (HR-MS-ESI-TOF) for compounds (**5**, **7**) were obtained at the University of Notre Dame. Infrared Spectra (IR) were run on a Nicolet iS10 FT-IR spectrometer (attenuated total reflectance). NMR Spectra (^1H NMR and $^{13}\text{C}\{^1\text{H}\}$ NMR) were acquired on a Varian *Mercury* 400 MHz NMR or Varian $^{\text{Unity}}$ *INOVA* 500 MHz NMR with VNMR 6.1C software. Chemical shift (δ) values are reported in parts per million (ppm) relative to Me_4Si (TMS) unless otherwise noted. X-ray crystallography was performed by Arnold L. Rheingold at the University of California, San Diego, La Jolla, California, USA, for compounds **14-18**. UV-Vis data were taken at room temperature on a Varian 50 Spectrophotometer. Electrochemistry was performed by Dr. Edward Wong using a Bioanalytical systems BAS 100B electrochemical work station with a glassy carbon working electrode, platinum wire auxiliary and silver /silver chloride reference electrode. Cyclic voltammograms were run at 200 mv/s. All solvents were reagent grade and were purified and dried as needed. All other reagents such as metal salts, drying agents, and alkylation material were obtained commercially and purified as needed as well.

4.2 Syntheses

All reactions were performed under N_2 atmosphere unless otherwise noted. Reactions above room temperature were run in flask using a condenser, oil bath, stir bar, and N_2 inlet. All routine solvent evaporations were carried out with a rotary evaporator under reduced pressure and trace solvent removal was done using a vacuum pump.

Hydrogen chloride ethanolic solution. HCl gas was prepared from the reaction of solid sodium chloride (40.04 g) with concentrated sulfuric acid (50 mL). This gas was bubbled into absolute EtOH (50 mL) (**Figure 4.1**). Titration of the resulting HCl ethanolic solution with standardized aqueous NaOH gave the molarity of the total HCl in solution. This stock solution was re-titrated before every use.

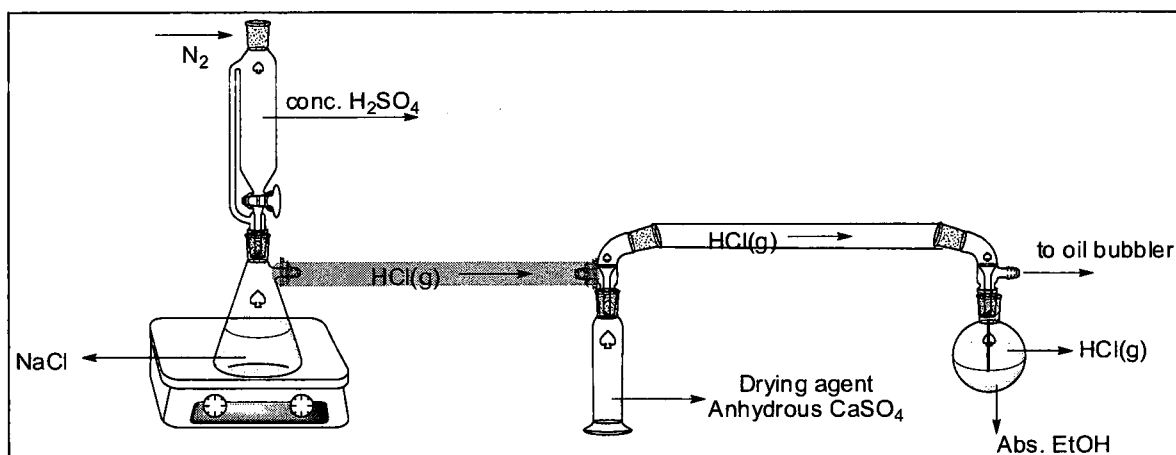


Figure 4.1: General design for bubbling dry HCl (gas) into absolute EtOH

1,4,7-triazacyclononane (1). **1** was prepared in 74% yield by a published procedure.^{6,9,12,58,59} 1,4,7-tritosyl-1,4,7-triazacyclononane (9.42 g, 15.90 mmol) in concentrated H_2SO_4 (85 mL) was heated and stirred for 84 hours at 100 °C. Solution was then allowed to cool at room temperature and placed into an ice bath to maintained the temperature below 10 °C. Cold absolute ethanol (85 mL) was added dropwise with

stirring and cooling followed by the addition of dry diethyl ether (130 mL). The formed precipitate was collected under N₂ and dissolved in H₂O (15 mL). Solution was adjusted to a pH ≥14 with NaOH pellets and extracted with cold CHCl₃ (7 × 40 mL). Portions of sodium chloride salt were added to the extraction funnel to increase the amount of extracted product. Chloroform extracts were dried with anhydrous Na₂SO₄ and filtered. Filtrate was then evaporated to obtain yellowish oil. Further drying in vacuum line gave product as a white solid. (1.513 g, 11.71 mmol, 74%). The ¹H and ¹³C{¹H}NMR were consistent with the literature spectra. This compound was used without further purification. However, in some cases further purification using kugelrohr distillation (100 °C air bath temperature / 100 millitorr) was required.

1,4,7-triazatricyclo[5.2.1.0^{4,10}] decane (3). **3** was prepared in 82% yield following a literature procedure^{55-58,60,61} (**Scheme 2.1**). Using a short path distillation set up, TACN (1.01 g, 7.82 mmol) was combined with N,N-dimethylformamide dimethyl acetal (0.94 g, 7.89 mmol) and stirred at 85 °C for 3 hours to obtain a brown-reddish solution. Crude material was cooled to room temperature and the byproducts of the reaction, MeOH and Me₂NH, were removed under reduced pressure. Crude material was then purified by Kugelrohr (50 °C Air bath / 60 millitorr) yielding 0.89 g of colorless oil. ¹H NMR (CDCl₃, 400 MHz) δ (ppm) 2.75-2.85 (m, 6H, XX' of AA'XX'), 3.04-3.14 (m, 6H, AA' of AA'XX'), 5.04 (s, 1H). ¹³C{¹H} NMR (CDCl₃, 100.51 MHz) δ (ppm) 52.11, 104.29.

1-Formyl-1,4,7-triazacyclonane (4). **4** was prepared according to a literature procedure (**Scheme 2.1**).^{55,56,57} **3** (910 mg, 6.51 mmol) were dissolved into 3 M HCl (23

mL) and stirred at room temperature for 7 hours. Clear solution was placed into an ice-water bath and a solution of cold 4 M NaOH (22 mL) was added dropwise or until pH was higher than 10. This aqueous solution was extracted with cold CHCl₃ (8 × 40 mL). Chloroform extracts were dried with anhydrous Na₂SO₄ and filtered out. Solvent was lastly evaporated to give 640 mg of white solid. A second extraction was performed to give 167 mg. ¹H NMR (CDCl₃, 400 MHz) δ (ppm) 1.76 (s, 2H, HN-CH₂CH₂NH), 2.71-2.79 (m, 4H), 3.03-3.14 (m, 4H), 3.34-3.48 (m, 4H), 8.15 (s, 1H). ¹³C{¹H} NMR (CDCl₃, 100.51 MHz) δ (ppm) 47.19, 48.78, 49.20, 49.88, 50.51, 53.14, 164.19.

1-Formyl-1,4,7-triazacyclononane-4,7-diacetic acid diethyl ester (5). This compound was reported in the literature⁶² but a different alkylation route was followed. Anhydrous sodium carbonate (194 mg, 1.83 mmol) and ethyl 2-bromoacetate were added to a solution of 1-formyl-1,4,7 triazacyclononane (**4**) (141 mg, 0.900 mmol) in anhydrous acetonitrile (7.5 mL). The heterogeneous mixture was stirred under N₂ atmosphere for 24 hours at 55 °C. The mixture was allowed to cool at room temperature and solvent was evaporated. The flask with the residue was then placed in an ice-water bath and the residue was dissolved by the addition of cold 20% aq NaOH (8.5 mL). This aqueous solution was extracted with cold CHCl₃ (8 × 40 mL) and the combined extracts were dried over anhydrous Na₂SO₄. Solvent was evaporated to give a yellowish oil (550 mg). The residue was chromatographed in ethyl acetate on a column of 50 grams of neutral alumina (M. Woelm, Eschwege, Germany) and eluted with same solvent (200 mL). The collected solvent was removed to give a clear oil (500 mg, 1.52 mmol, 88% yield). ¹H NMR (CDCl₃, 400 MHz) δ (ppm) 1.26-1.27 (t, 6H, CH₃-CH₂-O), 2.68, 2.76, 3.02, 3.24,

3.50 (6m, $6 \times 2\text{H}$, ring- NCH_2), 3.4 (s, 4H, N- $\text{CH}_2\text{-COOEt}$), 4.17-4.18 (q, 4H, $\text{CH}_2\text{-CH}_3$), 8.07 (s, 1H, N- CHO). $^{13}\text{C}\{^1\text{H}\}$ NMR (CDCl_3 , 100.51 MHz) δ (ppm) 13.30 ($\text{CH}_3\text{-CH}_2\text{-O}$), 46.11, 49.17 (ring- NCH_2 next to the CHO), 52.93 and 56.64, 53.65 and 57.08 (ring- NCH_2), 53.87 and 57.11 (N- $\text{CH}_2\text{-COOEt}$), 59.30 and 59.33 ($\text{CH}_3\text{-CH}_2\text{-O}$), 162.76 (CHO), 170.78 and 170.96 (COO). ^1H -NMR data were consistent with those reported by Kreher et al.,⁶² who prepared the compound from the precursor triazacyclononane orthoamide (**3**) rather than 1-formyl triazacyclononane (**4**). All chemical shifts from the $^{13}\text{C}\{^1\text{H}\}$ NMR spectrum were approximately one ppm up field than the reported shifts, although the number of resonances were consistent with the number of different carbons in the molecule. Additional characterization data were also acquired and consistent with the structure. ATR-IR 2909, 1735, 1663, 1443, 1415, 1370, 1183, 1134, 1059, 1027, 912 cm^{-1} ; HR-MS-ESI-TOF, m/z ($\text{M}+\text{H}$)⁺ exact mass for $\text{C}_{15}\text{H}_{28}\text{N}_3\text{O}_5$: 330.2023; Found: 330.2007 (error -1.6 mmu/-4.9 ppm); m/z ($\text{M}+\text{Na}$)⁺ exact mass for $\text{C}_{15}\text{H}_{27}\text{N}_3\text{NaO}_5$: 352.1843; Found: 352.1823 (error -2.0 mmu/-5.6 ppm).

1,4,7-Triazacyclononane-4,7-diacetic acid diethyl ester • 2HCl (6). The preparation of this compound was reported in the literature⁶³; however a different and more selective approach was followed. A solution of 1-formyl-1,4,7-triazacyclononane-1,4-diacetate diethyl ester (**5**) (500 mg, 1.52 mmol) in absolute EtOH (5 mL) was combined with a 2.05 M ethanolic solution of hydrogen chloride (see preparation above) (8.5 mL) and stirred at reflux for 24 hours. The cloudy yellowish solution was then allowed to cool down and the solvent was removed under reduced pressure to give an off-white solid (562 mg). Absolute EtOH (8.0 mL) was added to the crude material and

heated in a water bath until clear; this solution was cooled down in cold water bath to obtain tiny white crystals. Solid was separated by filtration, washed with a small portion of cold EtOH, and dried under vacuum to obtain 255 mg of the product. The filtrate was transferred to a round-bottomed flask and solvent was evaporated to give off-white crystals. The recrystallization process was repeated two more times to yield an additional 150 mg of the desired product for a total of 405 mg (1.08 mmol, 71% yield). ^1H NMR (D_2O , 400 MHz) δ 1.27 (t, 6H, $J = 7.2$ Hz, $-\text{OCH}_2\text{-CH}_3$), 3.28 (s, 4H, ring- $\text{N}(\text{CH}_2)_2$), 3.36-3.55(m, $4 \times 2\text{H}$, ring- $\text{NCH}_2\text{CH}_2\text{NH}$), 3.95 (s, 4H, $\text{N-CH}_2\text{-COOEt}$), 4.25 (q, 2H, $J = 7.2$ Hz, $-\text{OCH}_2\text{-CH}_3$); $^{13}\text{C}\{^1\text{H}\}$ NMR (D_2O , 100.51 MHz) δ 13.45 ($\text{CH}_3\text{-CH}_2\text{-O}$), 43.26, 49.77, and 50.92 (ring- NCH_2), 56.48 ($\text{N-CH}_2\text{-COOEt}$), 63.04 ($\text{CH}_3\text{-CH}_2\text{-O}$); ATR-IR 2924, 2534, 1738, 1434, 1290, 1247, 1202, 1174, 1118, 1096, 1051, 1010, 968 cm^{-1} ; Anal. Calcd. for $\text{C}_{14}\text{H}_{29}\text{Cl}_2\text{N}_3\text{O}_4$: C, 44.92; H, 7.81; N, 11.23; Cl, 18.94 %. Found: 44.65, H, 7.91, N, 10.98, Cl, 18.68%. $^{13}\text{C}\{^1\text{H}\}$ NMR data were consistent with those reported by Van Haveren et al.,⁶³ who prepared the compound from the precursor 1,4,7-triazacyclononane 1,4 diacetic acid (**11**).

1,4,7-Triazacyclononane-acetamide-4,7-diacetic acid diethyl ester (7).

Anhydrous potassium carbonate (250 mg, 1.81 mmol) was added to a solution of 1,4,7-triazacyclonane-4,7-diacetic acid diethyl ester $\cdot 2\text{HCl}$ (**6**) (233 mg, 0.622 mmol) in dry acetonitrile (23 mL) and stirred at room temperature for 10 min. Then 2-bromoacetamide (117 mg, 0.848 mmol) was added to the reaction mixture and stirred for 20 hours at 50 $^\circ\text{C}$. At this point, the reaction mixture was cooled down to room temperature and the white insoluble salt was filtered out and washed with CH_3CN . The combined filtrate was

evaporated and the residue was combined with cold aqueous solution of 4 M NaOH (13 mL). The aqueous mixture was extracted with cold (0-5 °C) CHCl₃ (7 × 40 mL) and the combined extracts were dried over anhydrous sodium sulfate. Solvent was then removed to give 194 mg, 87% yield of the desired compound as a yellowish oil. ¹H NMR (CDCl₃, 400 MHz) δ 1.26 (t, 6H, -OCH₂CH₃), 2.62-2.70, 2.80-2.90 (2m, 4×2H, ring-NCH₂CH₂N-amide), 2.84 (s, 4H, ring-N-CH₂CH₂N-ester), 3.27 (s, 2H, 4H, N-CH₂CONH₂); 3.38 (s, 4H, N-CH₂-COOEt), 4.15 (q, 4H, -OCH₂-CH₃), 5.43 and 9.29 (s, 2H, NH); ¹³C{¹H}NMR (CHCl₃, 100.51 MHz) δ 14.50 (-OCH₂CH₃), 55.41, 56.05, 58.42 (ring-NCH₂), 60.62 (N-CH₂-COOEt), 61.12 (N-CH₂-CONH₂), 172.04(CH₂-COOEt), 176.44 (CH₂-CONH₂); ATR-IR 3272, 2930, 2841, 1734, 1671, 1449, 1373, 1305, 1181, 1139, 1114, 1063, 1026, 910 cm⁻¹; HR-MS-ESI-TOF, *m/z* (M+H)⁺ exact mass for C₁₆H₃₁N₄O₅: 359.2289; Found: 359.2283 (error -0.6 mmu/-1.7 ppm).

Disodium-1,4,7-triazacyclononane-acetamide-4,7-diacetate (8) 1,4,7-triazacyclononane acetamide-4,7-diacetic acid diethyl ester (24 mg, 0.067 mmol) was combined with 1M NaOD (0.2 mL) and D₂O (0.5 mL) and stirred at room temperature for 45 min to give a D₂O solution of (8). ¹H NMR (D₂O, 400 MHz) δ 2.59-2.65, 3.23-3.27, 3.38; ¹³C{¹H}NMR (D₂O, 100.51 MHz) δ 52.19, 60.43, 62.25, 178.09, 180.72. The solvent of this solution mixture was evaporated and the residue was re-dissolved in D₂O. ¹H NMR (D₂O, 400 MHz) δ 2.40-2.60, 3.04-3.29, 3.75; ¹³C{¹H}NMR (D₂O, 100.51 MHz) δ 51.10, 51.57, 51.64, 59.97, 61.40, 62.06, 177.64, 179.89, 180.70 (refer to pages 32-33); ATR-IR 3300, 2807, 2841, 1679, 1583, 1406, 1335, 1291, 1258, 1121, 1054,

1011, 929 cm^{-1} . Since NMR spectra was non reproducible, further studies and characterization data are required for fully characterization of compound (8).

1-Formyl-1,4,7-triazacyclononane • copper(II) nitrate complex (13). Ligand 4 (41 mg, 0.26 mmol) and copper nitrate 2.5 hydrate (61 mg, 0.26 mmol) were dissolved with absolute ethanol (5.5 mL each) in separate vials. The solutions were combined and a blue-lilac precipitate formed. The mixture was stirred at room temperature under N_2 atmosphere overnight. The precipitate formed was then centrifuged and washed with cold ethanol and ether. Residual solvent was removed to give (89 mg, 98%) of the blue-lilac solid. ATR-IR 3305, 3260, 1676, 1469, 1400, 1355, 1286, 1245, 1210, 1173, 1131, 1064, 1085 cm^{-1} ; Anal. Calcd for $\text{CuC}_7\text{H}_{15}\text{N}_5\text{O}_7$: C, 24.39; H, 4.39; N, 20.31%. Found: C, 24.67; H, 4.45; N, 20.13%. UV-Vis(H_2O) $\lambda_{\text{max}} = 661 \text{ nm}$ ($\epsilon = 46 \text{ M}^{-1} \text{ cm}^{-1}$).

1-Formyl-1,4,7 triazacyclononane • zinc(II) nitrate complex (14). Ligand 4 (40mg, 0.25mmol) in absolute EtOH was combined with a solution of zinc nitrate hexahydrated (77 mg, 0.26 mmol) in absolute ethanol to obtain a white precipitate instantaneously. This mixture was stirred at room temperature for 16 hours. The white precipitate was collected by centrifuging and this solid was washed with cold ethanol and ether. Solvent evaporation gave the white solid product (28 mg, 27% yield). X-ray quality crystals were obtained by suspending a sample in ethanol and ether and allowing it to stand for several days. ^1H NMR (CDCl_3 , 400 MHz) δ 2.90-2.95 and 3.04-3.09 (2m, 4H, ring- $\text{NCH}_2\text{CH}_2\text{N}$ -amine) 3.12-3.17 and 3.24-3.29 (2m, 4H, ring- $\text{N-CH}_2\text{CH}_2\text{NCH=O}$), 3.50-3.54 and 3.57-3.62 (2m, 4H, $\text{N-CH}_2\text{CH}_2\text{NCH=O}$); ATR-IR 3519, 3285, 2978,

1656, 1464, 1427, 1404, 1378, 1361, 1289, 1262, 1226, 1181, 1137, 1114, 1100, 1067 cm^{-1} .

1-Formyl-1,4,7-triazacyclononane-4-acetate-7-acetic acid ethyl ester • copper (II) chloride complex (15) To a solution of 1-formyl-1,4,7-triazacyclononane-4,7-diacetic acid diethyl ester (**5**) (27 mg, 0.082 mmol) in absolute ethanol (2 mL) was added a light green solution of copper chloride dihydrate (14 mg, 0.085 mmol) in absolute ethanol (2 mL). The homogeneous green solution was stirred for 20 hours at room temperature. The solvent was evaporated and the residue was then re-dissolved in methanol and precipitated with the addition of ethyl acetate. The precipitate was centrifuged and washed with cold EtOH. Residual EtOH was removed *in vacuo* to yield the product as a green solid (26 mg). X-ray quality crystals were grown by slow diffusion of ethyl acetate into a solution of the crude material in MeOH. ATR-IR 2979, 2173, 1980, 1732, 1714, 1646, 1490, 1453, 1407, 1344, 1298, 1222, 1107, 1039, 1017 cm^{-1} ; Anal. Calcd for $\text{CuC}_{13}\text{H}_{22}\text{N}_3\text{O}_5\text{Cl}$ (NaCl) ($1.3\text{CH}_3\text{CH}_2\text{OH}$): C, 36.19; H, 5.80; N, 8.12; Cl, 13.70%. Found: C, 36.16; H, 5.73; N, 8.06; Cl, 13.78%. UV-Vis(H_2O) $\lambda_{\text{max}} = 666 \text{ nm}$ ($\epsilon = 69 \text{ M}^{-1} \text{ cm}^{-1}$).

1,4,7-Triazacyclononane-4,7-diacetate diethyl ester • copper(II) chloride complex (16). 1,4,7-triazacyclononane-4,7-diacetate diethyl ester • 2HCl (16 mg, 0.043 mmol) was dissolved with warm absolute ethanol (2 mL) and combined with a solution of cupric chloride dihydrate (7.6 mg, 0.045 mmol) in absolute EtOH (1 mL) and stirred at room temperature for 24 hours. Solvent was evaporated to give a light green solid,

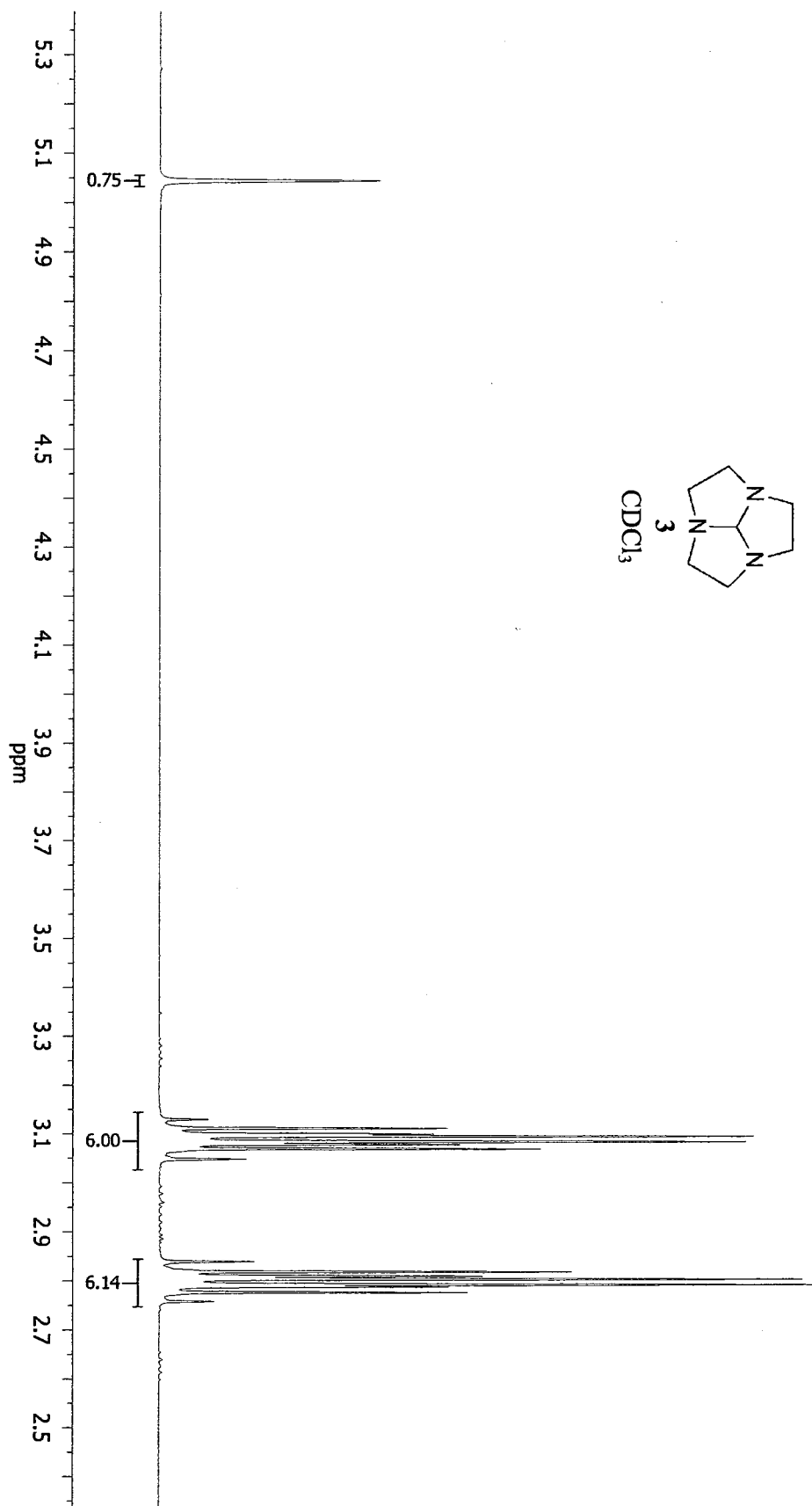
which was then combined with a small amount of absolute EtOH and heated until clear. This solution was allowed to cool to room temperature and then placed in the refrigerator overnight. Tiny blue crystals were obtained, which were washed with cold ethanol, and dried under vacuum to give (18.5 mg 92% yield). X-ray quality crystals were obtained from cooling a hot ethanolic solution of the complex. ATR-IR 3466, 3248, 2979, 2927, 1732, 1635, 1492, 1449, 1417, 1375, 1296, 1278, 1199, 1175, 1102, 1181, 1018 cm^{-1} . Anal. Calcd. for $\text{CuC}_{14}\text{H}_{27}\text{N}_3\text{O}_4\text{Cl}_2(0.5\text{H}_2\text{O})$: C, 37.80; H, 6.34; N, 9.45; Cl, 15.94 %. Found: C, 37.85; H, 6.33; N, 9.43; Cl, 16.13 %. UV-Vis(H_2O) $\lambda_{\text{max}} = 694 \text{ nm}$ ($\epsilon = 6 \text{ M}^{-1} \text{ cm}^{-1}$).

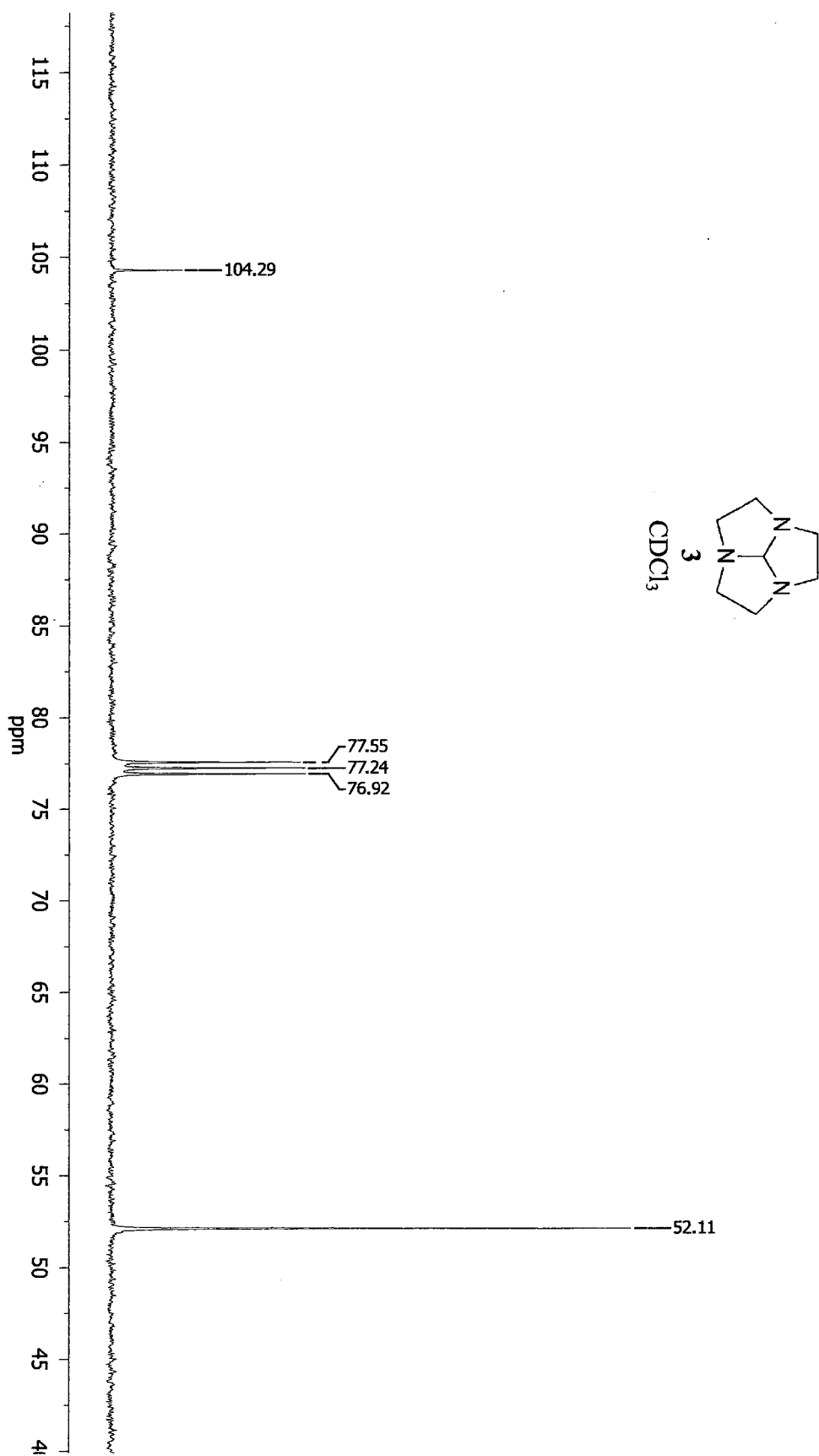
1,4,7-Triazacyclononane-1-acetamide-4,7-diacetate diethyl ester • copper(II) •chloride complex (17). To a solution of 1,4,7-triazacyclononane-1-acetamide-4,7-diacetate diethyl ester (23 mg, 0.064 mmol) (7) in ethanol (1 mL) a solution of cupric chloride dihydrate (11 mg, 0.064 mmol) in absolute EtOH (2 mL) was added dropwise and the reaction stirred at room temperature for 24 hours. Solvent was then evaporated and the residue was dissolved in a minimum amount of EtOH, ethyl acetate was added to induce precipitation. This precipitate was washed with a small amount of cold ethanol, separated by centrifuging, and dried under reduced pressure to yield light green crystals (24 mg, 72% yield). X-ray quality crystals were obtained by slow evaporation of an acetonitrile solution of the complex. ATR-IR 2930, 1728, 1658, 1591, 1452, 1420, 1375, 1295, 1203, 1180, 1098, 1053, 1018, 911 cm^{-1} . Anal. Calcd. for $\text{CuC}_{16}\text{H}_{30}\text{N}_4\text{O}_5\text{Cl}_2(0.3\text{NaCl})(0.7\text{H}_2\text{O})$: C, 36.74; H, 6.05; N, 10.71; Cl, 15.59 %. Found: C, 36.52; H, 6.05; N, 10.36; Cl, 15.51%. UV-Vis (H_2O) $\lambda_{\text{max}} = 716 \text{ nm}$ ($\epsilon = 57 \text{ M}^{-1} \text{ cm}^{-1}$).

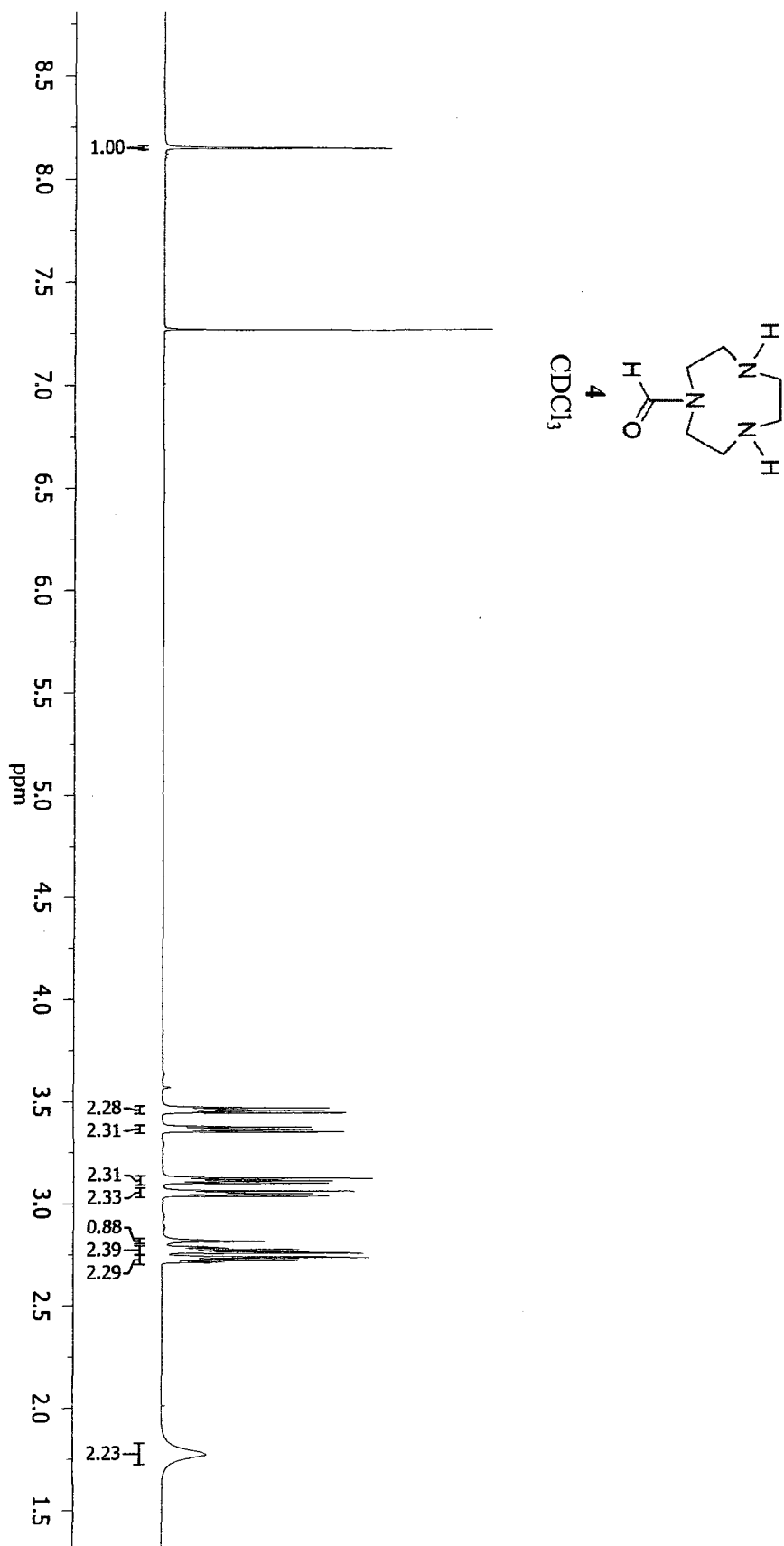
1,4,7-Triazacyclononane-1-acetamide-4,7-diacetate • copper(II) complex (18).

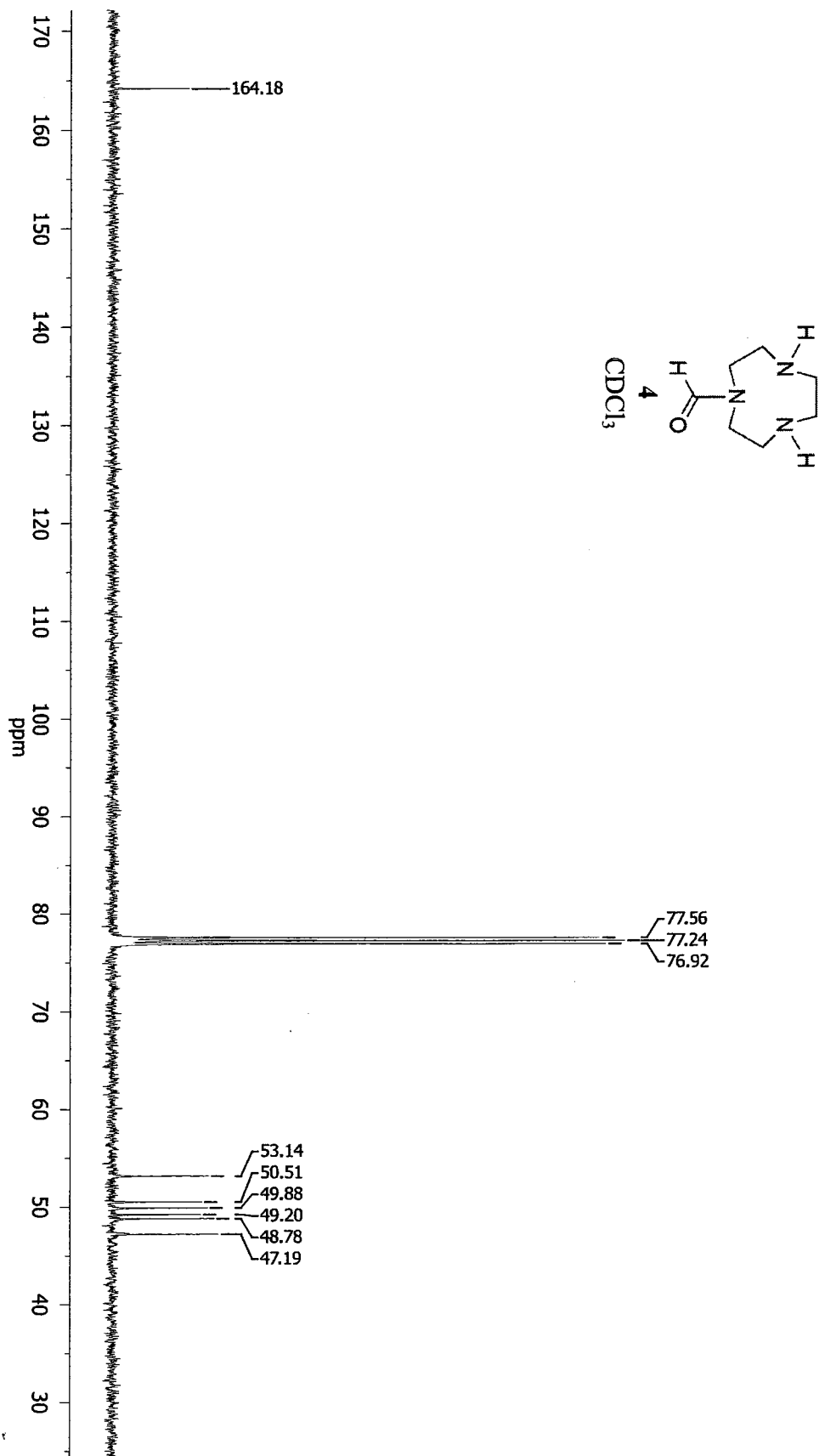
1,4,7-triazacyclononane-1-acetamide-4,7-diacetate-diethyl ester (7) (16.5 mg, 0.046 mmol) was combined with deionized (D.I.) water (0.5mL) and 1M aqueous NaOH (0.2 mL). This mixture was stirred until clear. A solution of copper chloride dihydrate (7.9 mg, 0.046 mmol) in D.I. water (1 mL) was added to give a blue solution. The pH of the final solution was adjusted to approximately 7 with 1 M NaOH. This was stirred at room temperature overnight to give a dark blue solution which was then evaporated to dryness under reduced pressure. The residue was treated with absolute ethanol and a light blue insoluble material was separated by centrifuging. This supernatant was dried under reduced pressure to give small dark-blue crystals (14 mg) 45% yield. X-ray quality crystals were grown from cooling a sample in a hot ethanolic solution containing a few drops of D.I. water. ATR-IR 3450, 3305, 1652, 1605, 1491, 1346, 1322, 1302, 1289, 1121 cm^{-1} . UV-Vis (H_2O) $\lambda_{\text{max}} = 719 \text{ nm}$ ($\epsilon = 68 \text{ M}^{-1} \text{ cm}^{-1}$).

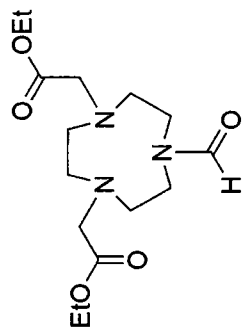
APPENDIX





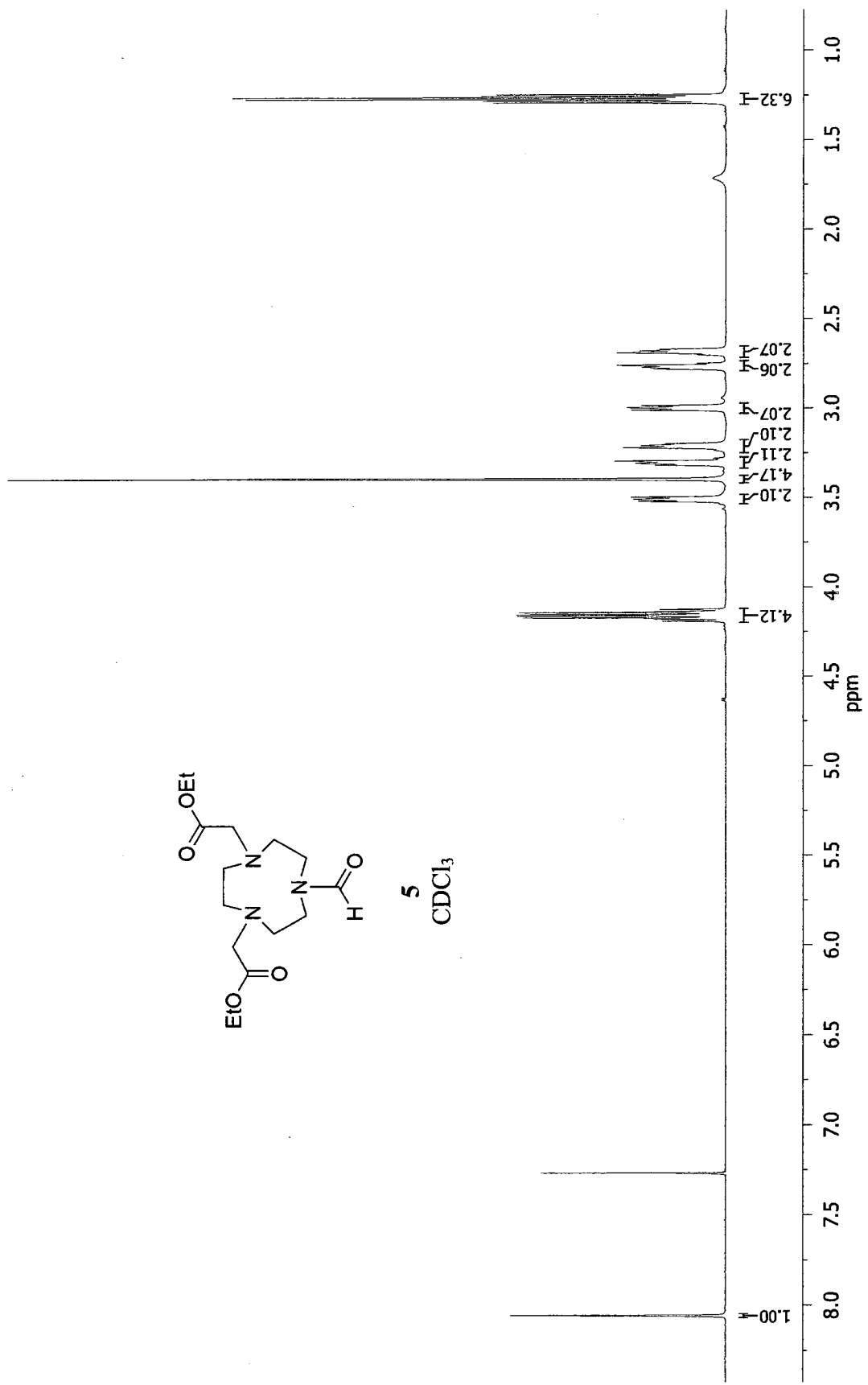


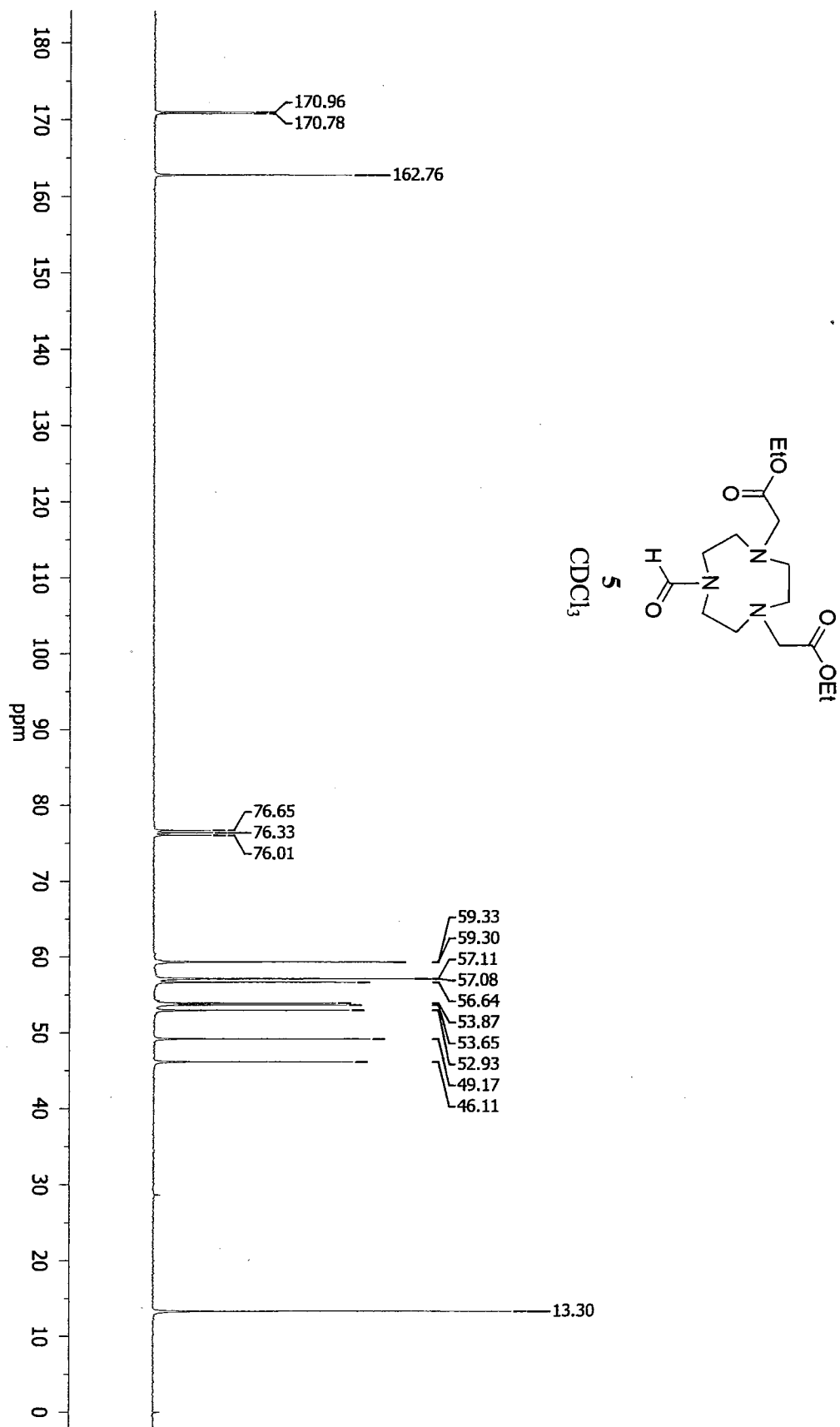


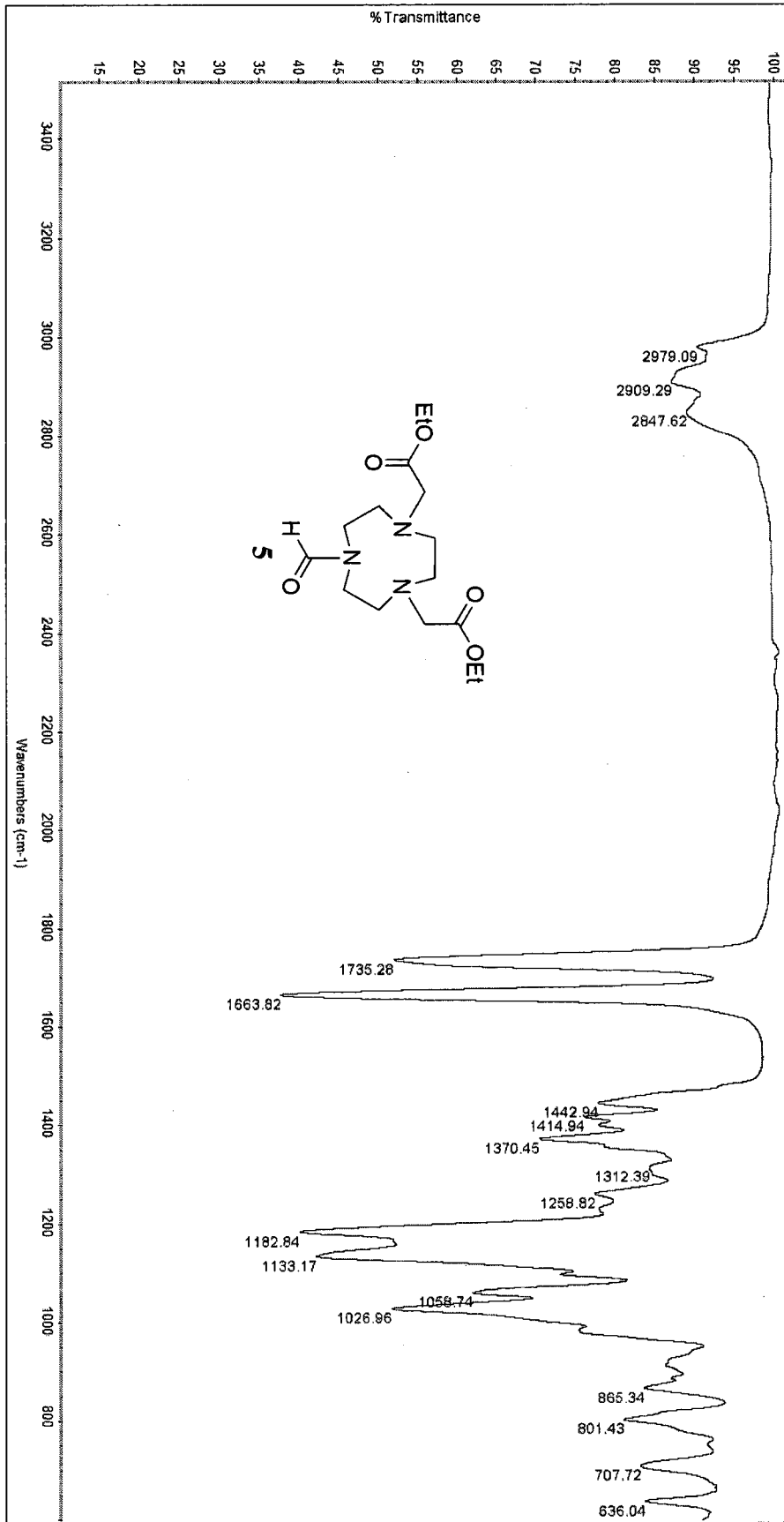


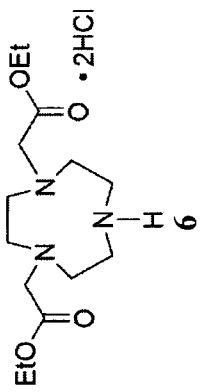
5

CDCl₃

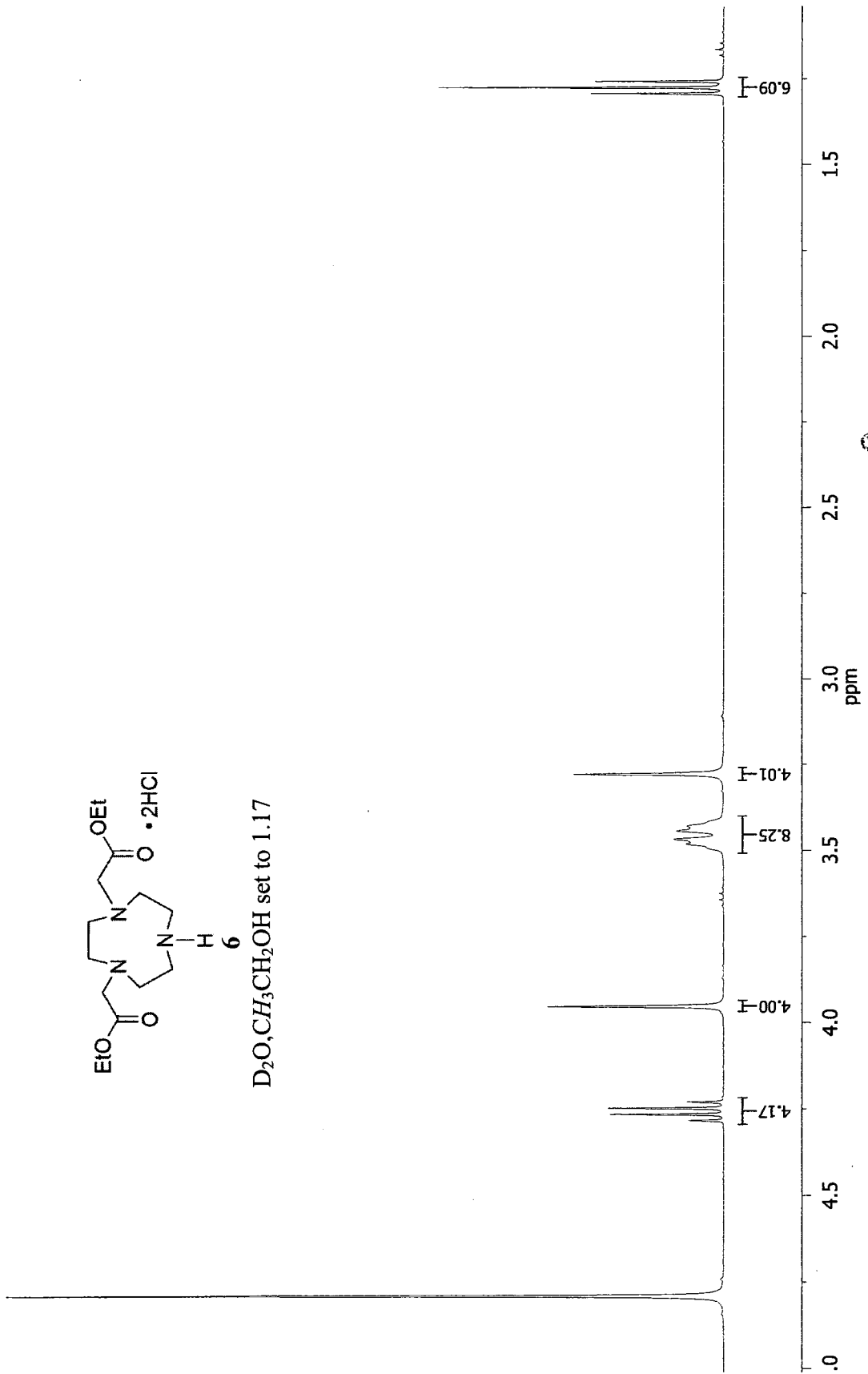


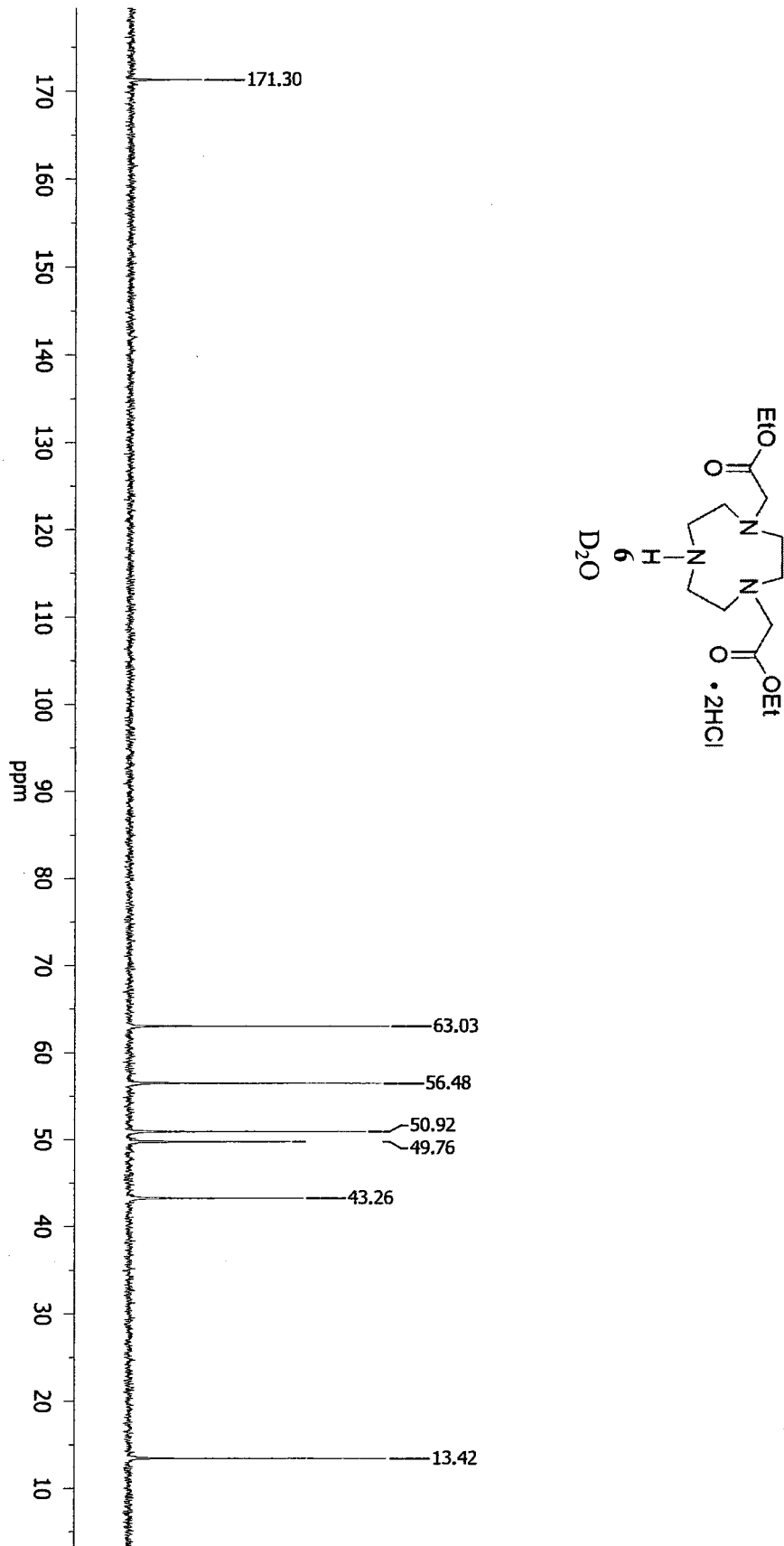


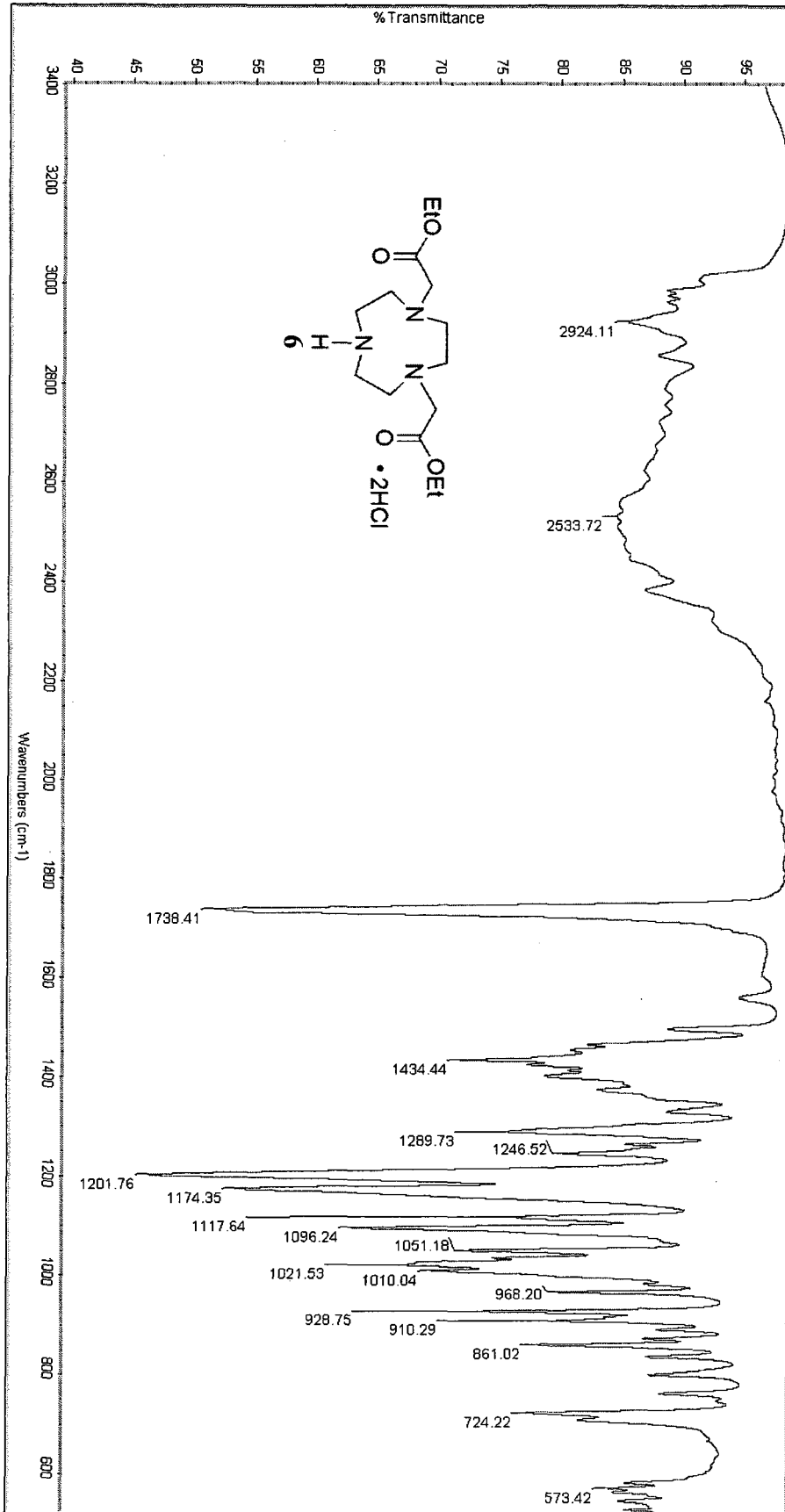


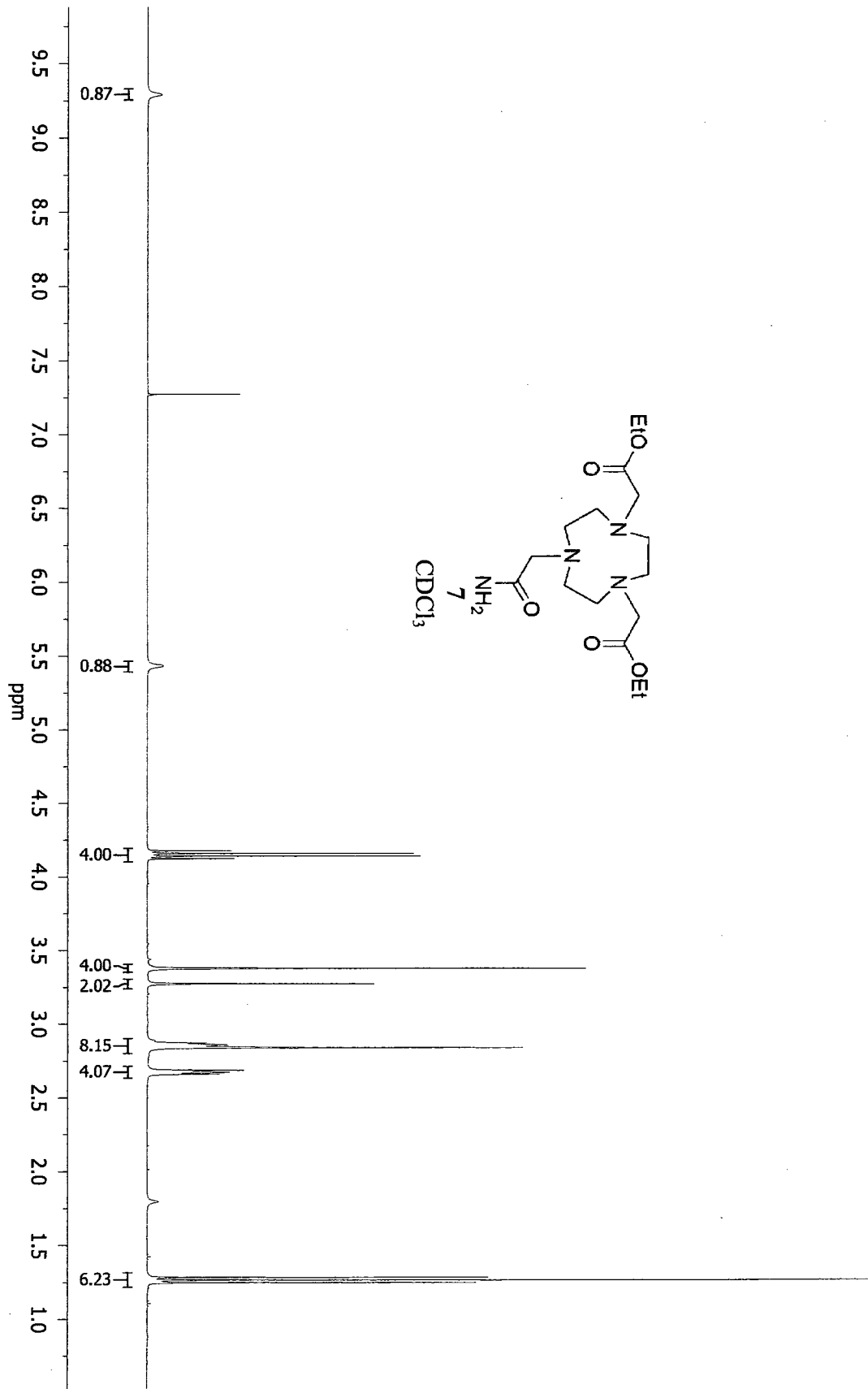


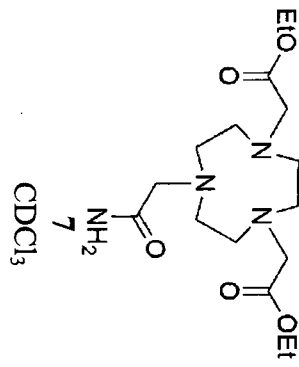
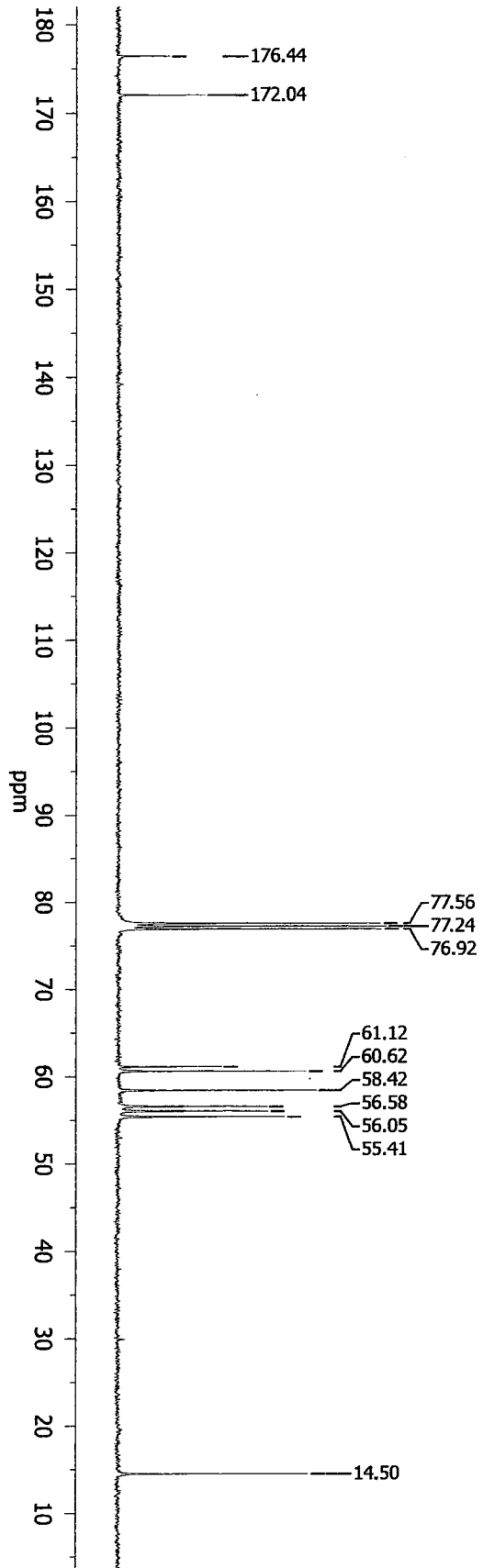
D₂O, CH₃CH₂OH set to 1.17

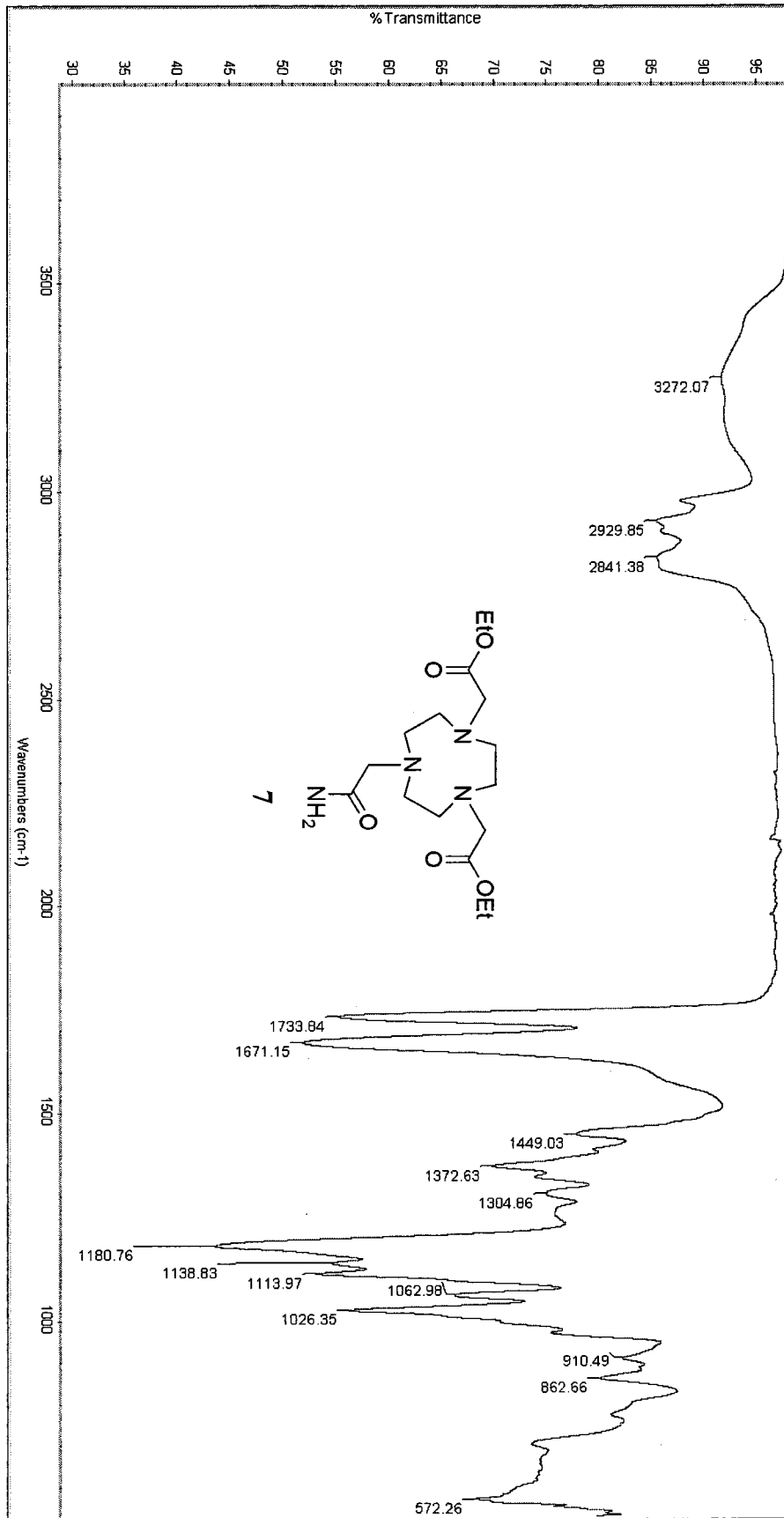


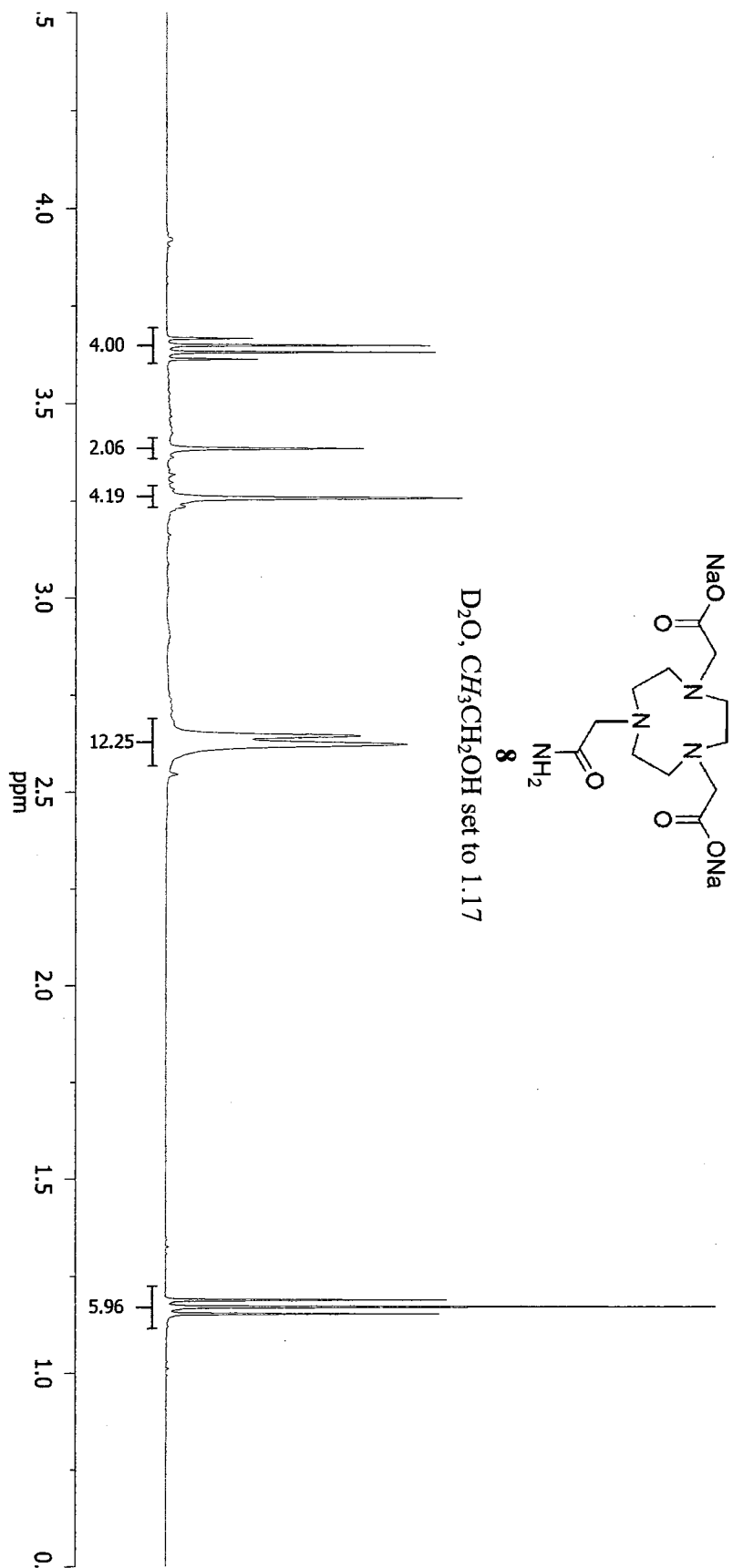


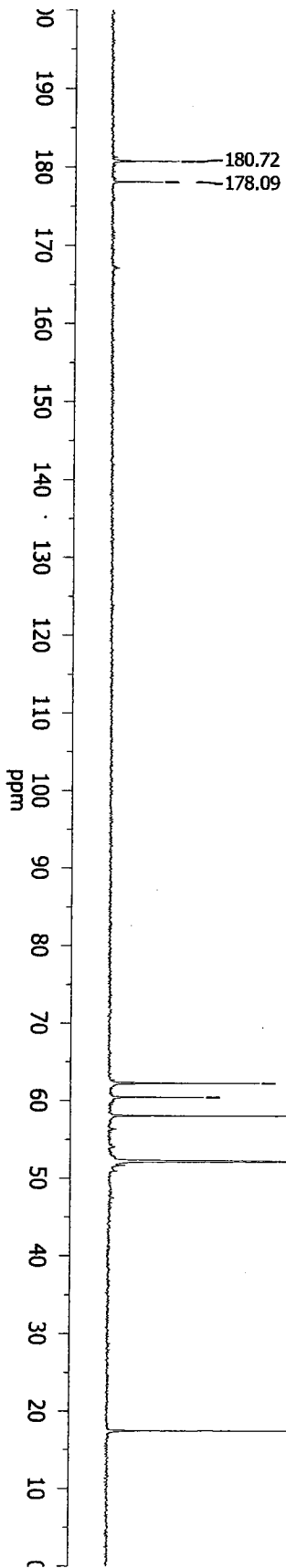




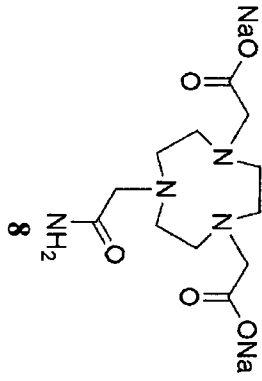


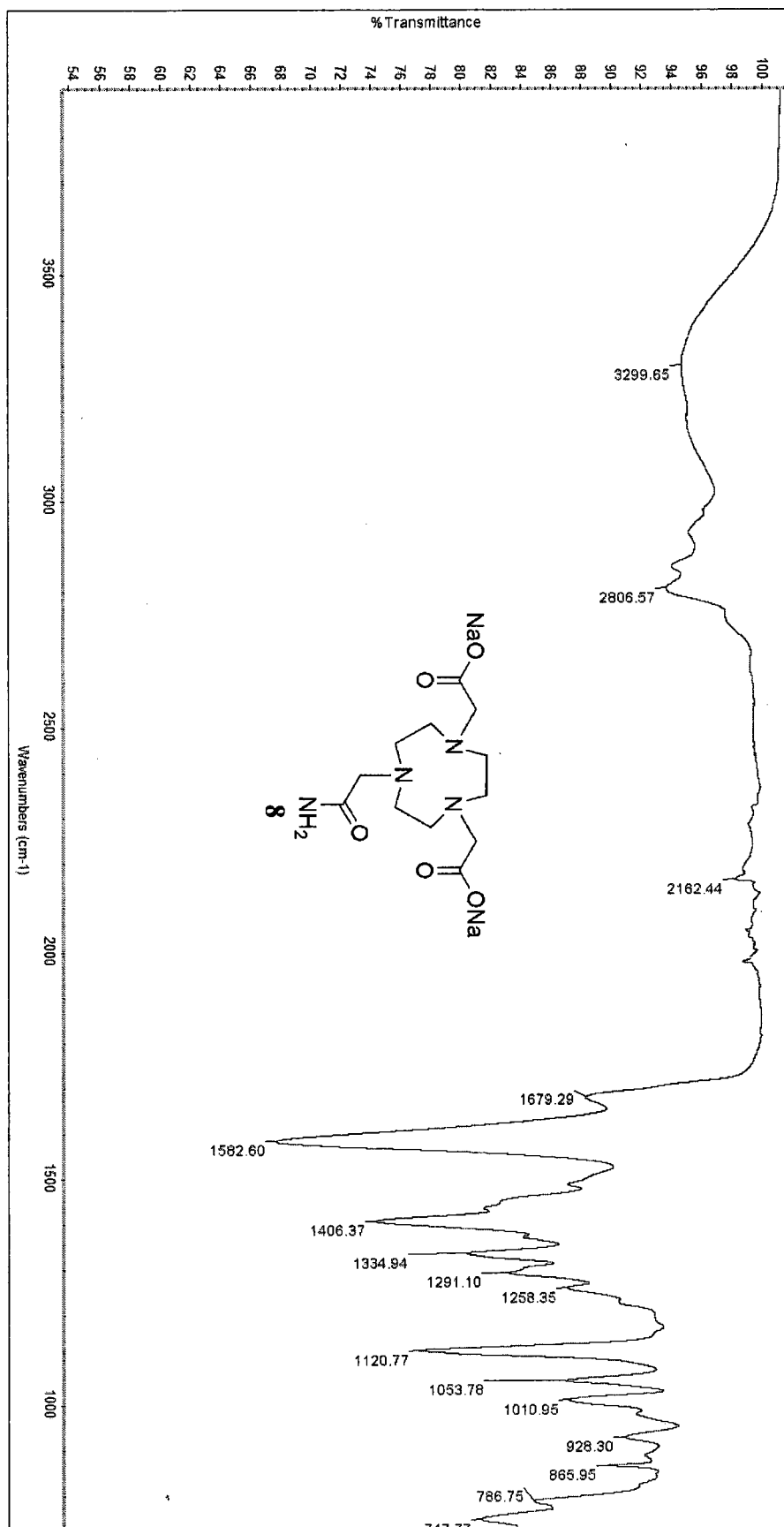


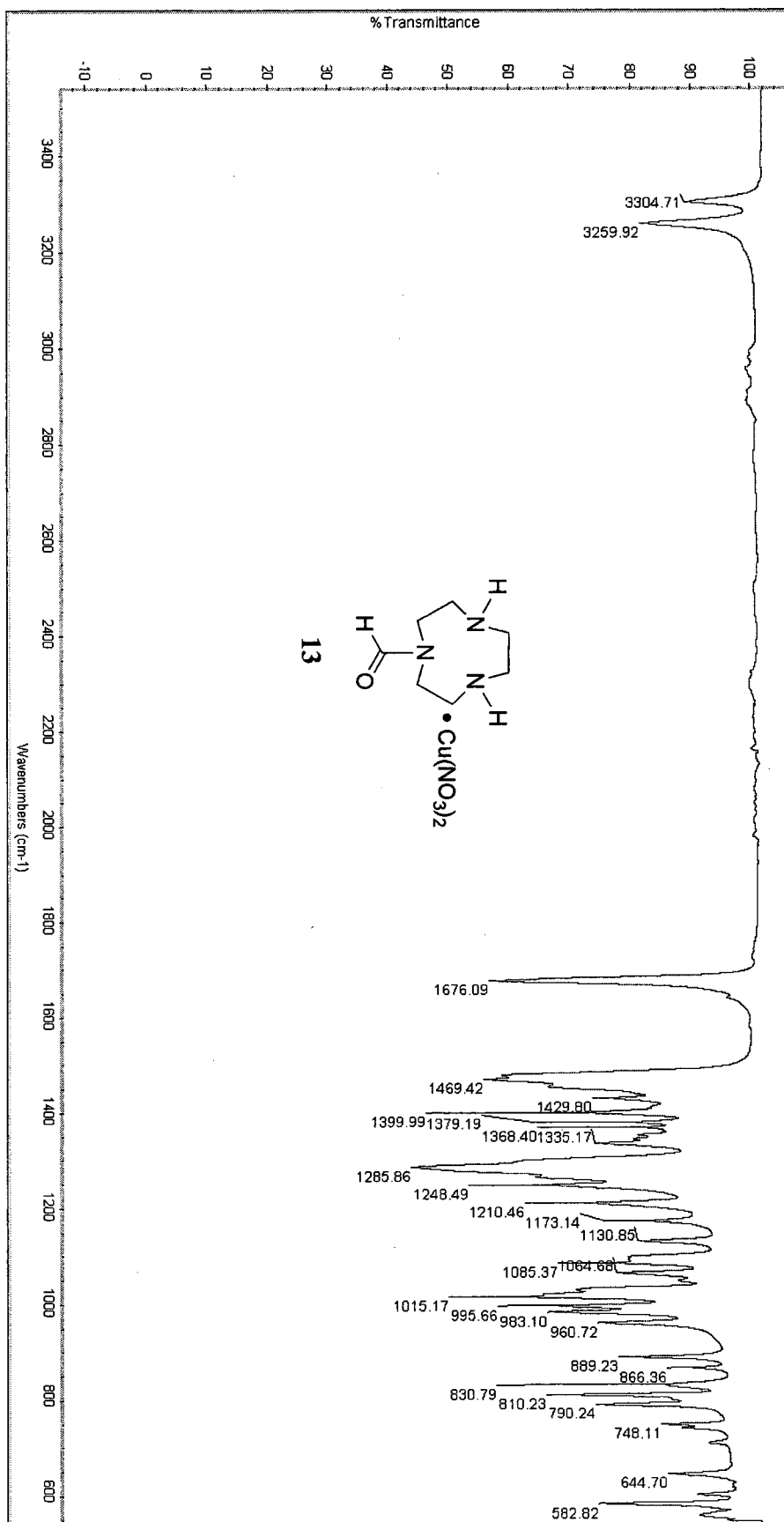


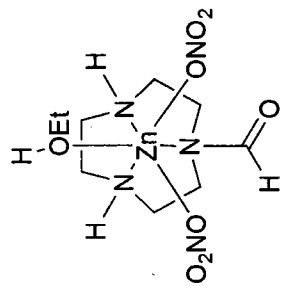


D_2O, CH_3CH_2OH set to 17.47



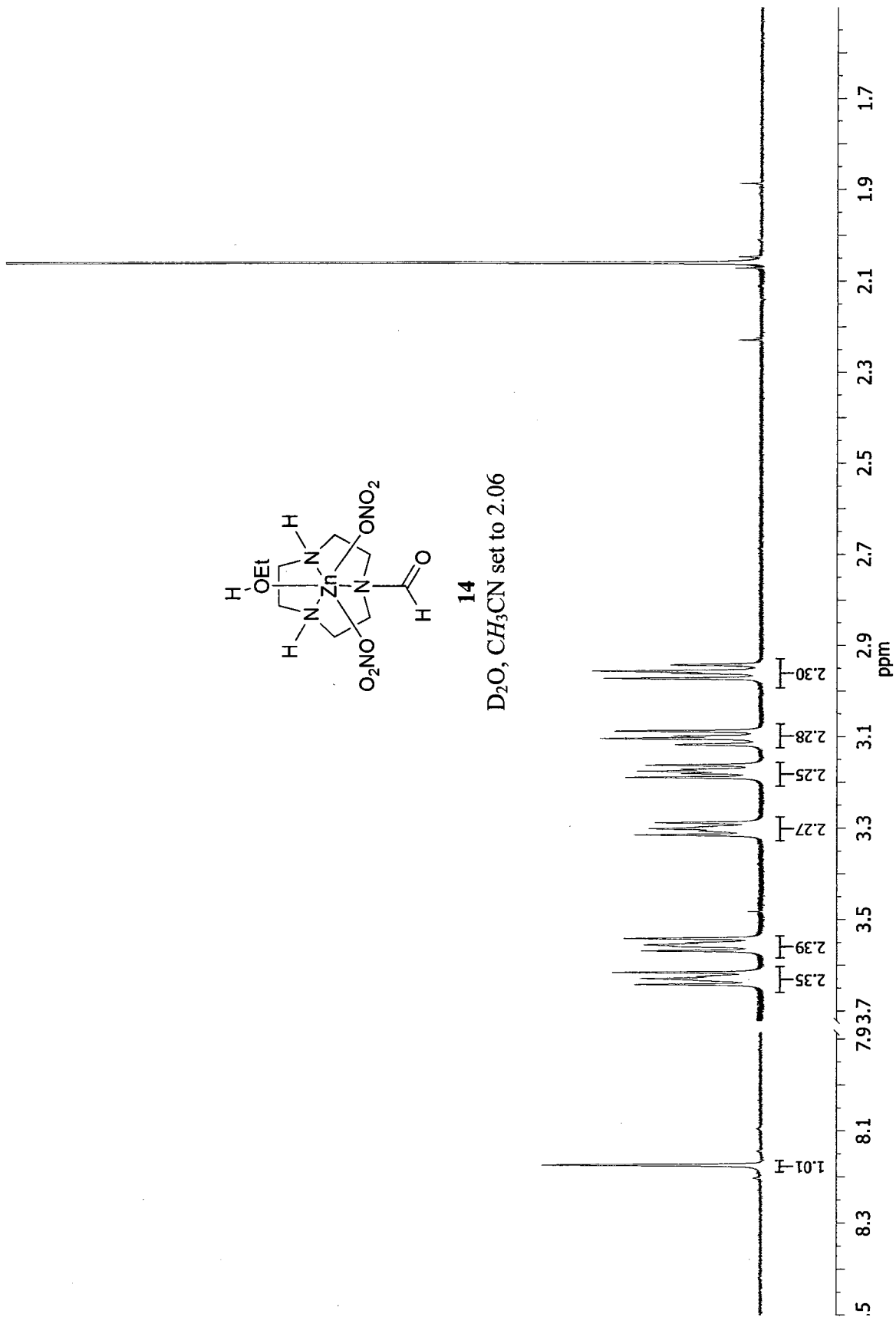


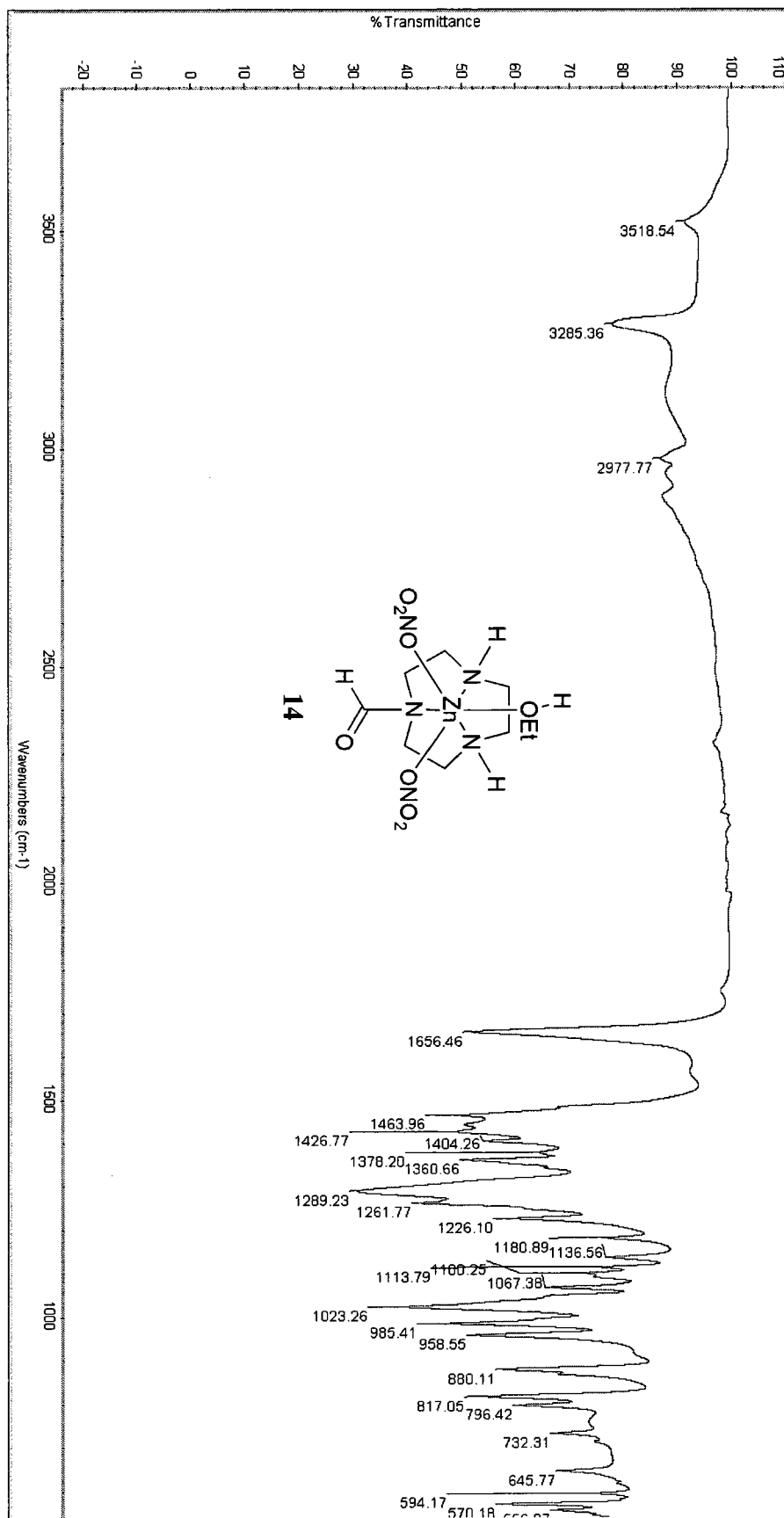


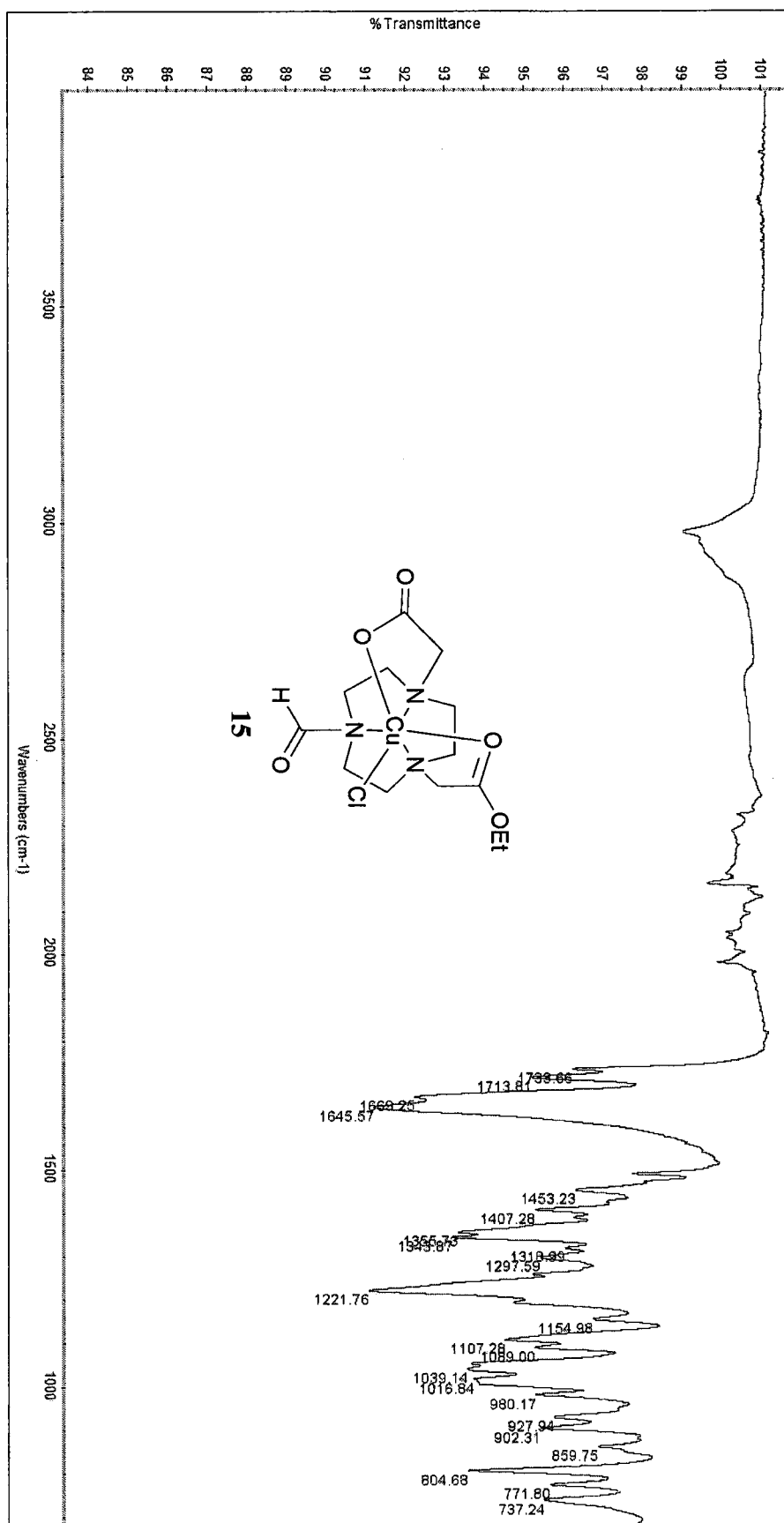


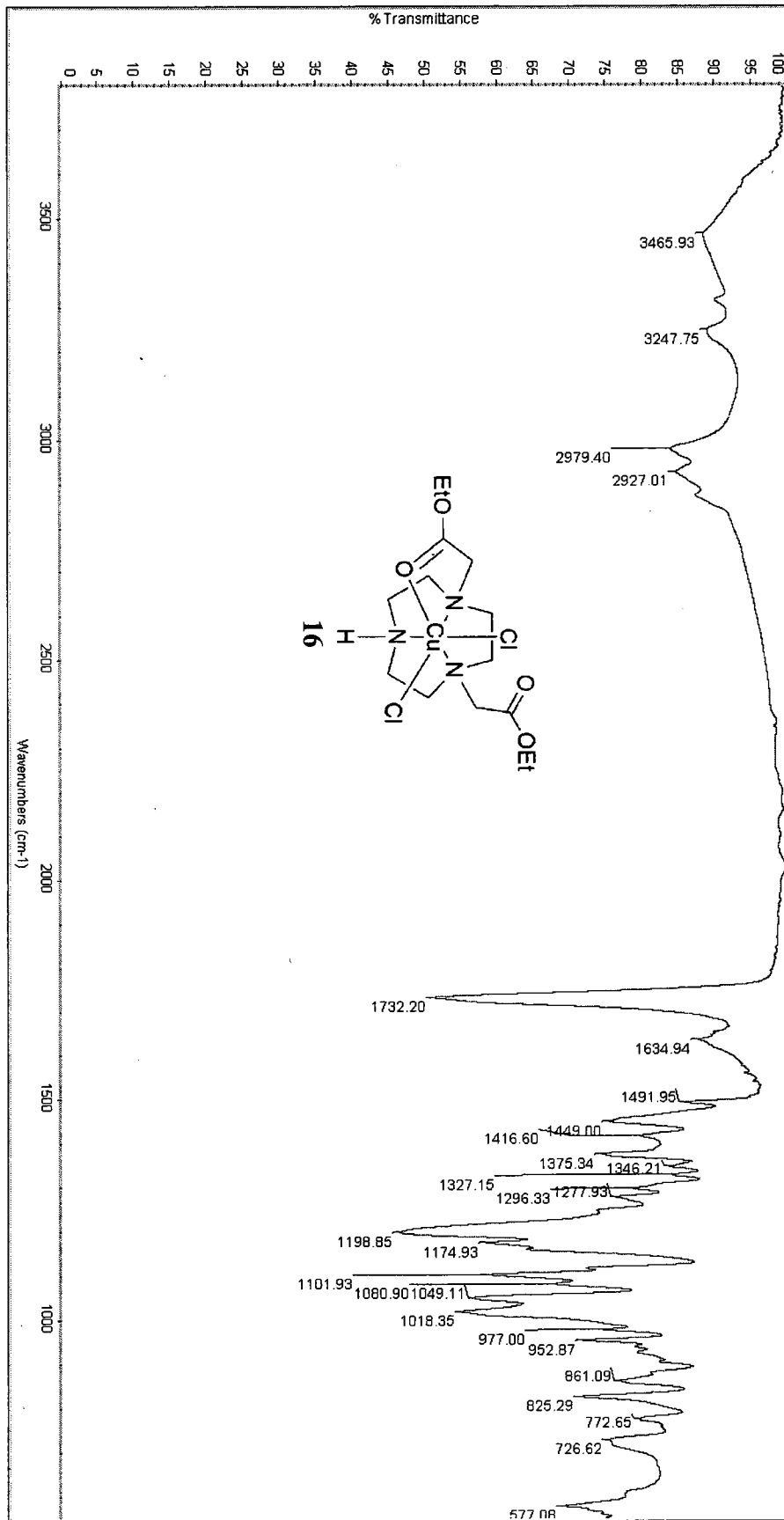
14

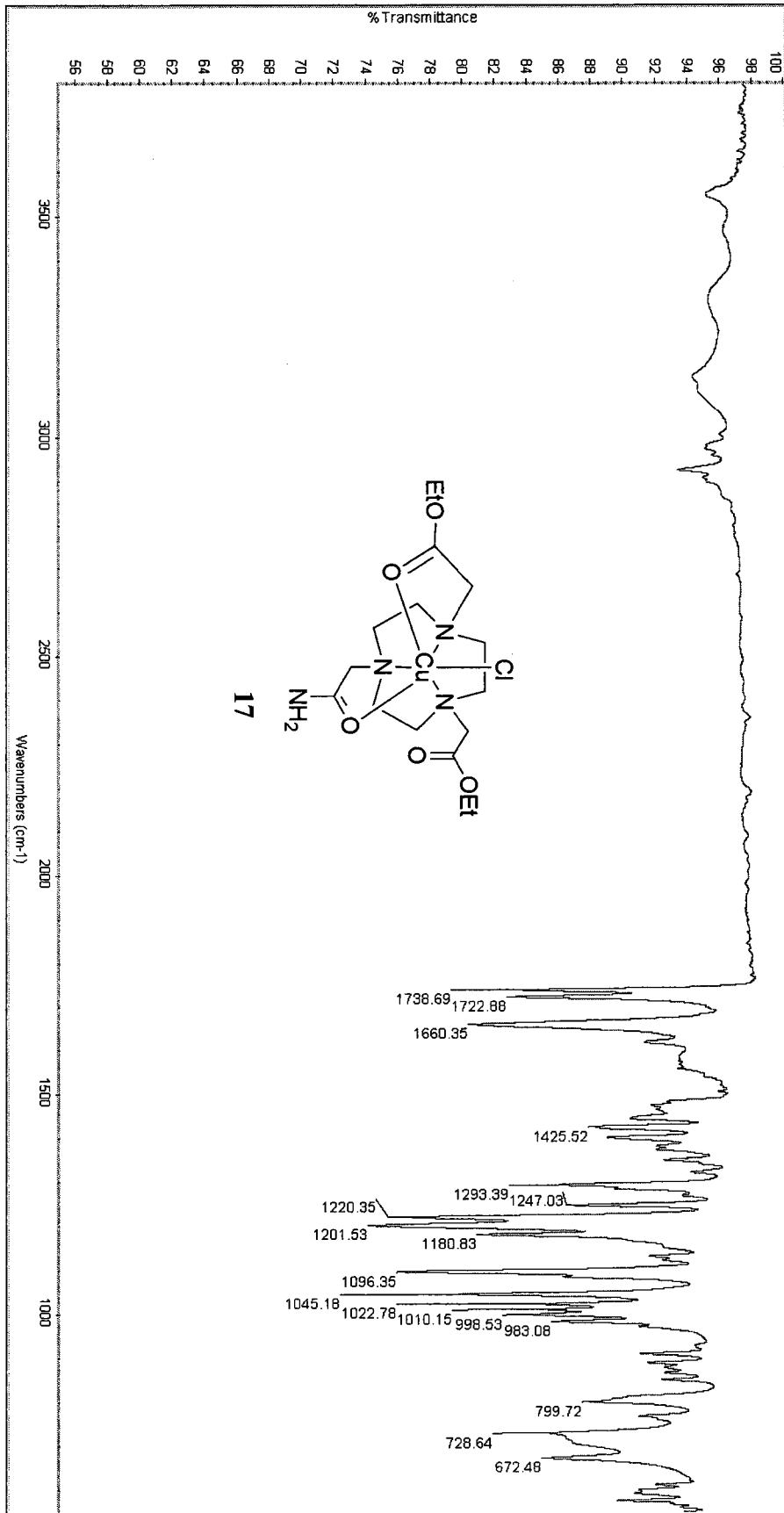
D₂O, CH₃CN set to 2.06

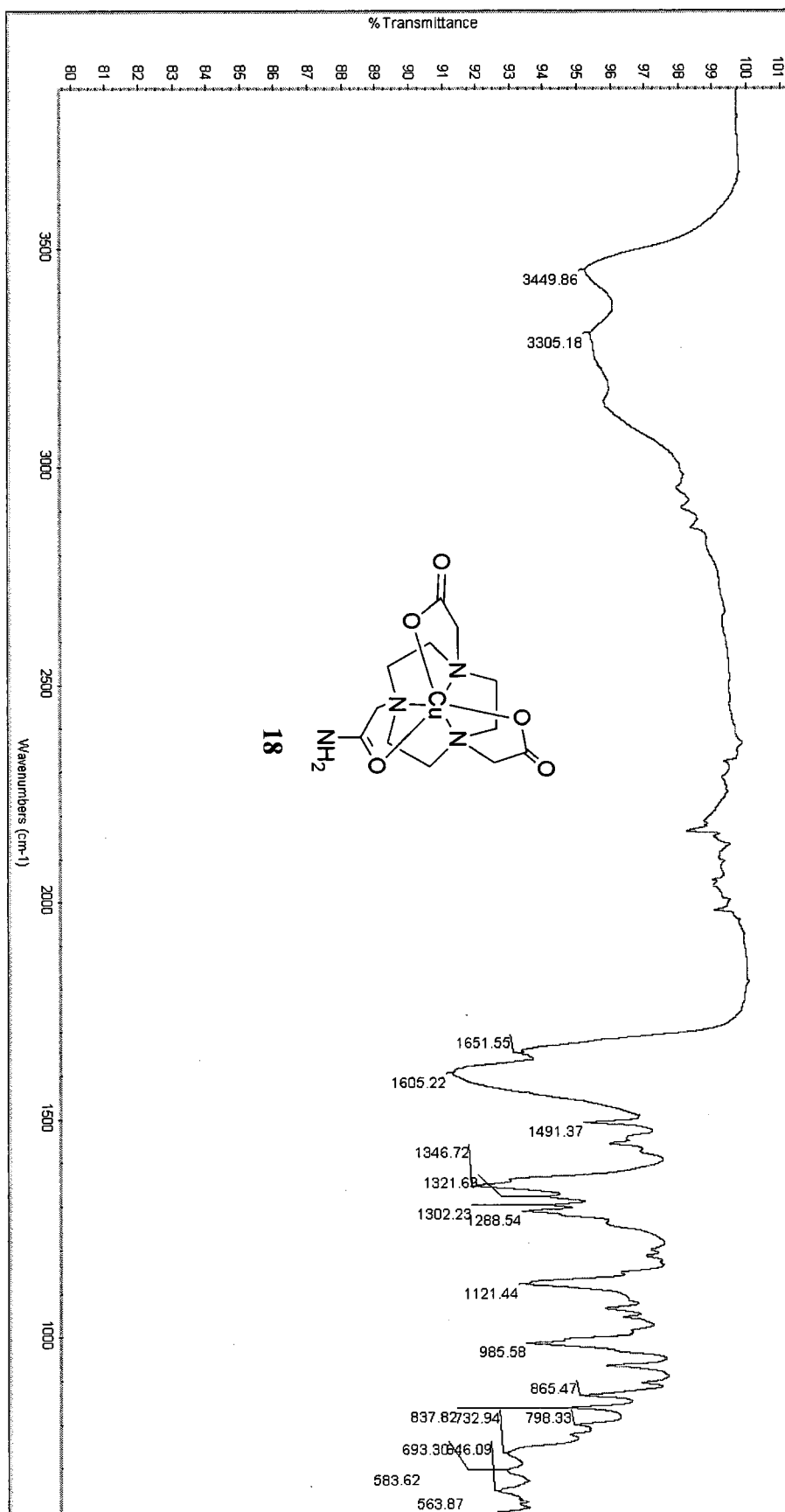












LIST OF REFERENCES

1. a) Chaudhuri, P.; Wieghardt, K. In *Progress in Inorganic Chemistry*; Lippard, S., Ed.; John Wiley & Son: New York, 1987; Vol. 35, pp 329-428. b) Wieghardt, K. *Pure Appl. Chem.* **1988**, 60, 509-516. c) Chomitz, W. A.; Arnold, J. *Chem. Eur. J.* **2009**, 15, 2020-2030.
2. Lindoy, L. F. *The Chemistry of Macrocyclic Ligands Complexes* Cambridge; University Press: London, 1989.
3. Hancock, R. D.; Martell, A. E. In *Metal Complexes in Aqueous Solutions*; Fackler, P. Ed.; Plenum Press: New York, 1996.
4. Lazar, I.; Kiraly, R.; Takacs, Z. *J. Coord. Chem.* **2000**, 51, 293-304.
5. Costamagna, J.; Ferraudi, G.; Matsuhira, B.; Campos-Vallette, M.; Canales, J.; Villagran, M.; Vargas, J.; Aguirre, M. J. *Coord. Chem. Rev.* **2000**, 196, 125-164.
6. Koyama, H; Yoshino, T. *Bull. Chem. Jpn.* **1972**, 45, 481-484.
7. Peacock, D. H.; Gwan, Y. S. *J. Chem. Soc.* **1937**, 1468-1471.
8. Stetter, H.; Roos, E.-E. *Chem. Ber.* **1954**, 87, 566-571.
9. Richman, J. E.; Atkins, T. J. *J. Am. Chem. Soc.* **1974**, 96, 2268-2270.
10. McAuley, A.; Norman, P. R.; Olubuyide, O. *Inorg. Chem.* **1984**, 23, 1938-1943.
11. Searle, G. H.; Geue, R. J. *Aust. J. Chem.* **1984**, 37, 959-970.
12. Chavez, F.; Sherry, A. D. *J. Org. Chem.* **1989**, 54, 2990-2992.
13. Vriesema, B. K.; Buter, J.; Kellogg, R. M. *J. Org. Chem.* **1984**, 49, 110-113.

14. Bossek, U.; Nühlen, D.; Bill, E.; Glaser, T.; Krebs, C.; Weyhermüller, T.; Wieghardt, K.; Lengen, M.; Trautwein, A. X. *Inorg. Chem.* **1997**, *36*, 2834-2843.
15. Fry, F. H.; Fallon, G. D.; Spiccia, L. *Inorg. Chim. Acta* **2003**, *346*, 57-66.
16. Chen, X.-Y.; Xia, J.; Zhao, B.; Cheng, P.; Yan, S.-P.; Liao, D.-Z.; Jiang, Z.-H.; Song, H.-B.; Wang, H.-G. *J. Coord. Chem.* **2004**, *57*, 231-237.
17. Braband, H.; Abram, U. *Inorg. Chem.* **2006**, *45*, 6589-6591.
18. Ware, D. C.; Olmstead, M. M.; Wang, R.; Taube, H. *Inorg. Chem.* **1996**, *35*, 2576-2582.
19. Shi, P.; Jiang, Q.; Lin, J.; Zhao, Y.; Lin, L.; Guo, Z. *J. Inorg. Biochem.* **2006**, *100*, 939-945.
20. Cabiness, D. K.; Margerum, D. W. *J. Am. Chem. Soc.* **1969**, *91*, 6540-6541.
21. Yang, R.; Zompa, L. J. *Inorg. Chem.* **1976**, *15*, 1499-1502.
22. Gasser, G.; Tjioe, L.; Graham, B.; Belousoff, M. J.; Juran, S.; Walther, M.; Künstler, J.-U.; Bergmann, R.; Stephan, H.; Spiccia, L. *Bioconjugate Chem.* **2008**, *19*, 719-730.
23. Arishima, T.; Hamada, K.; Takamoto, S. *Nippon Kagaku Kaishi* **1973**, 1119.
24. Hama, H.; Takamoto, S. *Nippon Kagaku Kaishi* **1975**, 1182.
25. Takahashi, M.; Takamoto, S. *Bull. Chem. Soc. Jpn.* **1977**, *50*, 3413-3414.
26. Wieghardt, K.; Bossek, U.; Chaudhuri, P.; Herrmann, W.; Menke, B. C.; Weiss, J. *Inorg. Chem.* **1982**, *21*, 4308-4314.
27. Sayer, B. A.; Michael, J. P.; Hancock, R. D. *Inorg. Chim. Acta* **1983**, *77*, L63-L64.
28. Moore, D. A.; Fanwick, P. E.; Welch, M. J. *Inorg. Chem.* **1989**, *28*, 1504-1506.
29. Beissel, T.; Buerger, K. S. Voigt, G.; Wieghardt, K.; Butzlaff, C.; Trautwein, A. X. *Inorg. Chem.* **1993**, *32*, 124-126.

30. Pavlishchuk, V.; Birkelbach, F.; Weyhermüller, T.; Wieghardt, K.; Chaudhuri, P. *Inorg. Chem.* **2002**, 41, 4405-4416.
31. Li, Q.-X.; Luo, Q.-H.; Li, Y.-Z.; Pan, Z.-Q.; Shen, M.-C. *Eur. J. Inorg. Chem.* **2004**, 4447-4456.
32. Belousoff, M. J.; Duriska, M. B.; Graham, B.; Batten, S. R.; Moubaraki, B.; Murray, K. S.; Spiccia, L. *Inorg. Chem.* **2006**, 45, 3746-3755.
33. Van der Merwe, M. J.; Boeyens, J. C. A.; Hancock, R. D.; *Inorg. Chem.* **1985**, 24, 1208-1213
34. Miessler, G. L.; Tarr, D. A. *Inorganic Chemistry: Coordination Chemistry*, 3rd Ed.; Pearson Prentice Hall: New Jersey, 2004.
35. Sprague, J. E.; Peng, Y.; Sun, X.; Weisman, G. R.; Wong, E. H.; Achilefu, S.; Anderson, C. J. *Clin. Cancer Res.* **2004**, 10, 8674-8682.
36. Chong, H.-S.; Ma, X.; Le, T.; Kwamena, B.; Milenic, D. E.; Brady, E. D.; Song, H. A.; Brechbiel, M. W. *J. Med. Chem.* **2008**, 51, 118-125.
37. Prasanphanich, A. F.; Retzlöff, L.; Lane, S. R.; Nanda, P. K.; Sieckman, G. L.; Rold, T. L.; Ma, L.; Figueroa, S. D.; Sublett, S. V.; Hoffman, T. J.; Smith, C. J. *Nucl. Med. Biol.* **2009**, 36, 171-181.
38. Reichert, D. E.; Lewis, J. S.; Anderson, C. J. *Coord. Chem. Rev.* **1999**, 184, 3-66.
39. Anderson, C. J.; Welch, M. J. *Chem. Rev.* **1999**, 99, 2219-2234.
40. Wadas, T. J.; Wong, E. H.; Weisman, G. R.; Anderson, C. J. *Curr. Pharm. Des.* **2007**, 13, 3-16.
41. Ametamey, S. M.; Honer, M.; Schubiger, P. A. *Chem. Rev.* **2008**, 108, 1501-1516.

42. Ma, D.; Lu, F.; Overstreet, T.; Milenic, D. E.; Brechbiel, M. W. *Nucl. Med. Biol.* **2002**, 29, 91-105.
43. Moi, M. K.; Meares, C. F.; McCall, M. J.; Cole, W. C.; DeNardo, S. J. *Anal. Biochem.* **1985**, 148, 249-253.
44. Bass, L. A.; Wang, M.; Welch, M. J.; Anderson, C. J. *Bioconjugate Chem.* **2000**, 11, 527-532.
45. Rogers, B.E.; Bigott, H. M.; McCarthy, D. W.; Manna, D. D.; Kim, J.; Sharp, T. L.; Welch, M. J. *Bioconjugate Chem.* **2003**, 14, 756-763.
46. Chen, X.; Park, R.; Hou, Y.; Tohme, M.; Shahinian, A. H.; Bading, J. R.; Conti, P. S. *J. Nucl. Med.* **2004**, 45, 1390-1397.
47. Sun, X.; Wuest, M.; Weisman, G. R.; Wong, E. H.; Reed, D. P.; Boswell, C. A.; Motekaitis, R.; Martell, A. E.; Welch, M. J.; Anderson, C. J. *J. Med. Chem.* **2002**, 45, 469-477.
48. Boswell, C.A.; Sun, X.; Niu, W.; Weisman, G. R.; Wong, E. H.; Rheingold, A. L.; Anderson, C. J. *J. Med. Chem.* **2004**, 47, 1465-1474.
49. Weisman, G. R.; Wong, E. H.; Hill, D. C.; Rogers, M. E.; Reed, D. P.; Calabrese, J. *C. J. Chem. Soc., Chem. Commun.* **1996**, 947-948.
50. Wong, E. H.; Weisman, G. R.; Hill, D. C.; Reed, D. P.; Rogers, M. E.; Condon, J. S.; Fagan, M. A.; Calabrese, J. C.; Lam, K.-C.; Guzei, I. A.; Rheingold, A. L. *J. Am. Chem. Soc.* **2000**, 122, 10561-10572.
51. Garrison, J. C.; Rold, T. L.; Sieckman, G. L.; Figueroa, S. D.; Volkert, W. A.; Jurisson, S. S.; Hoffman, T. J. *J. Nucl. Med.* **2007**, 48, 1327-1337.

52. Prasanphanich, A. F.; Nanda, P. K.; Rold, T. L.; Ma, L.; Lewis, M. R.; Garrison, J. C.; Hoffman, T. J.; Sieckman, G. L.; Figueroa, S. D.; Smith, C. J. *PNAS* **2007**, 104, 12462-12467.
53. Hoffman, T. J.; Smith, C. J. *Nucl. Med. Biol.* **2009**, 36, 579-585.
54. Sprague, J. E.; Peng, Y.; Fiamengo, A. L.; Woodin, K. S.; Southwick, E. A.; Weisman, G. R.; Wong, E. H.; Golen, J. A.; Rheingold, A. L.; Anderson, C. J. *J. Med. Chem.* **2007**, 50, 2527-2535.
55. Johnson, V. B. Ph. D. Dissertation, University of New Hampshire, 1982.
56. Vachon, D. J. Ph. D. Dissertation, University of New Hampshire, 1984.
57. Weisman, G. R.; Vachon, D. J.; Johnson, V. B.; Gronbeck, D. A. *J. Chem. Commun.* **1987**, 886-887.
58. Wang, Y. M.S. Thesis, University of New Hampshire, 1989.
59. West, C. A. Ph. D. Dissertation, University of New Hampshire, 1995.
60. Atkins, T. J. *J. Am. Chem. Soc.* **1980**, 102, 6364-6365.
61. Weisman, G. R.; Johnson, V.; Fiala, R. E. *Tetrahedron Lett.* **1980**, 21, 3635-3638.
62. Kreher, U.; Hearn, M. T. W.; Moubaraki, B.; Murray, K. S.; Spiccia, L. *Polyhedron* **2007**, 26, 3205-3216.
63. Van Haveren, J. ; DeLeon, L; Ramasamy, R.; Van Westrenen, J. V; Sherry, A. D. *NMR Biomed.* **1995**, 8, 197-205.
64. Geraldès, C. F. G. C.; Alpoim, M. C.; Marques, M. P. M.; Sherry, A. D.; Singh, M. *Inorg. Chem.* **1985**, 24, 3876-3881.
65. Lazar, I.; Kiraly, R.; Takacs, Z. *J. Coord. Chem.* **2000**, 51, 293-304.
66. Huskens, J.; Sherry, A. D. *J. Am. Chem. Soc.* **1996**, 118, 4396-4404.

67. Wulfsberg, G. *Inorganic Chemistry*; University Science Books: Sausalito, 2000.
68. Greenwood, N. N.; Earnshaw, A. *Chemistry of the Elements*; 2th ed.; Elsevier Butterworth-Heinemann: Oxford, 1997.
69. Cox, C.; Ferraris, D.; Murthy, N. N.; Lectka, T. *J. Am. Chem. Soc.* **1996**, 118, 5332-5333.
70. Blake, A. J; Fallis, I. A; Gould, R. O.; Parsons, S.; Ross, S. A.; Schröder, M. *J. Chem. Soc., Dalton Trans.* **1996**, 4379-4387.
71. Niklas, N.; Hampel, F.; Liehr, G.; Zahl, A.; Alsfasser, R. *Chem. Eur. J.* **2001**, 7, 5135-5142.
72. Niklas, N.; Heinemann, F. W.; Hampel, F.; Alsfasser, R. *Angew. Chem. Int. Ed.* **2002**, 41, 3386-3388.
73. Sibbons, K. F.; Al-Hashimi, M.; Motevalli, M.; Wolowska, J.; Watkinson, M. *Dalton Trans.* **2004**, 3163-3165.
74. Warden, A. C.; Spiccia, L.; Hearn, M. T. W.; Boas, J. F.; Pilbrow, J. R. *Dalton Trans.* **2005**, 1804-813.
75. Sigel, H.; Martin, R. B. *Chem. Rev.* **1982**, 82, 385-426.
76. Bannister, E.; Cotton, F. A. *J. Chem. Soc.* **1960**, 2276-2280.
77. Liu, Y.; Ren, T.; *Inorg. Chim. Acta* **2003**, 348, 279-282.
78. Song, Y.-F.; Berry, J. F.; Bill, E.; Bothe, E.; Weyhermüller, T.; Wieghardt, K. *Inorg. Chem.* **2007**, 46, 2208-2219.
79. Woodin, K. S.; Heroux, K. J.; Boswell, C. A.; Wong, E. H.; Weisman, G. R.; Niu, W.; Tomellini, S. A.; Anderson, C. J.; Zakharov, L. N.; Rheingold, A. L. *Eur. J. Inorg. Chem.* **2005**, 4829-4833.